Fire and High Temperature Behaviour of Thermal Mortars

Maria João Sobral Cordeiro Pupo Correia

Thesis to obtain Master of Science Degree in

Civil Engineering

Supervisors: Professor Doctor Inês dos Santos Flores Barbosa Colen

Doctor João Pedro Laje da Costa Firmo

Examination Committee

Chairperson: Professor Doctor Orlando José Barreiros D'Almeida Pereira

Supervisor: Professor Doctor Inês dos Santos Flores Barbosa Colen

Member of the committee: Professor Doctor Pedro Miguel Soares Raposeiro da Silva

July 2022

Statement

I declare that this document is an original work of my own and that it meets all the requirements of the University of Lisbon's Code of Conduct and Good Practices.

Acknowledgments

Resumo

A UE comprometeu-se a atingir a neutralidade carbónica até 2050. Nesse sentido, diversos países implementaram regulamentos e normas que impulsionaram a utilização de novos sistemas de revestimento de edifícios com materiais isolantes capazes de cumprir os requisitos de desempenho energético.

Seguindo esta abordagem, a utilização de argamassas térmicas à base de aerogel começou a ser explorada devido às suas propriedades melhoradas de isolamento térmico e potencial bom comportamento a temperatura elevada e ao fogo.

Neste contexto, o presente trabalho visa caracterizar o comportamento ao fogo e temperaturas elevadas de uma argamassa térmica inovadora com incorporação de aerogel e compará-la com uma solução convencional, uma argamassa térmica com granulado de poliestireno expandido (EPS), utilizando como referência uma argamassa à base de cal sem propriedades térmicas.

A campanha experimental incluiu (i) ensaios de caracterização mecânica; (ii) ensaios termofísicos; (iii) análises microestruturais; (iv) ensaios de reação ao fogo; e (v) ensaios de exposição ao fogo, cujos resultados foram utilizados para determinar/ calibrar a condutibilidade térmica e o calor específico a temperaturas elevadas.

Através destes procedimentos foi possível comparar o comportamento ao fogo e a temperaturas elevadas das argamassas térmicas, assim como propor parâmetros complementares (além das normas) para avaliar o seu desempenho nas referidas condições.

Os resultados mostram que ambas as argamassas térmicas são termicamente instáveis devido à suscetibilidade térmica dos constituintes poliméricos. Contudo, a argamassa com aerogel apresenta melhores propriedades residuais, provando que os seus constituintes (em particular, o aerogel) são menos degradados pela exposição a altas temperaturas.

Palavras-Chave

Aerogel; EPS; Argamassas térmicas; Comportamento ao fogo; Temperaturas elevada.

Abstract

The EU has committed to reach net-zero CO_2 emissions by 2050. The decarbonization pathways included the implementation of regulations and standards that have driven the use of new building envelope systems made of composite materials with insulating properties to fulfil energy performance requirements.

Following this approach, the use of aerogel-based mortars has begun to be explored due to its improved thermal insulation properties and potential good high temperature and fire behaviour.

In this context, the present work aims at characterizing the fire and post-fire behaviours of an innovative thermal mortar with aerogel incorporation, including the comparison with one conventional solution, a thermal mortar with expanded polystyrene granules (EPS), and using a lime-based mortar, as reference. To this end, an extensive experimental campaign was developed, including (i) mechanical characterization tests; (ii) thermophysical ones; (iii) microstructural analyses; (iv) fire reaction tests; and (v) fire exposure tests whose results were used to determine/ calibrate thermal conductivity and specific heat at elevated temperatures.

Within these procedures it was possible to compare the fire and high temperature behaviour of thermal mortars as well as suggest complementary parameters (beyond the standards) to evaluate their performance under these conditions.

The results showed that both thermal mortars are thermally unstable due to the susceptibility of polymeric constituents when subjected to high temperatures. Despite the referred instability, the aerogel-based mortar exhibited higher residual properties, proving that its constituents (in particular, aerogel) are less degraded by exposure to high temperatures.

Keywords

Aerogel; EPS; Thermal mortars; Fire behaviour; High temperatures

Table of Contents

List of Figures

List of Tables

Nomenclature

Roman Symbols

cp	Volumetric heat capacity	$[J/m^3.K]$
Cp	Specific heat capacity	$[J/(kg.K)]$
F_S	Flame spread	[mm]
G	Heat generation per unit volume per unit time	$[J/(m^3.s)]$
PCS	Gross calorific potential	$[MJ/kg$ or $MJ/m^2]$
T_{ig}	Time to ignition	[s]
U	Thermal transmittance	$[W/(m^2.°C)]$

Greek Symbols

θ	Temperature	[°C]
$\lambda_{10°C, dry}$	Thermal conductivity at 10°C and dry state	$[W/(m.K)]$
μ	Water vapour resistance factor	[-]
φ	Diameter	[mm]
ρ	Bulk density	$[Kg/m^3]$
σ_T	Flexural strength	[MPa]
σ_C	Compressive strength	[MPa]

Acronyms/ Abbreviations

ASTM	American Society of Testing Materials
CS	Strength Class
DECivil	Departamento de Engenharia Civil, Arquitetura e Georrecursos do IST
DEQ	Departamento de Engenharia Química do IST
EPS	Expanded Polystyrene
ETICS	External Thermal Insulating Composite System
EU	European Union
FIGRA	Fire growth rate used for classification purposes
GHGs	Greenhouse Gases
IFSTA	International Fire Service Training Association

IPCC	Intergovernmental Panel on Climate Change
ISO	International Organization for Standardization
IST	Instituto Superior Técnico
IUPAC	International Union of Pure and Applied Chemistry
LAMPIST	Laboratório de Mineralogia e Petrologia do DECivil
LC	Laboratório de Construção do DECivil
LERM	Laboratório de Estruturas e Resistência dos Materiais do DECivil
Micro CT	Micro Computed Tomography
MW	Mineral Wool
NFPA	National Fire Protection Association
PUR	Polyurethane
RCCTE	Regulamento de Características e Comportamento Térmico dos Edifícios
REH	Regulamento de Edifícios de Habitação
SEM	Scanning Electron Microscope
SMOGRA	Smoke growth rate
SSD	Sum Squares Differences
TGA	Thermogravimetric Analyses
THR	Total heat release
XPS	Extruded Polystyrene
XRD	X-Ray Diffraction

Chemical Substances

$CaCO_3$	Calcite
CO_2	Carbone dioxide
$Ca_2Al_2SiO_7$	Gehlenite
$CaSO_4$	Gypsum
CaO	Lime
$Ca(OH)_2$	Portlandite
SiO_2	Silica

1 Introduction

1.1 General framework and motivation

Until 20 to 25 years ago, the fire spread over and in facades played only a minor role during a fire event in buildings, as the outer walls comprised (mostly) non-combustible materials, such as brick masonry or concrete coated with non-combustible renders. However, with the adoption of new materials (with a significant number of them being combustible), fire spread in building's facades has become an increasing issue in recent years.

The EU has committed to reach net-zero CO_2 emissions by 2050. The decarbonization pathways included the implementation of regulations and standards that have driven the use of new building envelope systems made of composite materials with insulating properties to fulfil energy performance requirements. These measurements may have a significant importance on reaching the EU target since energy demand for daily use in the UE represents nearly 55% of the global energy consumption in buildings [1]. Heating is one of the biggest items in consumption of raw materials such as coal, oil, or natural gas.

The usage of new systems and coating technologies has launched a significant utilization of combustible materials which are used as thermal insulators due to their low thermal conductivity. However, the damage caused in case of fire can thus become considerable due to greater fire spread because most of them are combustible. In fact, fires on building facades have never been so prevalent [2]. According to a survey conducted at the Imperial College in 2018, the frequency of this type of fires has increased 7 times in 30 years [3]. This growth is also reflected on the graph presented in Figure 1.

To evidence and understand this occurrence, extensive research has been conducted about fire incidents involving buildings facades with multilayer coatings (annex A1) in which were reported a total of 66 events between 1990 and 2022. Most of the stated cases have caused catastrophic damages in terms of human lives, financial losses, and buildings' damages, either at a material and/or structural level; as consequence, the awareness and concerns about this issue have raised.
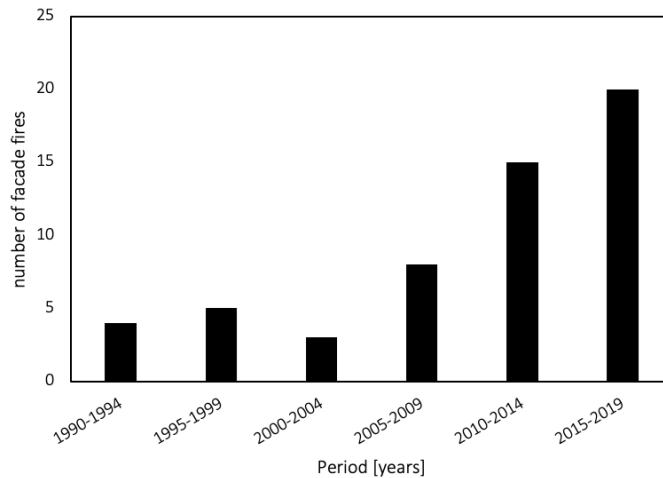
Figure 1. Number of fire facades with multilayer coatings worldwide every five years [4]

According to a report published in 2021 by the CTIF - International Fire Association of Fire and Rescue Services [5], worldwide there are, on average, 2.4 fires per 1000 inhabitants per year, of which 31.6% are in buildings and of these, 83.6% in residential buildings. It should be noted that only in Sweden, a country with approximately the same population as Portugal, 78 people died in fires in 2019 alone [5].

Despite the undoubtedly good thermal performance of External Thermal Insulation Systems, ETICS, which provide an improved thermal comfort and contribute to energy savings, their fire behaviour raises serious concerns when the insulation layer is made of combustible materials such as expanded polystyrene (EPS) and extruded polystyrene (XPS). In the reviewed cases presented in annex A1, cladding materials are generally composite multilayer systems including an infill insulation material consisting on EPS or polyurethane (PU) and, in some cases, low density polyethylene. These materials are highly combustible, contributing to fire spread. From the initial ignition, it can take around 20 min for a complete and uncontrollable propagation as happened in 2010 in a 38-storey building in South Korea with a 3mm polyethylene core on the facade (ID 22 – annex A1). Alongside the immediate and visible reported damages, when ETICS are subjected to fire, some hidden potential risks also exist. An independent study by the University of Central Lancashire [6] found significant amounts of toxins in soils and high concentrations of potentially carcinogenic residues in the burnt debris of the Grenfell tower (a building in UK completely destroyed by fire in 2017 in which 72 people lost their lives). Also, a study in the UK [7] showed that following the Grenfell fire, high concentrations of benzene were discovered 140 m away from the tower in amounts 25 to 40 times higher than normal. Based on the above, it can be concluded that good thermal performance it is often not balanced with sustainability and fire safety; in this context, innovative thermal mortars should be developed to fulfill both thermal performance and fire safety requirements.

These concerns about multilayer facade cladding systems have led to the interest in studying the layer with the greatest impact on system performance - the thermal insulation layer.

1.2 Objectives and main methodology

This work focused on studying the insulating layer/material that could be used in a multi-layered facade insulation composite system, commonly named as External Thermal Insulation Composite Systems (ETICS). For this insulating layer a thermal mortar was considered.

This dissertation aims at characterizing the fire and high temperature behaviour of an innovative thermal mortar with aerogel incorporation, including the comparison with a conventional solution, a thermal mortar with expanded polystyrene (EPS), and using a lime-based mortar as reference. The other main purpose is to define parameters to complement the standard evaluation of mortars, providing more detailed information that allows assessing the behaviour of these materials when exposed to elevated temperature or fire, by using small specimens.

To this end, an experimental campaign was developed including the following types of tests on the 3 different mortar types: (i) characterization tests: mechanical – compression and flexural resistance; and thermophysical – bulk density, thermal conductivity, specific heat, and thermogravimetric analyses (TGA); (ii) microstructural analyses of samples based on several techniques: XRD, SEM, and Micro CT; (iii) fire reaction experiments, in particular to determine the heat of combustion generated and the ignitability of these products, and (iv) fire exposure tests in which the mortars were subjected to a standard fire heating curve, ISO 834. Considering the peak temperatures on TGA (i.e. the temperatures where significant mass losses occur), samples were heated and then cooled down until room temperature. After that, tests (i) and (ii) were repeated to measure materials' residual properties.

The experimental programme described above included tests at a macro scale in order to reproduce a situation in which these mortars can be used and subjected to the fire action; complemented with micro scale analyses to understand what happens to the initial properties of the materials as well as what components are degraded that justify such performance during and after high temperatures exposure.

Finally, a numerical inverse analysis was carried out to calibrate the thermal properties of the 3 mortars, namely, their specific heat (Cp) and thermal conductivity (λ) as a function of temperature; to this end, a thermal program and an optimization routine developed in *matlab* software was used. The input were temperature distributions over the mortars thickness obtained in (iv).

1.3 Dissertation Outline

This dissertation is organized into six chapters, in order to simplify the interpretation of the results obtained in each phase of the work. The structure of each chapter is presented in the following paragraphs.

The present chapter (Introduction) provides the background of the subject, describing the worldwide concern with thermal comfort inside homes and energy consumption that this can generate, presenting new trends in building facade cladding driven by new thermal requirements, highlighting the lack of safety in fire situations. Then, the objectives to be achieved are described, the main methodology is presented, and, finally, the structure and organization of the various chapters are briefly explained.

In the second chapter, a literature review on relevant topics for this dissertation is presented. In the first phase, a more general description of buildings' performance is given both in terms of thermal efficiency and of fire behaviour. Then, the constructive solutions in terms of thermal claddings are described, and at the end of the chapter introduces the concept of nanomaterial and describes silica aerogels. Afterwards, research studies found in the literature about mortars incorporating aerogels are presented, and, finally, studies on fire behaviour of external cladding systems are examined.

Chapter three explains the research methodology adopted in the present study; firstly, the mortars (and their constituent materials) are described and then the organization of the experimental program is presented, followed by the description of experimental procedures.

The fourth chapter presents the results and discussion of experimental tests. This includes (i) the characterization tests: mechanical – compression and flexural resistance; and thermophysical – bulk density, thermal conductivity, specific heat, and thermogravimetric analyses (TGA); (ii) microstructural analyses: XRD, SEM, and Micro CT; (iii) fire reaction experiments: ignitability, gross calorific potential, cone calorimeter, and bomb calorimeter; and (iv) fire exposure tests.

The fifth chapter presents the numerical study developed with the objective of determining the thermophysical properties of the mortars through inverse numerical analysis using the experimental thermal distributions obtained in (iv) fire exposure tests described in chapter 3.

Chapter 6 comprises the general conclusions of the work carried, with a critical analysis of the data obtained in the present research followed by proposals for future developments.

Finally, the literature references used as basis for the development of this work are listed. At the end of the dissertation, the annexes contain supporting data for the six chapters mentioned above.

2 Literature review

2.1 General framework

In the present chapter, the importance of the thermal insulation of facades is briefly described, with particular interest in the opaque envelope, where thermal mortars are used.

Firstly, it is analysed the building performance in case of fire, the possible fire-induced structural damage and how the different facade systems influence the fire spread. The standard tests which aim at evaluating the fire reaction and fire resistance and the regulatory requirements concerning these topics are also briefly analysed.

Then, it is examined the new thermal requirements in buildings which has led to the novel approach in terms the facades' function as thermal insulation barrier. In order to balance the multiple objectives, facade design combines layers of varied materials [8], in which polymers are often adopted, as they are high-performing, affordable, and their thermal and mechanical properties can be tailored to meet different needs.

In this chapter it is also included a clarification on the types of cladding systems which are more adopted nowadays (section 2.3), including their main differences and the pros and cons of using each solution. Special emphasis is given to thermal mortars since they are seen to have the best potential to match good thermal performance, combining comfort and safety.

Section 2.4 starts with the description of the main characteristics and proprieties of aerogel, how it behaves under exposure to high temperature, and in which products it can be incorporated in; this section ends with a description of the main characteristics of commercially available aerogel-based thermal mortars.

Finally, in section 2.5, a compilation of different studies available in the literature about the fire behaviour of cladding systems is analysed and the research needs are identified (section 2.6).

2.2 Buildings' performance

The classification of concrete structures depends on the choice and disposal of structural elements which affect the way on how the building will behave when subjected to vertical and horizontal loads. They can be classified as: framed structures (columns and beams), laminar structures (walls) and mixed structures (frames and walls).

In Portugal, the most used system is the mixed one, as it presents a better performance against horizontal loads when compared to framed structures. It also presents lower costs when compared to laminar structures. This makes sense, since the country has relevant seismic activity, and it is intended to meet the Eurocode 8 [9] requirements.

In mixed structures vertical loads are transmitted by the slabs to the beams (for flat or waffled slabs, vertical loads are transmitted directly to vertical elements) and from these to the columns and walls; there is a rigid connection between columns, walls, and beams, so the bending effects on beams due to vertical loads are also transmitted to columns and walls. Horizontal loads are resisted exclusively by the beams, columns, and walls; the introduction of resistance walls, especially on the contour of the structure, allows reducing the effects of torsion and the displacements.

The action of fire is particularly worrying in buildings, and especially in high-rise buildings. It is important to mention that besides the behaviour of the structure during fire, its residual (i.e. post-fire) capacity and the feasibility of repair/rehabilitation are also critical issues.

Not only do walls and slabs constitute compartmentalization elements with watertightness and insulation capacity, but also the collapse of a concrete structure exposed to the fire action rarely occurs. The most serious damages are associated to the global effects of the deformations imposed [10].

Despite the traditional building structures (e.g. made of the reinforced concrete) have a good fire performance, the materials which are used on the building envelope and on finishes may represent a significant hazard for the fire spread. In fact, those elements which cover the walls play a key role for the thermal insulation and energy efficiency of the building.

The main purpose of a building envelope is to isolate the inside from the outside. It serves as an outside barrier to ensure the quality and control of the indoor conditions irrespective of transient outdoor conditions. The building vertical envelope (i.e. the facade) consists of transparent and opaque parts. Opaque parts include external walls, roof and floors and transparent parts include windows, skylights and glass doors [11].

According to Najjar et al. [12], 20% of heat losses through residential buildings envelopes happen through walls, 13% through de roof, 15% through the floor and the remain through the openings. This means that the walls represent the biggest impact in heat losses. Indeed, thermal insulation of the opaque areas of the facade presents itself as a decisive factor in exterior insulation, given their large exposure area to the external environment.

The heat transfer is usually a combination of heat conduction, heat convection and heat radiation as shown in Figure 2 [13]. As a result, an ideal thermal insulation layer/coating should resist heat transfer, reflect, and radiate the solar energy actively.

This insulation can be from the inside or outside of the facade walls: the insulating material can be placed in the air gap between the masonry panels or through the placement on the outside of the facade walls of blocks/systems with improved thermal characteristics [14]. The latter have the main advantage of mitigating thermal bridges by significantly reducing energy losses.
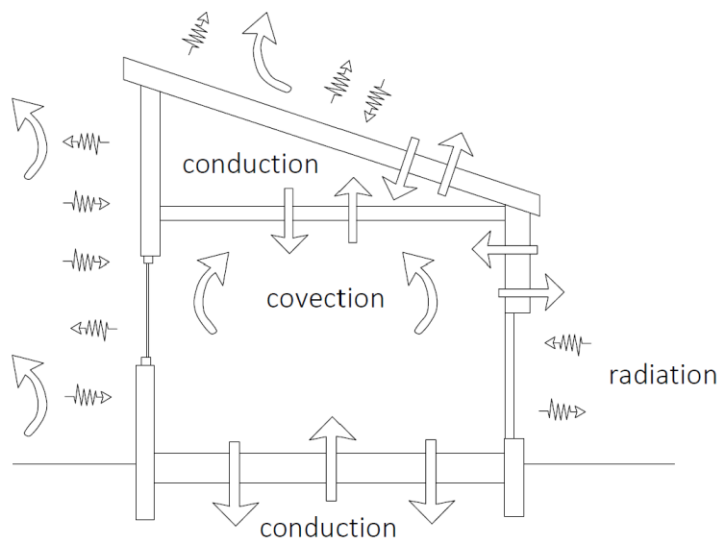
Figure 2. Schematic heat transfers in buildings. Adapted from [13]

2.2.1 Fundamentals of fire in buildings

Fire is an oxidation process in which heat is released. The sudden release of energy causes temperature rise, smoke, and toxic gases release. The three needed components of a fire are fuel (something that will burn), heat (enough to make the fuel burn) and air (oxygen). Fire will last until one or more components are removed.

The development process of a building fire inside a typical room is illustrated in Figure 3 through temperature-time evolution [15]. This evolution depends on a wide range of variables (fuel load, ventilation, compartmentation characteristics etc.,) which cause a significant variation in the dynamics of each fire [16,17].
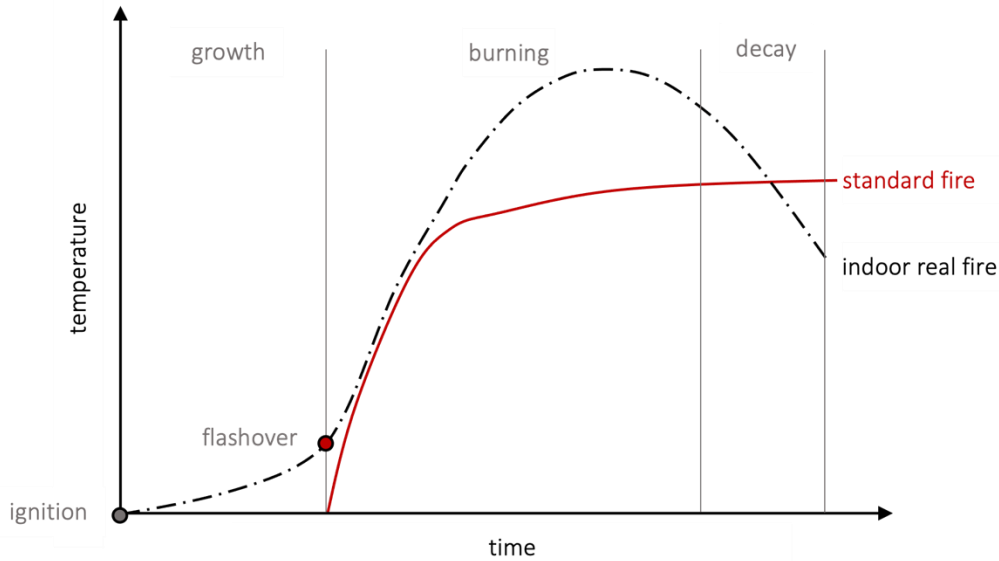
Figure 3. Building fire development process inside a typical room. Adapted from [15]

Briefly explaining, ignition is the start of combustion. The fire is then in growth phase, the heat-release rate increases, but the fire remains localized. The transition from growth stage to the fully developed stage involve a flashover. Flashover is the short stage at which all surfaces and objects within a space have been heated to their ignition temperature and flame breaks out almost at once over the surface of all objects in the space [18]. Once in the burning period, the temperatures and radiant heat flux are so high that all exposed surfaces are burning, and the heat release rate is governed by the available ventilation - this is stage that has most impacts on the structural elements and compartment boundaries. When the fuel burns out and temperature drops, comes the decay period, where the burning rate becomes a function of the remaining fuel itself rather than of the ventilation.

To simulate the action of fire, there have been many studies that aimed at defining standardized temperature *vs.* time curves. Internationally, there are a few time-temperature curves which were defined in the following standards: ISO 834 [19], BS 476 [20], ASTM 119 [21], NFPA 251 [22]. However, the choice of a single curve is far from being unanimous, since fires are variable and depend on a variety of properties and circumstances, therefore, these standard curves are, in some situations, far from a real fire as shown in Figure 4. As fire tests have shown, the maximum temperature of real fires can exceed the ISO-curve, but after the peak, it decreases again, whereas the ISO-curve rises continuously [23]. Therefore, many papers have been published that focused on the definition on suitable/realistic time-temperature curves [24,25]. Research on fire spread from adjacent floors levels through exterior walls have been carried out for many years [26,27]. Generally, fire can spread upon building external walls in three principal ways. The first is an

internal spread mechanism where fire leaks through gaps and cracks between floor slabs and exterior walls. The second is an external spread mechanism, window to window, where combustible materials inside an upper window are ignited due to the intense heat from flames projected out of a lower window. The last one is a surface spread mechanism where fire propagates upward along the exterior walls' assembly [15,16].
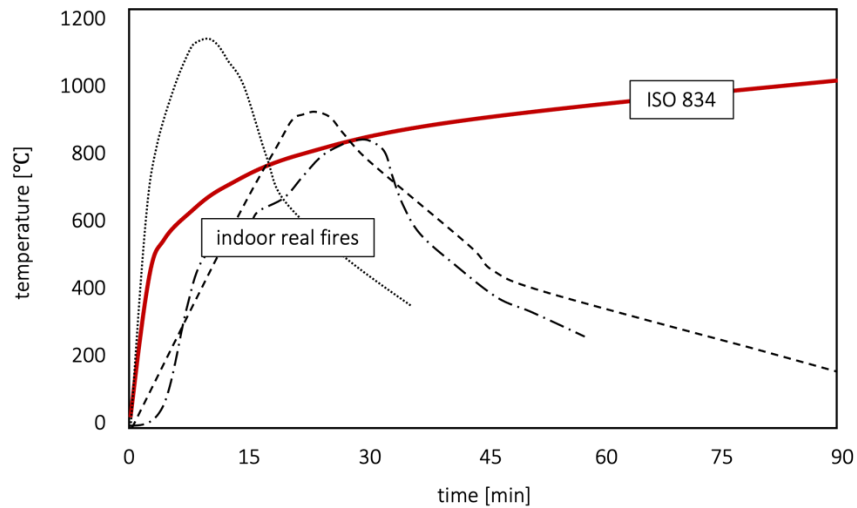
Figure 4. Comparison of temperature-time curves in natural fires with ISO 834 standard curve [23]

2.2.2 Classification of construction materials regarding fire reaction

The prevention of fire in buildings as the minimization of its consequences depends to a significant extent on the fire reaction behaviour of the materials used in constructions. Some crucial factors that can compromise the successful evacuation of buildings are the ease and speed with which materials burn/decompose and the emission of toxic gases during that burning/decomposition process during fire exposure.

To classify a construction product under European Classification, a product must pass up 4 test methods that simulate the first 3 stages of a fire development, which correspond to 3 different levels of thermal exposure: i) small flame action, EN ISO 11925-2 [28]; ii) effect of an isolated object on combustion (SBI), EN 13823 [29]; iii) generalised fire, EN ISO 1182 (ISO furnace) [30] and ISO 1716 [31](calorimetric bomb). In an effort to achieve a consensus and standardization of the fire reaction classification of construction materials, the European standard EN 13501-1 [32] was created. According to results of the tests mentioned above, 7 classes of reaction to fire are proposed, as presented in Figure 5. As illustrated in this figure, materials are classified into Euroclasses from A1 to E, where A1 means the material does not fuel and does not contribute to fire, while E means that the material is considered fuel and causes flashover before 2

9

minutes. Additionally, there is a classification s1, s2, s3 for smoke release and d0, d1, d2 for flaming droplets or particles. Figure 5 summarizes the classification according to EN 13501-1 [32].

Fire reaction classification EN 13501-1

		A1	**EN ISO 1182** ΔT ≤ 30°C + Δm ≤ 50% + t ≤ 0s
EN ISO 1182 ΔT ≤ 50°C + Δm ≤ 50% + t ≤ 20s	or	**EN ISO 1716** PCS ≤ 3 MJ/Kg	A2	**EN ISO 13823** No lateral flame spread FIGRA ≤ 120 W/s + THR ≤ 7.5 MJ

EN ISO 11925-2 Exposure time = 30s F_S ≤ 150mm within 60s	B	
	C	No lateral flame spread FIGRA ≤ 250 W/s + THR ≤ 15 MJ
	D	FIGRA ≤ 750 W/s
Exposure time = 15s F_S ≤ 150mm within 20s	E	
No test	F	
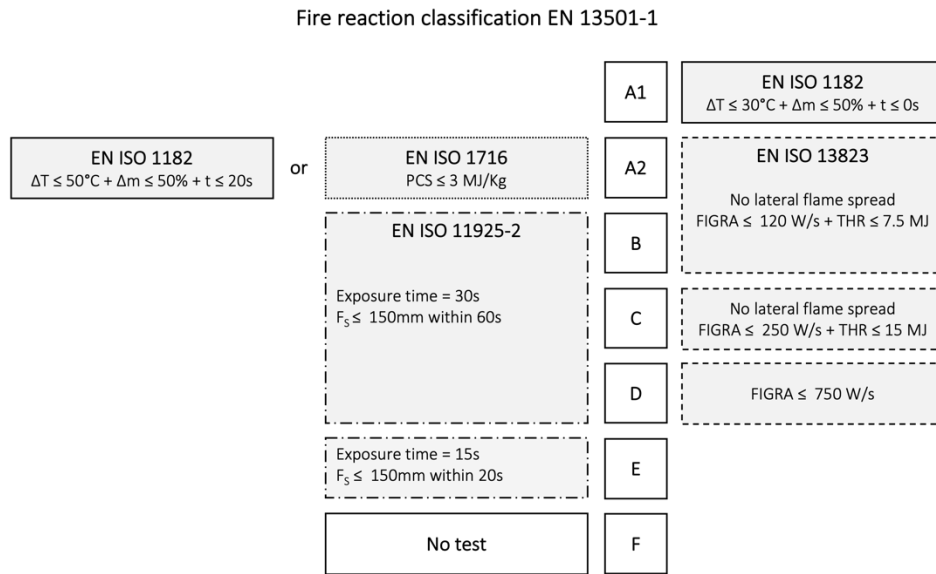
ΔT = temperature rise; Δm = mass loss; **FIGRA** = fire growth rate; **PCS** = gross calorific potential; **THR** = total heat release

Figure 5. Scheme of fire reaction classification according to EN 13501-1

It is important to mention the key differences between reaction to fire and resistance to fire. Reaction to fire is the measurement of how a material will contribute to the fire development and spread, particularly in the initial stages of a fire when evacuation is crucial. Fire resistance is the measurement of the ability of a building/construction element to maintain its load bearing capacity and to prevent the passage of fire from one distinct area/building compartment to another. The fire resistance rating of a building element is normally expressed in minutes of fire containments. It basically includes the load bearing capacity, integrity, and isolation. The design procedures are ruled at European level by the parts 1.2 of structural Eurocodes [33].

2.2.3 Energy requirements

Over the last few decades, the concerns about climate change have grown, particularly, when it comes to global warming due to the increasing of extreme weather events.

According to Intergovernmental Panel on Climate Change (IPCC) specialists, an intergovernmental panel created to provide policymakers with regular scientific assessments on climate change, its implications, and potential future risks, the greenhouse gases emissions (GHGs) have been the main booster of climate change process. Those concerns lead EU to aim climate neutrality by 2050 which means an economy with

net-zero greenhouse gas emissions. This objective is the core of the European Green Deal [34] and in the line with the EU commitment to global climate action under the Paris Agreement [35].

The EU Strategy for long-term greenhouse gases emission reduction [36] outlines a vision of the economic and societal transformations required, engaging all sectors of economy and society, emphasizing the ones which contribute the most for GHGs emissions.

Building stock is responsible for approximately 26% of all CO_2 emissions in European Union. By including the emissions from the building construction industry, this share increases to 38%. In terms of electricity consumptions, building operations represent nearly 55% of global electricity consumption [1]. Indeed, evaluating the final energy consumption in EU, 50% is used for heating and cooling, 80% of which is used in buildings [37]. The magnitude of the numbers underlines the importance of reducing the energy demand and carbon emissions in buildings by adopting retrofitting solutions in facades with an increased thermal performance. Energy Efficiency Plan 2011 [36] emphasised this need reinforcing that "The greatest energy saving potential lies in buildings".

At European level, the relevance of improving the thermal performance in the framework building's rehabilitation is significant, since the relatively low percentage of new construction (in which thermal efficient claddings are being applied) is not sufficient to achieve the proposed targets. This is accentuated because in the residential sector, the age of a building is likely to be strongly linked to the level of energy use in buildings, meanwhile, the ones that have not undergone renovation need to improve their energy performance. More than 40% of the buildings date back from 1960, 80% before 1990 [38], and it is predictable that the vast majority of them, 75%-90%, will remain occupied in 2050 [39].

As shown in Figure 6, in Portugal, in 2011, about 68% [40] of the existing buildings had been built before 1990, the year of the first legal code (RCCTE – *Regulamento das Características de Comportamento Térmico dos Edifícios* [41]) that imposed thermal requirements on new buildings. The main purpose of this regulation was to improve thermal comfort without increasing energy consumption. The first version of this regulation contributed to a widespread use of thermal insulation in construction. A new thermal regulation was published in December of 2013, DL no. 118/2013 [42], REH – *Regulamento dos Edifícios de Habitação* in which the requirements on thermal transmittance, U_{max}, have been reduced (i.e. the value required in vertical opaque walls is 1.75 W/(m^2.°C) compared with 1.80 W/(m^2.°C) on RCCTE).
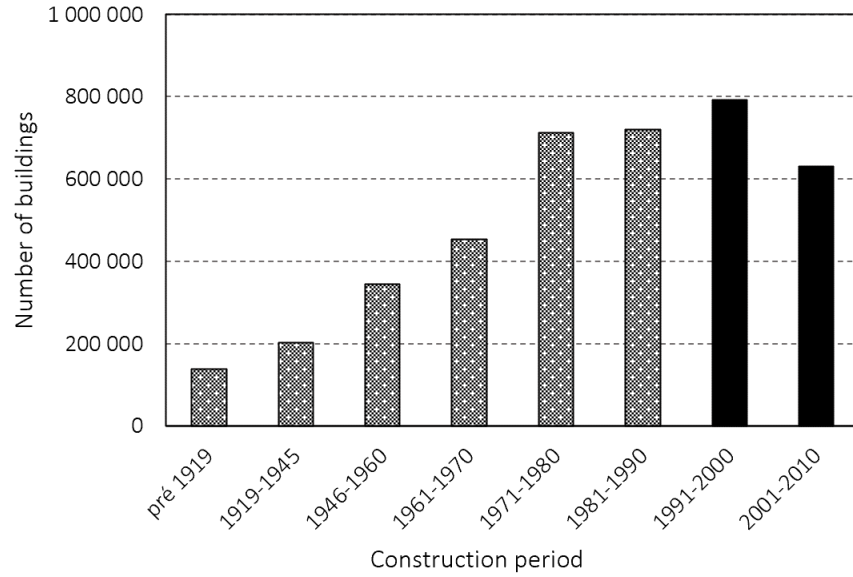
Figure 6. Number of existing buildings in 2011 per construction period in Portugal [40]

Also, in other European countries, such as in UK, there has been a substantial change in the requirement for thermal performance of external walls. Between 1965 and 2016 the claim on the thermal transmittance, the U value, increased more than 70% [43], as shown in Figure 7.
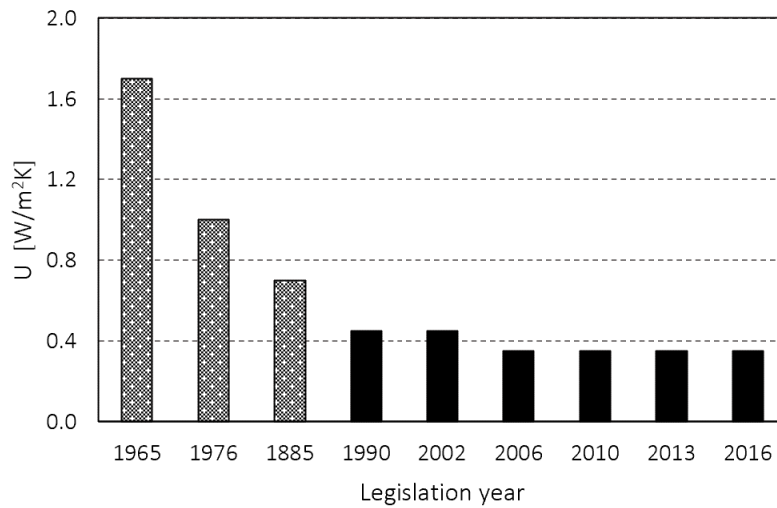
Figure 7. Progression of the regulated U-values for Buildings in UK [43]

2.3 Constructive solutions

2.3.1 Facade thermal insulation solutions

The need to change construction habits is unquestionable. New requirements and concerns are emerging to boost demand and research. This path has been traced over the last few decades. The decline in the use of conventional solutions and the option for innovative alternatives with improved performance is noticeable. Figure 8 highlights the increase in the application of ETICS versus the option for dry mortars.
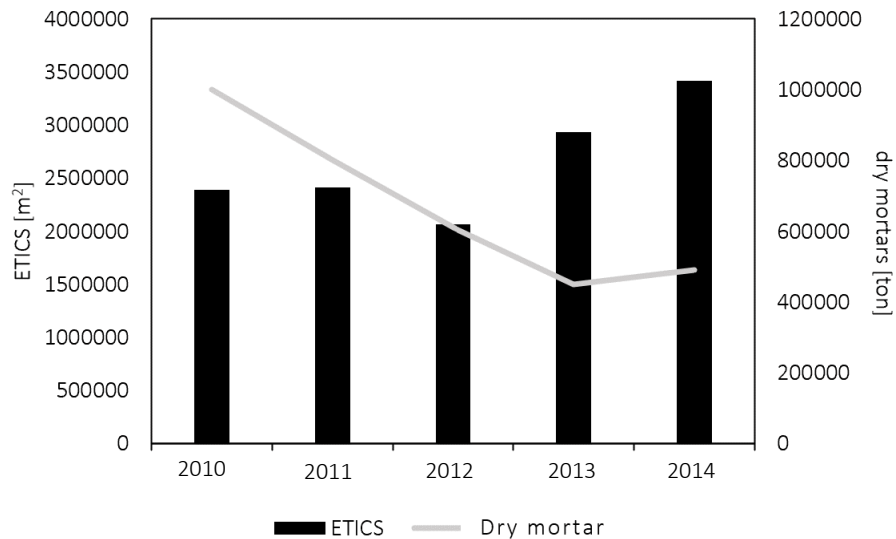
Figure 8. Evolution of the use of dry mortars and ETICS in Portugal. Adapted from APFAC [44]

Although other constructive wall solutions were used, such as double-leaf walls where expanded or extruded moulded polystyrene (EPS and XPS, respectively) boards are placed in the air cavity between them, their thermal efficiency is often compromised due to thermal bridges, and inefficient execution [45,46].

According to the literature, the most effective ways to save energy in buildings is through the use of thermal insulating materials on their envelope [47,48], as external walls and ceilings can be responsible for ≈ 80% of the total heat losses [49].

The increasing use of ETICS, which combines different layers of materials with thermal insulating properties, can be explained by their high commercial availability, but also by their low thermal conductivity (*e.g.*, ETICS with EPS show values of 0.032 W/(m.K) [50]). However, they present some drawbacks: lack of stability for increased thicknesses (needed to fulfil increasingly demanding legislation requirements); low fire reaction rating; difficulty in applying them on uneven surfaces; among others.

To improve some of those aspects, an significant effort has been made to develop innovative materials with improved thermal performance [51], especially with the aim of thermal conductivities lower than 0.020 W/(mK), compared to the 0.030–0.040 W/(m.K) of conventional materials (e.g mineral wool (MW) or glass wool), and compared to transition materials, such as polyurethane or propylene with a range of values between 0.020 and 0.030 W/(m.K). Lower thermal conductivities allow lower thicknesses to satisfy the same thermal requirements, which represents one of the main reasons why innovative materials are particularly appropriate for rehabilitation of buildings.

In terms of characteristics, conventional ETICS and systems incorporating thermal mortars are similar systems that are often used as external cladding of facades. As Figure 9 shows, both are multilayer systems, being the substantial difference between them the thermal insulation layer. While in conventional ETICS this layer is a plate of EPS, XPS, MW or expanded cork agglomerate (ICB) that can be glued or mechanically fixed to the wall, in the other one the insulation layer is made of a projected thermal mortar. A thermal mortar is a mortar in which the aggregates (sand) are replaced by lightweight materials (EPS, perlite, cork, aerogel). Both systems are made up, in sequence, of an insulation layer that is applied in the regularised facade wall; a glass-fibre mesh is typically applied between the base and the finishing coat.

The most significant handicap of conventional ETICS is the difficulty of application in buildings dated before 1945, due to incompatibility with the support. Thermal mortars have the advantage of being able to be applied in a wider range of subtracts, to have a high vapour permeability and can be applied by mechanical projection, increasing the efficiency of the process.

When analysing thermal plasters currently available on the market, they show relatively high average thermal conductivity, λ, and low water vapour permeability coefficients, μ ($\lambda \approx 0.050$ to 0.100 W/(mK), $\mu \approx 15$) [52]. Considering conventional thermal insulation products, such as EPS boards, they show low thermal conductivity coefficients but poor water vapour permeability ($\lambda \approx 0.032$-0.038 W/(mK), $\mu \approx 30$-70) [53].
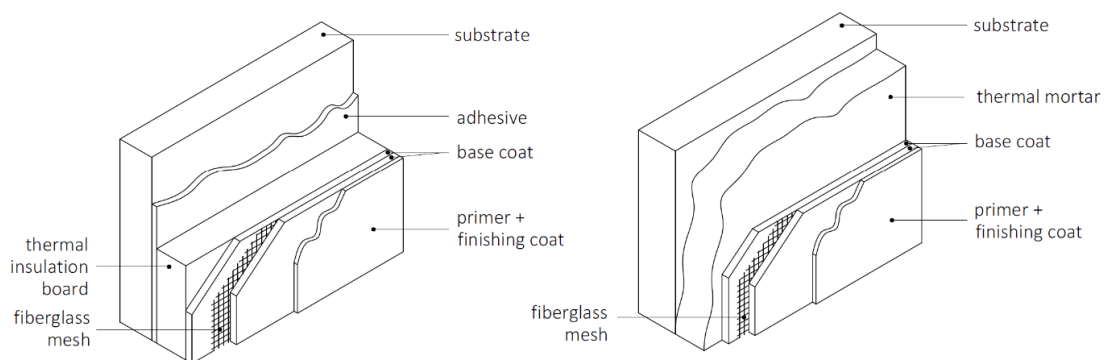
Figure 9. Multilayer insulation systems components: conventional ETICS (left), thermal mortar (right). Adapted from [53]

The most common insulating materials for application in ETICS are EPS, XPS, MW and ICB, with fire performance ratings of A1 or A2 for MW and E for the remaining materials, and similar thermal conductivities, according to the APFAC data presented in Table *1*, obtained through indicative values collected from various manufacturers.

Table 1. Characteristics of common insulation materials for application in ETICS [53]				
Property	**EPS**	**XPS**	**MW**	**ICB**
λ [W/(m.K)]	0.031 – 0.038	0.033 – 0.037	0.035 – 0.038	0.037 – 0.040
FR [class]	E	E	A1/ A2	E

λ = thermal conductivity; **FR =** fire reaction Euroclass

It is thus clear that, despite good thermal performance, most of these systems have poor fire behaviour. In addition, other disadvantages are worth referring, such as difficult application on uneven surfaces and lack of stability for high thicknesses. To mitigate these aspects, during the last years, several types of thermal mortars have been developed.

2.3.2 Thermal mortars

One of the ways to improve the thermal behaviour of buildings is to minimise thermal losses and gains through an opaque envelope. This can be achieved using thermal insulation materials, where thermal mortar presents itself as a possible solution.

Thermal mortars not only have the function of a conventional mortar (i.e finishing), but also improve the thermal resistance of building walls. In this sense, aggregates (sand) are normally replaced by lightweight aggregates (EPS, cork, perlite, aerogel).

EN 998-1 [54] identifies a set of requirements (Table *2*) to classify a mortar as a thermal one. The thermal performance of these mortars is, in general, lower than ETICS. In a study where the properties of various thermal mortars with EPS, expanded cork, clay and silica aggregates are compared, it is possible to conclude that this type of mortars presents, on average, a thermal conductivity of 0.083 W/(m.K), therefore, being clearly higher than that typically presented in the ETICS solutions [52].

Given the advantages of these coatings, such as, high vapour permeability, direct application on the substrate, mechanical projection, making it possible to use them on rough, irregular supports and on non-standard architectural details; there is an urgent need to study ways to improve their thermal performance.

Given this scenario, the incorporation of new materials with improved thermal properties is being studied. One of these materials is aerogel. However, one the most important obstacles to the industrial production of aerogel mortars is (still) its high cost [55,56].

Table 2. Summary of requirements and declared values according to EN 998 [54]

Test parameter	Method of test	Category	Range values
Dry bulk density	BS EN 1015-10	-	Declared
Compressive strength	BS EN 1015-11	CS I - CS IV	[(0.4 a 2.5) to (≥6)] MPa
Adhesion	BS EN 1015-12	-	-
Capillary water absorption	BS EN 1015-18	W1	$c \leq 0.4$ kg/m^2.min^{0,5}
Water vapor permeability coefficient	BS EN 1015-19	-	$\mu \leq 15$
Thermal conductivity	BS EN 174:2002	T1 or T2	(≤0.1 or ≤0.2) W/(m.K)
Reaction to fire	BS EN 13501-1	A1[*] to F	≤0.01[*]
Durability	-	-	Declared

[*] in case of organic material, otherwise it is necessary to perform an experiment

2.4 Aerogel and applications in the construction industry

2.4.1 Synthesis and properties

According the European Commission recommendation of 18 October 2011 (2011/696/EU) [57], a material composed by 50% or more of particles with external dimension between 1 nm and 100 nm can be classified as a nanomaterial .

Aerogel is a gel composed of a microporous solid in which the dispersed phase is a gas [58]. It is created by combining a polymer with a solvent to form a gel, then the liquid part of the gel is replaced by air. It was discovered by Kistler in 1931 - the date of his first article in Nature [59].

The structure of the aerogel is composed of small spherical agglomerates of silica (SiO_2 particles), generally with dimensions between 2 and 5 nm, which are linked together in a chain shape forming a porous spatial network in which the pores present an average dimension of 20 to 40 nm, varying between 1 and 100 nm. Thus, aerogels with different particle and pore sizes can be obtained, as well as different porosity values, which in general are around 75 to 98% [60–63].

Those characteristics lead silica aerogels to be materials with unusual properties such as: high specific surface area (500-1200m^2/g) [64], high porosity (80-99.8%) [65] and low thermal conductivity value (0.005 W/(m.K)) [66].

Aerogels entered the construction sector in the 1980s due to their high thermal performance [67,68]. Until that date aerogel had been used mostly in the aerospace industry, the chemical industry and for sports equipment.

Silica aerogel is the best known insulator by mass and volume and it transmits 100 times less heat than normal density glass [69]. It has a great potential to be incorporated in different construction materials (such as in thermal mortars), improving their thermal performance and, in the case of insulation layers, allowing for the use of lower thicknesses of material for the same thermal requirements.

2.4.2 High temperature behaviour

Silica aerogels not only act as high-performance thermal insulators but also have an inorganic structure, therefore, they are non-combustible.

Previous studies on aerogels have showed that at 200°C the viscosity of aggregated nanoparticles decreases enough so that there is relative movement between them to achieve structural relaxation. This translates into a shrinkage of the pores and a decrease in the volume of the material. As the temperature increases, the viscosity of the particles becomes sufficiently low so that there is an increased aggregation and densification of particles, which can alter the transparency and thermal conductivity of the material. Upon reaching the glass transition temperature (≈0-800°C) the extreme densification and particle aggregation drastically changes the nanostructure within hours [70].

A study on the microstructural evolution of silica aerogels with temperature [71] found that the pore volume increases slightly up to 300°C and then a rapid decrease is observed up to 1100°C, where the pore volume practically disappears. It was concluded that until 200°C occurs the evaporation of water and ethanol (possibly) that causes the pore volume to increase and the specific surface also to increase in 20%. The oxidation of organic residues is the cause of the 6% mass loss.

In view of this behaviour, there have been studies aiming to design aerogels capable of maintaining their mechanical and thermal properties at elevated temperatures.

Cai et al. [72] conducted the synthesis of silica aerogels with different particle sizes through mono-dispersed silica sol and studied their properties at room and elevated temperatures. They concluded that these silica aerogels were able to maintain a stable structure up to 900°C and a relatively complete structure up to 1000°C with about 35% volume shrinkage after 2h.

Ye et. al. [73] produced an aerogel through and cationic amylopectin and clay whose structure they dubbed "brick mortar bridges" with a temperature resistance of 1400°C.

In view of overcoming the brittleness and sintering behaviour of silica aerogel at elevated temperature, Ma et al. [74] produced an alumina modified silica aerogel. They obtained a specific surface area of 278 m^2/g, and a compressive strength of more than 2.17 MPa. By heating this innovative formulation and an ordinary silica aerogel to 1000°C they found that the performance of the former was far superior.

Regarding these studies, it is believed that the performance of aerogel under elevated temperatures depends on its composition and on the process of synthesis which was used to produce it. However, it is undeniable that being a non-combustible material, aerogel can be considered as an alternative to lightweight aggregates in thermal mortars, which highlights the importance of understanding the degradation of aerogel with temperature and its interactions with the different mortars' components.

2.4.3 Aerogel applications

Aerogel is already used as a component in various insulation solutions and building elements. There are two main types of materials, Opaque Silica Aerogel-Based Materials and Translucent Aerogel-Based Materials. The first refers to opaque sheets or mats and the latter to translucent materials [75]. In Table 3, some applications of silica-based aerogels are presented.

Table 3. Construction elements based on silica aerogels [75]	
Translucent	*Opaque*

Granular silica aerogel
    Solar collectors
    Translucent glasses
	Aerogel-based composite materials
	    concretes
	    renders/ plasters

Monolithic aerogel Windows	Vacuum insulation panels

	Fibre-reinforced silica aerogel
	    panels
	    blankets
	    wallpapers
	    plasterboards

Regarding elements with translucent or transparent characteristics, it was investigated how to develop super-insulating windows using granulated and monolithic aerogels [76,77]. Another investigation was on the performance of solar collectors. It was concluded that a solar collector with aerogel operating at a temperature 60° C higher than the air temperature, requires a solar radiation of 90 W/m^2, while a current collector, is only able to operate above 240 W/m^2 [69,78]. Vacuum insulation panels (VIPs) are a type of very thin insulation already extensively applied in insulating refrigerators, building cladding, and refrigerated warehouses. However, with increasing internal pressure, the performance of the insulation degrades,

resulting in a service life of 5 to 25 years. In an investigation where the preparation of VIPs with aerogel cores were studied, it was concluded that 1.8- 20% by volume in fibres with aerogel of density 50-143 Kg/m^3 are able to achieve a service life of over 50 years [79].

There are also preliminary studies where the use of cement and aerogel mortars is suggested as a strategy to protect the lining of high-performance concrete tunnels. However, more in-depth research is required to prove these promising findings [80].

2.4.4 Aerogel-based thermal renders

Mortars with silica aerogel have proven to be extremely insulating, therefore they can be particularly useful when walls are to be insulated without increasing excessively the thickness [81,82].

There is a study comparing the required insulation thickness of different materials (aerogel, EPS, XPS, PUR, PIR, cork, glass wool) to achieve a U of 0.3 W/(m^2.K), as well as the embodied energy (where the whole life cycle is accounted for) in each of them. It was concluded that aerogel was the material that required the lowest thickness and, evaluating embodied energy, contained only 10% more than glass wool, which was the material with lower embodied energy [51].

Aerogel thermal renders are made of lime or cement as binders and use silica aerogel as (lightweight) aggregate. Aerogel contributes to a low-density mass, an increase in thermal and acoustic insulation, and, potentially, to an improved fire resistance. Owing to the hydrophobic nature of aerogel, the renders incorporating this material have the advantage of being water repellent, which avoids water absorption, while they are water vapour permeable and more breathable than conventional renders, which prevents surface wetness [56]. The incorporation of silica aerogels into coating materials has only been recently investigated, with the first publication on the subject appearing in 2012 [81]. Stahl et al. [81] presented a cementitious mineral hydrophobic mortar with high thermal performance (0.025 W/(m.K)) and a density mass of 200 kg/m^3, with the incorporation of aerogel in 60 to 90% of the total volume, and some additions to improve workability, which were not identified. However, the study did not refer to the mechanical performance, water behaviour or other fundamental properties that allow a complete evaluation of the mortars under study. Indeed, there are already a few aerogel mortars on the market. The first one has the commercial name of "FIXIT222", with an announced thermal conductivity, λ, of 0.0261 W/(m.K) and a fire reaction class A2 [83], which has boosted several studies with it [84,85].

Following the studies of Buratti et al. [86] it was developed another commercial silica aerogel-based mortar named "Tilica Pasta" which is obtained by manually mixing slaked natural hydrated lime with granular silica aerogel. This combination led to a product's high porosity (>90%) and favourable thermal behaviour and

breathability. The presence of hydrated lime as a binder makes it not being putrescible and antibacterial. The product data sheet declares a thermal conductivity, λ, of 0.00175 W/(m.K) and a fire reaction class A1 [87].Table 4 shows some mortars containing aerogel available on the market, as well as some existing formulations in the bibliography. Due to the potential of using aerogel-based renders in historic buildings, these products are being studied particularly in the field of cultural heritage. The recent Italian state incentive ("facade bonus", 2020), which supports the improvement of renovations of existing building envelopes in Italy by allowing the deduction of 90% of the facades' refurbishment costs, makes aerogel-based renderings a topical issue [88]. These kinds of initiatives promote the development of research activities on aerogel-based thermal renders in order to optimize their overall performance and costs.

In fact, the studies of these materials are complex since they consist in a mixture of many components. Apart from binders and aggregates, these mortars include some additives to be able to give the final material some specific and mandatory characteristics such as workability, adhesiveness, avoid segregation and allow the bond with water since aerogel is a hydrophobic material. The type of additives used (sometimes polymeric ones) and the percentage of them can affect the way the final material will perform.

Table 4. Mortars containing aerogel

Product	Main components	Aerogel [%(vol.)]	ρ [Kg/m³]	Th. [mm]	λ [W/(m.K)]	Reference
Aerogel render	• Mineral and cement binder • Silica aerogel	60-90	≈200	12-13	0,025	[81]
FIXIT 222 RÖFIX	• Hydraulic lime • White cement • Silica aerogel granules • Mineral aggregates	>50	220 (dry)	Min 30	0,028	[83]
Hydraulic mortar by *Chiraema* + 25% aerogel	• NHL 3.5 • Silica aerogel granules	25	735,6	-	0,1151	[89]
Hydraulic mortar by *Chiraema* + 70% aerogel	• NHL 3.5 • Silica aerogel granules	70	260,7	-	0,0311	[89]
Aerogel render	• NHL 3.5 • Silica aerogel	80-90	300-275	-	0,050-0,045	[86]
Aerogel render	• NHL 3.5 • Silica aerogel	96-99	125-115	-	0,016-0,014	[86]
Tilica pasta	• NHL 3.5 • Silica aerogel	-	700 (wet) 170 (dry)	≤5,8	0,0018	[87]

ρ = density; Th. = thickness; λ = thermal conductivity

2.5 Studies on fire behaviour of external cladding systems

The increased number of fire incidents associated with combustible cladding materials have raised awareness and concerns regarding non-compliant materials. As response to this new challenge, the Australian Government, in 2020, commissioned an ongoing Senate inquiry that has identified non-conforming materials that do not meet the fire safety regulatory standards major fire risks [90] and worldwide some measures have been taken. However, it is still noticeable an overall the lack of understanding and, therefore, additional research is needed. To better understand the phenomena, many studies on fire behaviour of exterior cladding systems have been carried out, as described in the next paragraphs.

The fire safety of high-rise buildings represents a major vulnerability. To analyse and investigate the phenomena, there was a case study done in "Torre Regione Piemonte", that is one of the highest offices buildings in Italy with 45 floors and 183.61m of height, in which was concluded that prescriptive fire codes could not be sufficient to ensure a proper fire safety level [91].

Peng et al. [92] discussed 3 high-rise buildings fire cases (TVCC, Beijing, 2009. Residential building fire, Shangai, 2010. Wanxin complex, Shenyang, 2011) involving rapid exterior wall fire spread by analysing the fire causes, propagation mechanisms and problems. They found that the use of combustible insulation in exterior wall claddings would potentially cause rapid fire spread and severe damage and loss. It was also showed that the combustibility of the insulation used in exterior wall claddings played a significant role on the fire spread via exterior walls.

In ventilated facades, there are two main factors influencing flammability: the cladding and the air cavity. The air cavity has a major influence on fire performance and enhances flame spread comparing to a simple vertical surface. The three most significant factors justifying this event are: radiation being enhanced by the cavity, increased upward spread from the chimney effect and a decrease in the amount of connective cooling from external air. The combination of these effects causes the extension of flamed heights in the cavity [93] and facilitates the ignition of the combustible material inside the cavity [94].

Comparing the performance of different systems of facades, in a research based on KRESNIK database containing 252 commercial facade tests, it was found that ETICS facade perform better than the ventilated ones [4].

Some investigations using large scale test, since they better simulate a real situation, were also carried out. One of those studies presented in literature [95] describes the experimental setup, procedure, and results

of 5 large scale fire tests which were carried out on a flat facade with ETICS based on EPS, concerning fire loads at the ground in front of the facade. The 5 tests differed on fire load, heat release rate, number of fire barriers and the existence of openings in the wall. By the comparison between the performance of each setup test it was found out that a fire barrier in each story can lead to a significant increase in fire safety of ETICS with EPS. Apart from that, the fire tests showed that the fire load at the base of the facade has a crucial effect on the fire behaviour of the facade.

Zhou et al. [96] found that in a large fire (2 m high facade panel already burnt), even the thickest fire barriers tested (mineral wool extending horizontally across the width of the facade and over 40 cm high), could not prevent the spread of flames. The destruction of the exterior render allows drops of thermoplastic insulation to burn, and they can ignite further down the facade.

In the above-mentioned context, there is no doubt about the insecurity of ETICS with EPS insulation layer, therefore, it is mandatory to search and investigate other alternatives. Indeed, it is crucial to understand how the whole facade system will perform in case of a fire. However, there are some gaps in knowledge blocking the understanding of facade fires. Firstly, there are numerous design decisions to fulfil its objectives within a building, and secondly, there is no theory, model, or comprehensive data series that can reliably explain or predict facade's performance under fire.

Despite large-scale fire testing remains the more reliable route, they are time consuming, expensive, and the results cannot be extrapolated to assorted designs. In the context, it has emerged the need to develop a methodology to evaluate facade flammability and to evaluate how the materials properties change during fire exposure.

2.6 Concluding remarks and research needs

In this chapter, the importance of thermal insulation of the opaque envelope in the thermal balance of a building was presented, as well as some advantages and disadvantages about the use of thermal mortars compared to other current insulation materials/systems.

However, most of the commercially available thermal mortars still have the disadvantage of having a higher thermal conductivity than current insulation systems (e.g. ETICS), therefore, significant efforts have been made on the development of innovative thermal mortars with improved thermal performance. Within this context, new materials, including silica aerogel have begun to be studied in the last decade. Silica aerogel, being a nanostructured material with high total porosity and reduced pore size (mesoporous structure),

presents unique thermal insulation characteristics, with thermal conductivity values between 0.012 and 0.021 W/(m.K), and, given its inorganic nature, with a potentially good performance under fire exposure.

The characteristics of aerogels allows a range of applications that are worth of exploring, with thermal insulation being the most relevant in the construction industry. In fact, several ways have been investigated to take advantage of the characteristics of silica aerogel to benefit the thermal comfort of buildings and reduce energy consumption.

Studies addressing the incorporation of silica aerogels in mortars or cement-based materials has been recently developed; as a results of these recent research, aerogel-based thermal mortars are now commercially available in some EU countries and are suitable to be applied in a multilayer cladding system. However, most of the existing publications have only analysed the thermal component of mortars with silica aerogels, not exploring other important properties of the thermal mortar, such as mechanical strength, fire performance, and high temperature behaviour.

The potential of innovative thermal mortars lies not only on its thermal properties but also on its high temperature and fire behaviour. Indeed, the concerns about fire risk on buildings have increased over the last few years driven by the increased number of fire incidents on buildings facades. These cladding systems contain combustible materials, used as thermal insulators, which are considered to be the main responsibles for fire spread. So, the importance on finding alternatives for the conventional thermal insulation layers is unquestionable. Investigations on how thermal mortars behave during and after fire exposure are, therefore, needed, as well as the development of appropriate experimental methodologies for its assessment. In the next chapter the experimental research methodology is presented.

3 Research methodology

3.1 Objectives and overview of the experimental programme

The application of mortars with improved thermal performance in multilayer systems for exterior thermal insulation is becoming increasingly common. They can contribute to overcome (or in some cases aggravate) some of the disadvantages identified in these systems over the last few years. The most harmful disadvantage is related to the fact that the insulation layer is the main engine for fire spread in building facades, as discussed on the previous chapter. Therefore, the present experimental study focused exclusively on the characterization of this layer (i.e. the thermal mortars that are part of multilayer systems).

The objective of this study was to compare a conventional thermal mortar with EPS granules with an aerogel-base one, namely in terms of their performance under exposure to elevated temperatures and fire; as well as their post-fire (i.e. residual) behaviour; a traditional lime-based mortar was used as reference since it is a mortar widely used in the market and has the most favourable fire reaction, class A1.

The goal was not only to characterize the thermophysical properties of the mortars at different elevated temperatures, but also to understand the degradation of the materials after exposure to high temperatures, namely, in terms of residual mechanical resistance and changes in their microstructure.

The EPS-based mortar is representative of a common thermal mortar widely used in interventions in buildings' facades (new construction or thermal retrofitting), whose properties are also known. The potential interest of the research is focused on the mortar containing a nanomaterial as aggregate, the silica aerogel.

The work developed, summarized in Table 5, can be divided in two main categories: an experimental campaign and a numerical analysis (better explained in chapter 5). Altogether, were carried out 13 different types of testes within a total of 89 practical experiments. The range on experiments is one of the strengths of this work, from the analysis of material's performance in terms of reaction to fire, until microscopic chemical analyses.

Table 5. Summary of dissertation main work

			28 days	Nº of tests	Post heating	Nº of tests	Total nº of tests
Experimental Campaign	(i) Characterization tests	Mechanical	Compression strength	✓	3x3	✓	2x3	15
			Flexural strength	✓	3x3	-	-	9
		Thermophysical	Thermal conductivity	✓	2x3	✓	1x3	9
			Specific heat	✓	2x3	✓	1x3	9
			TGA	-	1x3	-	1x3	6
	(ii) Microstructural Analyses	XRD		✓	1x2	✓	1x2	4
		Micro CT		✓	1x2	✓	1x2	4
		SEM		✓	1x2	✓	1x2	4
	(iii) Fire Reaction tests	Ignitability			-		3x1	6
		Gross Calorific Potential			-		3x1	3
		Cone calorimeter			-		4x2	8
		Bomb calorimeter			-		3x1	3
	(iv) Fire exposure tests			1x3				3
								89

Numerical analyses	Calibration of thermal conductivity and specific heat at high temperatures using data (iv)

Legend	✓	done	-	not applicable	NxM	M type of mortars tested N times each

The experimental campaign began with specimens' preparation in which different shapes and sizes were moulded according with the tests' requirements. The wide variety of experiments led to specimens with multiple sizes: from a few milligrams (for TGA), until specimens with 1600 cm^3 (for fire exposure tests) which is important to have the perception of the different scales of analysis. The experimental programme included the following main types of experiments: (i) material characterization tests to evaluate the flexural and compressive strengths, and thermophysical ones to measure thermal conductivity and specific heat. These tests were performed on reference specimens (i.e. without thermal damage) and on specimens after being subjected to a significant thermal damage (exposure up to 400 °C), to understand how these

properties were affected by temperature. Within thermophysical testing, thermogravimetric analysis (TGA) was also carried out. (ii) Microstructural analyses: XRD, Micro CT, and SEM were useful to assess the performance and response of materials to heating. (iii) Fire reaction tests were also performed, giving values used by EU norms, therefore, essential to compare with commercial products and to understand how the materials contribute to fire development. Finally, (iv) fire exposure tests, in which specimens of the three thermal mortars were subjected to standard fire curve ISO-834 [19]. During the experiments, the temperature across the thickness was measured. These data were then used in an inverse numerical procedure in which thermal conductivity and specific heat at high temperatures were calibrated based on experimental thermal distributions.

The production of specimens was carried out at the Construction Laboratory of DECivil – IST (LC), as well as the mechanical tests, thermophysical, while the fire exposure ones took place at Engineering and Strength of Materials Laboratory at DECivil – IST (LERM). The normalized experiments of fire reaction, the ignitability test and gross calorific potential test were performed at ITECONS, while the remaining fire reaction tests were made at DTU facilities. The X-Ray diffraction (XRD) and Micro CT took place at Laboratory of Mineralogy and Petrology of DECivil – IST (LAMPIST). The TGA was carried out at a Chemistry Lab of DEQ – IST.

3.2 Organization of experimental campaign

In Figure 10 is presented an overview of experimental' campaign organization. The experimental campaign started with the production of different shaped samples according to the tests that were predicted. After the 28 curing days, the characterization tests, thermophysical and mechanical were carried out, as well as the preliminary microstructural analyses.

According to the thermograms obtained in TGA, peak temperatures were found (temperatures in which the mass loss was most significant). Then, a few samples were heated up until those temperatures in a muffle and then cooled down at room environment. Finally, that samples were mechanically tested, the thermophysical properties (thermal conductivity and specific heat) were measured, and their microstructure was analysed with different techniques.

To evaluate the fire behaviour performance, fire reaction and fire exposure tests (whose results were used to calibrate thermophysical properties at high temperatures) were also carried out.

28 days curing + heating at
and cooled down

definition of **peak temperatures**

TGA

Thermophysical tests

Thermophysical prop.

Mechanical tests

Microstructural
analyses

Samples
production

28 days curing

Fire reaction

Fire exposure

Thermophysical prop.

Mechanical tests

Microstructural
analyses

described on chapter 5

Numerical analyses

Iterative process
matlab routine

Figure 10. Flowchart explaining the experimental campaign

3.3 Materials

3.3.1 Material characterization

The experimental campaign focused on the following 3 pre-dosed mortars: i) a conventional coating mortar based on natural hydraulic lime (Lime.m); and 2 thermal mortars, ii) one with EPS (EPS.m) aggregates and iii) the second one with silica aerogel granules (Aero.m). Table 6 summarizes the main properties of the mortars; for Lime.m and EPS.m the values were provided by the manufacturer, while the ones from the Aero.m were collected from a PhD thesis [97] that focused on the effect of adding fibbers to an aerogel-based mortar developed at PEP project *(P2020 POCI-01-0247-FEDER-017417)* . The comparison is made, therefore, between two commercial mortars and a non-commercial one which was developed in the framework of the above-mentioned project.

The thermal mortars, with lower density (consequence of the incorporation of lightweight aggregates) and with better thermal properties (lower thermal conductibility) than that of the reference one (Lime.m), are also formulated with polymeric additives to ensure better workability. On the other hand, these additives may affect the thermal performance of mortars when exposed to elevated temperatures (cf. chapter 2.3.2).

The aerogel-based thermal render is composed of a blend of mineral binders (Portland cement and calcium aluminate cement), rheological agents, resins, hydrophobic agents, among others, while also containing, as lightweight aggregate and thermal insulation material, a commercial supercritical hydrophobic silica aerogel available in granules (particle size ≤ 3500 μm, apparent density ≤ 90 kg/m^3, particle compressive strength ≤ 0.80 MPa, and a thermal conductivity ≤ 0.020 W/(mK)) [98]. The mineral binders represented a total of 20 % (m/m), and silica aerogel hydrophobic granules a total of ≈ 37% (m/m), with the remaining quantities allocated to the other components [99].

ID	ρ kg/m^3	$\lambda_{10°C, dry}$ W/(m.K)	μ	σ_T N/mm^2	σ_C N/mm^2	FR	Reference
Lime.m	1500 - 1600	0.82	≤ 15	≤ 1.5	≤ 3.5	A1	[100]
EPS.m	150 ± 5	0.042	≤ 5	≥ 0.25	CSI (0.4 - 2.5)	B	[101]
Aero.m	160 ± 3	0.0293	7.8 ± 0.1	0.099 ± 0.004	0.227 ± 0.002	-	[99]

Table 6. Properties of the mortars in study

ρ = dry bulk density; $\lambda_{10°C, dry}$ = thermal conductivity at 10°C and dry state; σ_T = flexural strength; σ_C=compression strength; FR = fire reaction class

3.3.2 Production of specimens

The production of the industrial renders, Lime.m and EPS.m followed the recommendation of EN 1015-2 [102] and those provided by the manufacturer, namely regarding the amounts of water that should be added to the powder product. The water/ powder ratios were: 160 ml/kg for Lime.m and 1300 ml/kg for EPS.m.

For Aero.m production there are a few details which must be taken in consideration. Before weighting the water and the powder with the ratio of 1270 ml/kg, it was essential to mix the powder in a polyethylene bag to guarantee homogeneity. Then, the water was added to the mixing recipient and then the render in powder state. All the components were then well mixed manually until they began to show visual and tactile signs of proper mixing. Finally, the mixture was put into a mechanical mortar mixture, in slow rotation for 2 minutes. After mixing, the render was placed in several molds according to the test procedure which were planned.

For all the mortars produced, the curing followed the procedure indicated in EN 1015-11 [103], which consists in placing the samples in a chamber with a temperature of 20 ± 2 °C and a relative humidity of 65% ± 5% for 28 days, where during the first 7 days the samples remained inside a polyethylene bag; at 12 days they were demoulded. After this curing period, the mortars were tested in their hardened state at 28 days.

The type and dimension of the specimens produced, as well as the correspondent tests, are presented in Table 7.

Table 7. Type and dimensions of specimens produced for each test

ID	Type	Mortar(s)	Dimensions [mm]	Test
A	Normalised prismatic	Lime.m + EPS.m + Aero.m	160 x 40 x 40	Mechanical tests
B	Prismatic	Lime.m + EPS.m + Aero.m	40 x 40 x 40	Mechanical tests
C	Cylinder	Aero.m	ϕ = 40, h = 100	Thermal cond. + Cp
D	Cylinder	Lime.m + EPS.m	ϕ = 60, h = 20	Thermal cond. + Cp
E	Prismatic	Lime.m + EPS.m + Aero.m	200 x 200 x 40	Fire exposure
F	Prismatic	Aero.m	250 x 90 x 40	Ignitability
G	Prismatic	Lime.m + EPS.m + Aero.m	100 x 100 x 30	Cone calorimeter

3.4 Experimental methods

3.4.1 Mechanical tests

The mechanical performance of materials at the hardened state was evaluated to by means of compressive and flexural tests. Considering the requirements of the EN 998-1 [54], the minimum value of compressive strength is associated to class CS I, which is 0.40 MPa, while for flexural strength no requirements are defined.

The maximum compressive and flexural stresses were measured with a *Form+Test* (*model 505/200/10/DM1*) equipment as presented in Figure 11, with a load cell of 200kN for the compression test (testing speed of 5 mm/min) and 10kN for the flexural test (testing speed of 10 mm/min), using square prisms of 160x40x40 mm^3 and following the EN 1015-11 standard [103].

The specimens used for the flexural tests, after resulting in two halves, were used for carrying out the compressive tests.

To calculate the flexural strength, Equation (1) was used, while for the compressive strength, it was followed the formula presented in Equation (*2*).

$$\sigma_T = M/w = \frac{3F_T L}{2bh^2}$$ (1)

where σ_T : Flexural strength   [MPa]

               F_T : Applied load   [N]

               L : Distance between supports   [mm]

               b : Specimen's width   [mm]

               h : Specimen's height   [mm]

$$\sigma_c = F_C/A_c$$ (2)

where σ_c : Compressive strength   [MPa]

               F_c : Applied load   [N]

               A_c : Specimen's area   [mm^2]
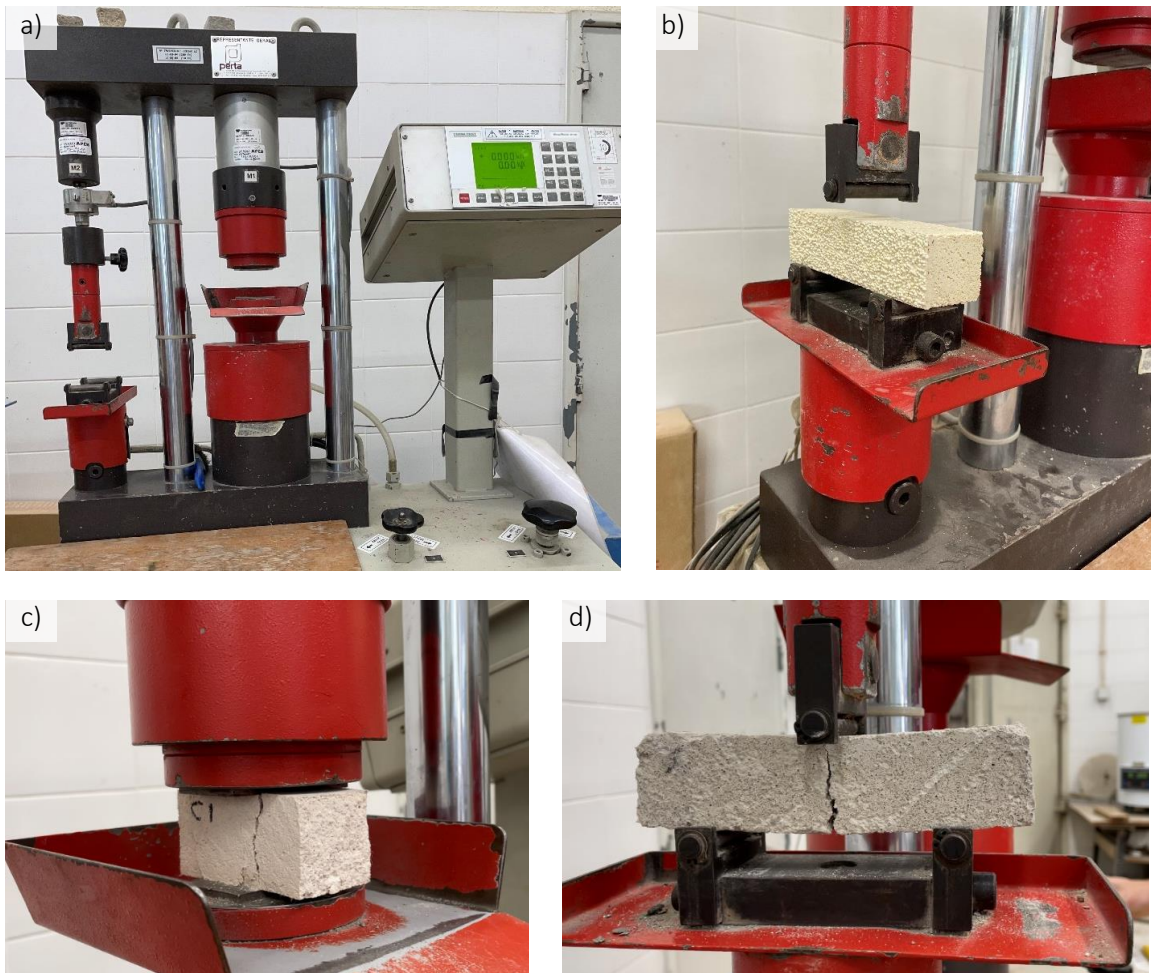
Figure 11. a) Equipment used in mechanical tests; b) Flexural strength test in progress (EPS.m); c) Compressive strength test in progress (Lime.m); d) Flexural strength test in progress (Aero.m)

These procedures were followed at i) room temperature, after 28 days of curing, for both flexural and compressive strength and using the normalised prismatic specimens (specified in Table 7, ID-A) and ii) after the specimens had been heated up to 400°C to measure the residual compressive strength using the normalised prismatic specimens (specified in Table 7, ID-B). The residual flexural strength was not measured since the magnitude of this value was expected to be extremely low.

The heating process was set up in a muffle furnace at LAMPIST, as shown in Figure 12, from room temperature until 410 °C at rate of 10°C/min. To measure the temperature inside the material during heating, dummy specimens were instrumented with a thermocouple in their geometrical centre. The specimens were introduced inside the muffle until had passed 5 min since the interior of the material reached 400°C. Then, the equipment was turned off and the specimens were cooled down up to room temperature. Not only due to the limited dimensions of the equipment, but also due the expected different heating times of thermal mortars (EPS.m and Aero.m) when compared to the reference one (Lime.m), the specimens were heated separately.

Figure 12. Test setup: a) general view; Specimens' placement post heating b) Lime.m and c) EPS.m and Aero.m

3.4.2 Thermophysical tests

i) Thermal conductivity and specific heat

The evaluation of the thermal conductivity and specific heat was carried out, after the 28-day curing period, through a transient method with the ISOMET 2114 equipment [104], which follows the ASTM D5930-9 standard test [21]. The equipment directly provides the value of thermal conductivity, λ, as well as the volumetric heat capacity, cp. The specific heat, Cp, is calculated by dividing the volumetric heat capacity by the bulk density, ρ. The bulk density was determined according to EN ISO 1015-10 [105].

The principle of measurement is based on analysis of the sample's temperature response to heat flow impulses. Heat flow is imposed by electrical heating a resistor heater inserted into the probe, which is in direct heat contact with the tested specimen. The evaluation of thermal conductivity is based on periodically temperature records as function of time.

In order to obtain the best measurement accuracy on specific materials, two general probe types were used: needle probes and surface probes. According to equipment's' manual, needle probes are recommended to be used in materials with low thermal conductivity. The expected minimal material thickness surrounding the needle is 40 mm and a minimum depth of insertion 80 mm. In case of the surface probe, it is recommended to have a flat surface of 60 mm diameter and a minimum thickness of 20 mm.

To analyse the aerogel-based mortar, cylindrical specimens with 40 mm diameter and 100 mm of height were made (specified in Table 7, ID-C), and it was used the needle probe exhibiting a measurement range between 0.015 and 0.050 W/(m.K), with an accuracy of 5 % of the reading value + 0.001 W/(m.K) and reproducibility of 3 % + 0.001 W/(m.K). For EPS.m and for Lime.m samples with 60 mm diameter and 20 mm of thickness were produced (specified in Table 7, ID-D), and it was used the surface probe exhibiting a measurement range between 0.04 and 6 W/(m.K) with an accuracy of 10 % of the reading value and reproducibility of 3 % + 0.001 W/(m.K) [104].

The procedure took place at i) room temperature, after 28 days of curing and ii) after the specimens had been heated up to 400°C to measure the residual thermal conductivity. The heating process was the same as the one described in chapter 3.4.1.

ii) TGA

The mortar samples were analyzed using a *Netzsch STA 409 PC* thermobalance, under air flow (oxidizing atmosphere), and at a heating rate of 25°C/min. The samples, 60-100 mg (fragments), were heated from room temperature to 1100°C using alumina crucibles. The heating rate was optimized to make the different

thermal decomposition processes clear and with as lower overlap as possible. For each thermogram acquired the thermal decomposition rate (DTG), which is the derivate of the initial thermogram, was calculated using the Proteus software of the equipment.

3.4.3 Microstructural techniques

The microstructural tests were only carried out on thermal mortars, EPS.m and Aero.m. The techniques used were X-Ray diffraction (XRD) and Micro computed tomography (Micro CT), both at room temperature and after the specimens had been heated up to 300°C[1] in a muffle at LAMPIST and cooled down. These procedures were used to analyse the changes on microstructure due to high temperature exposure.

i) X- Ray diffraction (XRD)

The X-ray diffraction (XRD) test allows the qualitative identification of the crystalline compounds in the sample and evaluates the presence of amorphous phases.

The technique consists in subjecting the material sample to X-rays which are used because they have a similar wavelength to the spacing between atoms in the sample, so that the diffraction angle is similarly affected by the spacing between atoms in the material. As the beams pass through the sample, they change direction and are reflected at different angles [106].

This phenomenon gives rise to diffraction based on Bragg's law, thus obtaining a diffractogram of the sample with the representation of the intensity of the diffracted radiation as a function of the diffraction angle or the characteristic interplanar distance [107].

A diffractogram contains several peaks that are characterized by their position, intensity and shape. Each phase/substance has a characteristic X-ray diffractogram.

Phase identification is performed by comparing the diffractogram of an unknown sample with diffractograms from a reference database (PDF4 ®).

An X-ray diffractometer (*X'Pert PRO* from *Panalytical*) was used for this test, with a copper ampule (K-Alpha 1.541). The current intensity used was 35 mA, with a voltage of 40 kV. Scans were performed from 5° to 70° of 2θ, with a step of 0.033° and t=75 seconds per step.

---

[1] This temperature was set to take advantage of the fact some preliminary specimens had been heated up to 300 °C (before the target value of 400 °C had been decided based on the TGA results).

ii)   Micro computed tomography (Micro CT)

Micro computed tomography is a 3D, high-resolution X-ray imaging. The obtained radiographs are strongly dependent on the composition and microstructure of the studied objects. With this methodology there´s no need of destructive sectioning, critical for sensitive samples.

The technique consists of getting hundreds of radiographs (2D images) while sample is rotating throughout the 180/360° interval.

The series of X-ray projection images is then computed into cross-sectional images (slices) through the computational process called "reconstruction" [108] using NRecon® Program. The overall set of images can be seen as a 3D object in the visualization program (CTVox®).

The acquisition was made with the SKYSCAN 1144 (Brucker) scanner, with 59 kV Source Voltage and 167 µA Source Current. The Image Pixel Size is 5.07 µm, and the rotation step is 0.3°, using 5 frame averaging and a 180° scan.

iii)   Scanning electron microscope (SEM)

The scanning electron microscope provides high-resolution images since it uses a beam of accelerated electrons, which have short wavelengths, as the source of illumination.

When the electron beam interacts with the sample, it loses energy through a variety of mechanisms. The lost energy is converted into alternative forms, such as heat, emission of low-energy secondary electrons and high-energy backscattered electrons, light emission, or X-ray emissions. These provide signals that carry information about the properties of the sample surface. The image displayed maps the varying intensity of any of these signals in the image to a position corresponding to the position of the beam on the sample when the signal was generated [111].

Scanning electron microscopy (SEM) analysis was carried out using both a SEM Hitachi S-2400, working at an acceleration voltage of 20kV and coupled with an Oxford Inca X-Sight energy dispersive X-ray spectrometer, and a SEM Thermoscientific Phenom ProX G6, working at an acceleration voltage of 15 or 20 kV. Samples were previously sputtered with a Pt-Au coating.

3.4.4 Fire reaction tests

i) Ignitability test

The ignitability test can be considered as a small-scale reaction-to-fire test; its main objective is to determine the ignitability of a material by exposing a sample positioned vertically to a small flame inside a combustion chamber -a detailed description is provided in ISO 11925-2 [28] .

The evaluation of ignitability is established by measuring the flame propagation distance and total duration of the test. The ignition of the filter paper positioned under the sample due to falling drops and ignited particles is also observed.

The sample to be tested shall be 250 mm x 90 mm and a maximum thickness of 60 mm (specified in Table 7, ID-F).

The test takes place in a combustion chamber and the method involves two conditions of exposure to the applied flame - surface exposure and edge exposure - the application of which depends on the type of dimensional characteristics and internal constitution in the material under study.

In the surface exposure condition, the flame is exposed at 45°, centered on the vertical axis of the specimen at a position of 40mm measured from the lower edge. In the edge exposure condition, the flame is applied directly to the lower edge of the sample at positions defined depending on the number of constituent layers and thickness [112].

The duration of the test depends on the time of imposition of the flame, which will be 15s or 30s depending on the reaction to fire class that is intended to be assigned. For a 15s imposition, the total test time corresponds to 20s, relative to a 30s imposition, the total test time will be 60s.

During this time, it is intended to determine whether the distance of 150 mm is reached (the flame spread (F_S) in mm is measured), as well as to assess the combustion of the filter paper placed inside the chamber.

The specimens were made at LC in IST and sent to ITECONS where the test took place.

ii) Gross calorific potential test

To determine the calorific value according to EN ISO 1716 [31], the sample is subjected to complete combustion in a constant volume containing oxygen under pressure with high purity. The occurrence of combustion is indicated by a temperature rise, which allows the determination of the calorific value.

This quantity is intended to characterise the amount of heat released by the material per unit mass (PCS – gross calorific potential), in MJ/kg, when subjected to complete combustion.

A sample of material reduced to powder and of known mass is mixed with the same quantity of paraffin and introduced into the calorimetric pump where the test is carried out.

The value obtained is then converted into MJ/m^2 according to the mass and thickness of the material.

The specimens were made at LC in IST and sent to ITECONS where the test took place.

iii) Cone calorimeter

The cone calorimeter uses radiant heat to ignite the samples (Figure 13a). To avoid ignition of the edges of the specimen, the sample is enclosed in a steel frame (Figure 13c), that ensures ignition of the surface.

This equipment is used to calculate the time to ignition of a material. The specimens used are 10 cm x 10 cm in cross section and 3 cm in thickness (specified in Table 7, ID-G).

The material sample is measured and weighed before it is placed in the steel frame; then the samples is placed 25mm below the cone and the test is ready to begin. The cover of the heating element is opened, and the piloted spark ignition is activated. From opening the cover, a timer is started to measure the point where the sample ignites.

The test is performed (Figure 13b)) with different heat fluxes until the critical flux is found, i.e. the minimum heat flux to ignite the surface.

The specimens were made at LC in IST and the test took place at a Fire Lab in DTU.
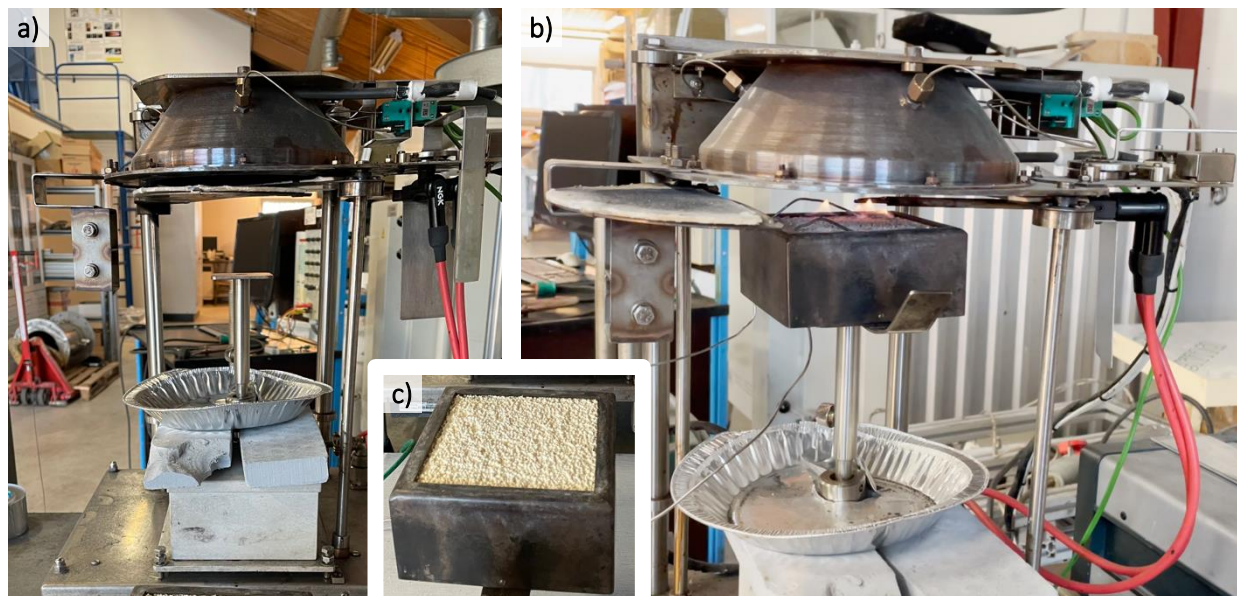
Figure 13. Cone calorimeter test: a) equipment, b) ongoing test, c) specimen inside steel frame

iv)   Bomb calorimeter

Combustion calorimeters measure the heat released from a combustible material (solid or liquid). This is done by weighing a precise measure (a few milligrams) of the sample substance into a crucible which is placed inside the "bomb," a sealed metal cylinder called vessel, filling the vessel with oxygen (~ 30 bar), and igniting the substance. The sample burns and the resulting temperature increase of the vessel is measured and from it the calorific value is calculates by comparing it to a previous combustion of a known substance, calibration. The experimental procedure is summarized in Figure 14.

The substance used for calibration was benzoic acid. Then, the experiments were performed with 2 different samples: an EPS based mortar and an aerogel-based mortar. The lime-based mortar was not evaluated since it is classified as class A1 which means it is a non-combustible product.

The specimens were made at LC in IST and the test took place at a Fire Lab in DTU.
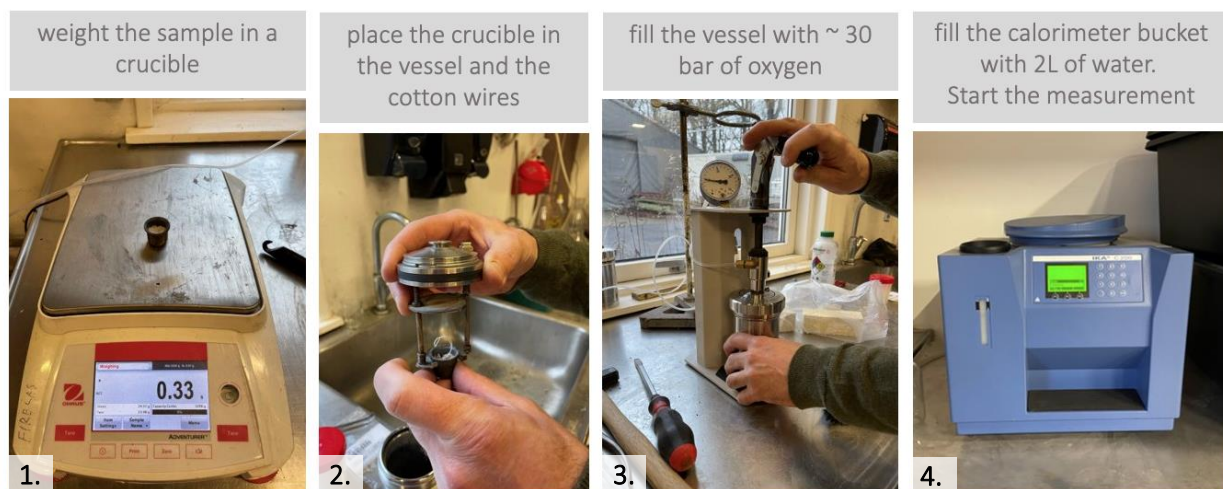
Figure 14. Bomb calorimeter's experimental procedure

3.4.5 Fire exposure tests

The experimental campaign included fire exposure tests, in which the specimens are subjected to a heating curve according to the standard fire defined in ISO 834 [19]. The main objective of these tests was to characterize the thermal response of the different materials and, then, to use the experimental data to calibrate (based on the numerical inverse analysis – described in chapter 5, section 5.2) their thermal conductivity and specific heat as a function of temperature. For this purpose, the 3 mortars were applied with a thickness of 40 mm on 5 mm thick steel plate, where the thermal action took place. To perform the

temperature measurements along the mortar thickness, type K thermocouples (conductor diameter of 0.25 mm) were positioned with a vertical spacing of 10 mm (Figure 15 d)) during the samples' preparation.

The temperature measurements were acquired at a 1 Hz rate, using a datalogger (*HBM, model Quantum X MX1609*) connected to a computer. The test duration was defined according to the temperature up to which the properties were intended to be calibrated. The limit was set at 800 °C, as the degradation of thermal mortars was already significant due to the presence of polymeric compounds.

The tests took place in a furnace with exterior dimensions of 2.10 m (height) x 1.25 m (width) x 1.20 m (depth) and a top opening area of 0.60 m x 0.30 m (Figure 15b)). The steel plate had the exact same dimensions to cover the opening. As the mortar area was 0.20 m x 0.20 m, the remain part of the plate was covered with an insulation material – ceramic wool; this procedure guaranteed proper insulation of the lateral sides of the mortar which was especially relevant since it was pretended the heat flow to be unidirectional – ascending (Figure 15 a) c)).

The minimization of convection phenomena in the air above the mortar was accomplished by covering the space between the exhaust system and the specimen with a non-flammable fabric.
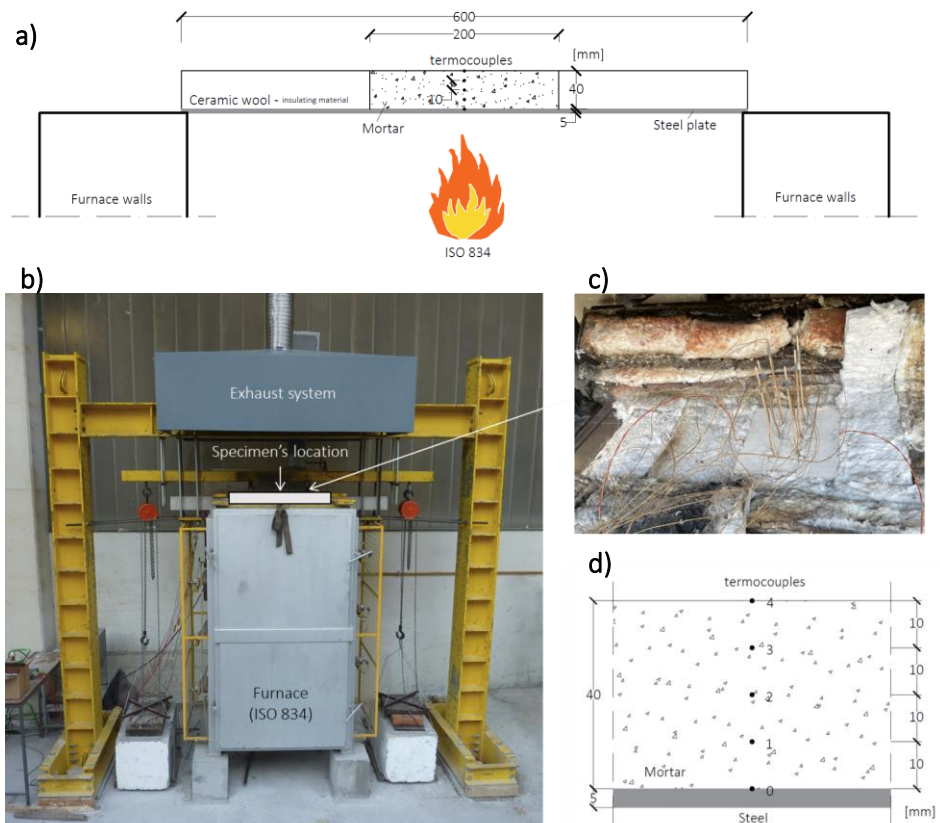
Figure 15. Test setup: a) Scheme of the front view, b) General view, c) Top view of the specimen, d) Scheme of thermocouples disposal inside the material in height

3.5 Synthesis of the chapter

This chapter described the experimental study carried out in this dissertation to characterize and compare different thermal mortars in terms of fire performance and post exposure to high temperatures and fire. Firstly, the materials and their main characteristics were described, as well as the main steps of the production of the. Then, the experimental methods and their main objectives were presented. Table 8 summarizes the different types of tests carried out in the experimental campaign and the corresponding parameters analysed/measured. A wide variety of experiments were performed, from the material's performance in terms of reaction to fire, until microscopic chemical analysis. This range involved the study of a variety of scales, not only in terms of samples dimensions (e.g. a few milligrams for XRD compared with a prismatic shape with 4 cm of thickness used in fire exposure tests), but also in terms of duration (e.g. few seconds to measure compressive strength and almost an hour on fire exposure tests). Overall, a total of 89 tests were performed.

In the next chapter, the results of experimental campaign will be presented and analysed.

Table 8. Synthesis of the tests and parameters measured during the experimental campaign

Type of test			Measured/ analysed parameter(s)
(i) Characterization tests	Mechanical		Compression strength, σ_C
			Flexural strength, σ_T
	Thermophysical	Using ISOMET 2114	Thermal conductivity, λ
			Specific heat, Cp
		TGA	% of mass loss in function of temperature
(ii) Microstructural Analyses	XRD		Identification of mineral compounds
	Micro CT		Zoomed 3D pictures
	SEM		High resolution images (microscope)
(iii) Fire Reaction tests	Ignitability		Flame spread, F_S
	Gross Calorific Potential		Gross calorific potential, PCS
	Cone calorimeter		Time to ignition, T_{ig}
	Bomb calorimeter		Heat release
(iv) Fire exposure tests			Temperature along thickness while exposure to fire curve

Note: The leftmost column of the table is labelled vertically "Specimens' production".

4 Results and discussion

4.1 introductory remarks

This chapter presents the results obtained during the experimental campaign, followed by a detailed analysis of them. Finally, a global evaluation of the measured parameters is presented established in order to define and verify their relevance and importance for the objective of this study.

4.2 Mechanical tests

Table 9 presents the temperatures of the air inside the muffle (cf. Figure 12 in section 3.4.1) as well as the ones inside the samples at the end of the heating process; the corresponding time-temperature curves are shown in annex A2.

It is worth mentioning that although the target temperature inside the mortar had been set as 400 °C, much higher values were reached in both thermal mortars (cf. Table 9); this may stem from the exothermic nature of the decomposition process of the polymeric components/additives (e.g. EPS granules; resins). Notwithstanding these differences in temperatures measured inside the samples, the residual mechanical tests were performed after the cubic samples had been exposed to an environment (i.e. temperature of the air inside the muffle) of 426 °C for Lime.m (434 °C in the material - cubes), whereas for both thermal mortars were exposed to 397°C, (internal temperatures of 707 °C for EPS.m and 657°C for Aero.m). The comparison between the temperatures measured inside the cubic samples lead to the conclusion that EPS.m releases more heat during the thermal decomposition of its components than Aero.m.

Table 9. Final temperatures of muffle heating process			
Mortar	T_{air} [°C]	T_{cube} [°C]	$T_{cilinder}$ [°C]
Lime.m	426	434	493
EPS.m	397	707	651
Aero.m	397	657	622

Considering the mechanical properties at room temperature, thermal mortars have significant less flexural and compressive strength than Lime.m (Figure 16). However, this is not a problem insofar as this type of mortars is to be used as part of a system that already foresees this vulnerability and, therefore, relies on a fiberglass mesh as reinforcement. As observed in Figure 16, Aero.m present the lowest initial mechanical

properties; this can be related to the high percentage (≈37%) of aerogel granules in this mortar since aerogel is fragile and has a porous matrix.

When comparing the residual compressive strength with the values obtained at room temperature and looking at Figure 16, it can be seen that Lime.m presents a slight decrease of 4% in the compressive strength. By evaluating the thermal mortars, the pattern is completely different. The highest decrease in compressive strength is observed in EPS.m (91%) that reaches lower values than the ones obtained for Aero.m, which can be justified by the higher polymeric content of the former mortar.
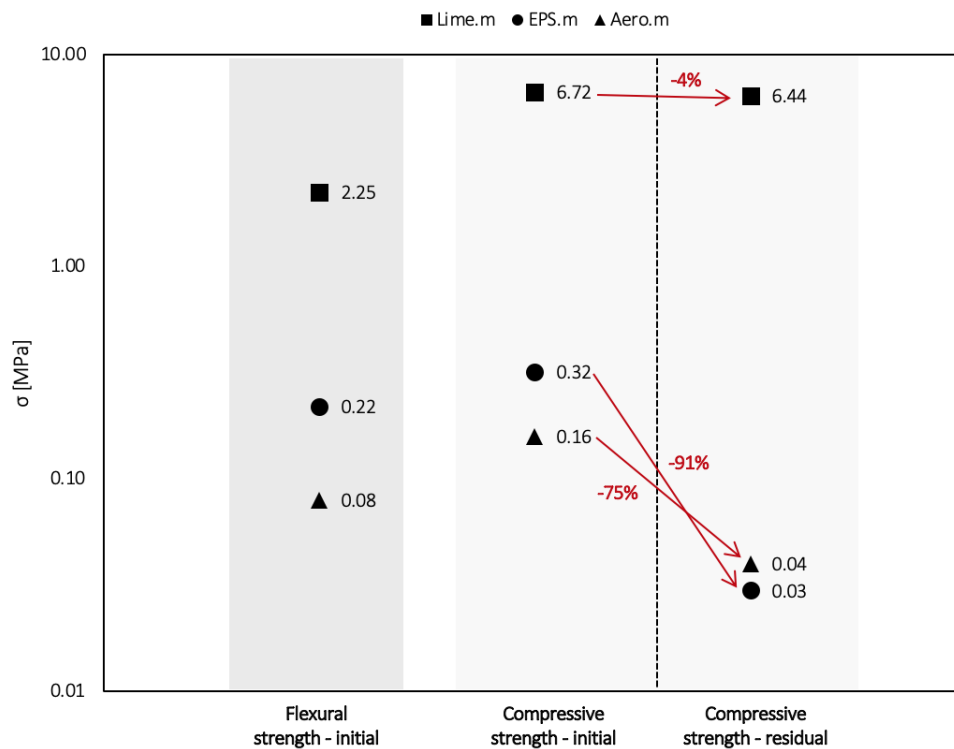
Figure 16. Average values of the initial and residual mechanical properties strength (after exposure to ≈ 400 ℃)

An observation followed by qualitative comments on the post-heated samples was also carried out. From the pictures of mortars after the residual compressive strength test presented in Figure 17, it is clear that EPS.m was the mortar which presented a higher degradation level; indeed, the EPS granules disappeared, and air gaps replaced them. The handling of EPS.m samples had to be very delicate because a simple touch would cause the sample to crumble. Regarding Aero.m, both aggregates and the cementitious matrix seem to be less degraded despite the crumblier texture when comparing with pre-heated specimens. In Lime.m samples, no visible thermal damages were observed at the surface of the material, only the slight reduction on the compressive strength revealed the effects of thermal exposure.

Figure 17. Specimens after residual compressive strength test: Lime.m (left), EPS.m (middle), Aero.m (right)

4.3 Thermophysical characterization tests

i) Thermal conductivity and specific heat

The specific heat of a material is the amount of heat per mass unit required to raise the temperature of the material in 1°C, while thermal conductivity can be defined as the rate at which heat flows through the material, indicating its ability to conduct heat. It is worth mentioning that although the comparison between the initial and residual properties (that will be presented next paragraph) does not have a direct practical application, they can be used to indirectly evaluate/compare the susceptibility of the mortars to fire/elevated temperature exposure.

When comparing the results obtained for the initial and residual specific heat and thermal conductivity shown in Figure 18, it is noticeable that the Cp of Aero.m is the most affected by temperature, whereas the one less affected is that of Lime.m. The higher susceptibility of the Cp of Aero.m can be justified by the degradation of (high) polymeric content (which is incorporated in these mortars to improve its initial mechanical properties). Since these components are no longer present after heating, the thermal properties changed; this result means that it is required less energy to raise the temperature in Aero.m, which means lower Cp.

Regarding the influence of temperature on density, Table 10 shows variations of 18% and 26% for Aero.m and EPS.m, respectively. These results also justify the ones obtained on the compression tests. The loss of compression resistance on EPS.m was also greater than the one on Aero.m. Regarding Lime.m, both the bulk density and compression strength decrease less than 5%.

Regarding effect of temperature on the thermal conductivity (Figure 18), it can be concluded that thermal mortars have almost no variation while Lime.m decreases its λ in about 28%. This significant reduction observed on Lime.m, may be due to the mass loss (water evaporation) and the consequent increase of

empty spaces/ pores, causing an improvement (i.e. reduction) on λ; additionally it can also be related the degradation on some components that had a higher thermal conductivity than the air that fill the remnants voids.

Table 10. Results on bulk density at initial conditions and post-heating

Mortar	$\rho_{initial}$ [kg/m^3]	$\rho_{residual}$ [Kg/m^3]	$\Delta\rho$
Lime.m	1675.55	1617.19	-3.48%
EPS.m	216.61	161.20	-25.58%
Aero.m	160.18	130.73	-18.39%
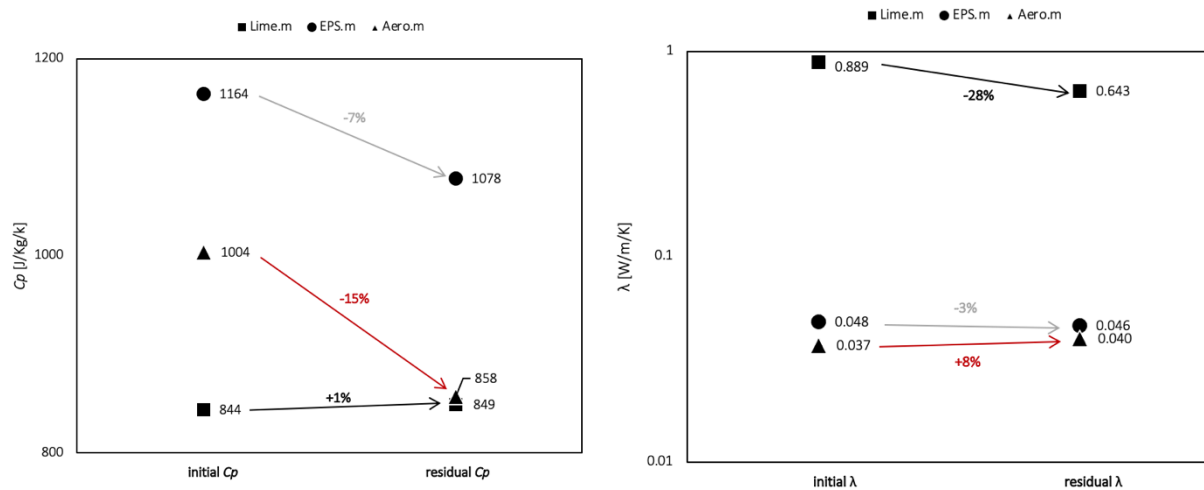
Figure 18. Initial and residual specific heat (left) and thermal conductivity (right)

ii)   TGA

The thermograms of the thermal mortars with EPS and aerogel are distinct from the thermogram of the lime-base (reference) mortar, as can be clearly seen in Figure 19; the thermogram of the latter mortar exhibit an expected peak centered at around 850 °C, which corresponds to the decarbonation process of $CaCO_3$. The temperature range at which this process occurs depends on factors such as the size of the $CaCO_3$ particles and their degree of crystallinity [113]. This process also includes decarbonation of the calcium silicates in the mortar [114]. The mortar with aerogel has less calcite than the remaining two samples. Both thermal mortars exhibit a complex decomposition process between 250°C and 450°C, absent in the reference mortar. The decomposition process of the polymer component and polystyrene (at 350 °C) is visible for the EPS mortars. The thermal mortars also show decomposition processes at low temperature attributable to the dehydration of CSH, ettringite and stratlingite (225°C, only in the one with aerogel).

The three mortars analyzed present different residual masses at 1100 °C, due to their different percentages of calcite, portlandite and organic material from polystyrene and aerogel. It is worth mentioning the fact that the samples used in thermogravimetry have a small volume, therefore the results presented above may have a limited representativeness of a real application, in which relatively thick layers (i.e volume) of mortar are used.
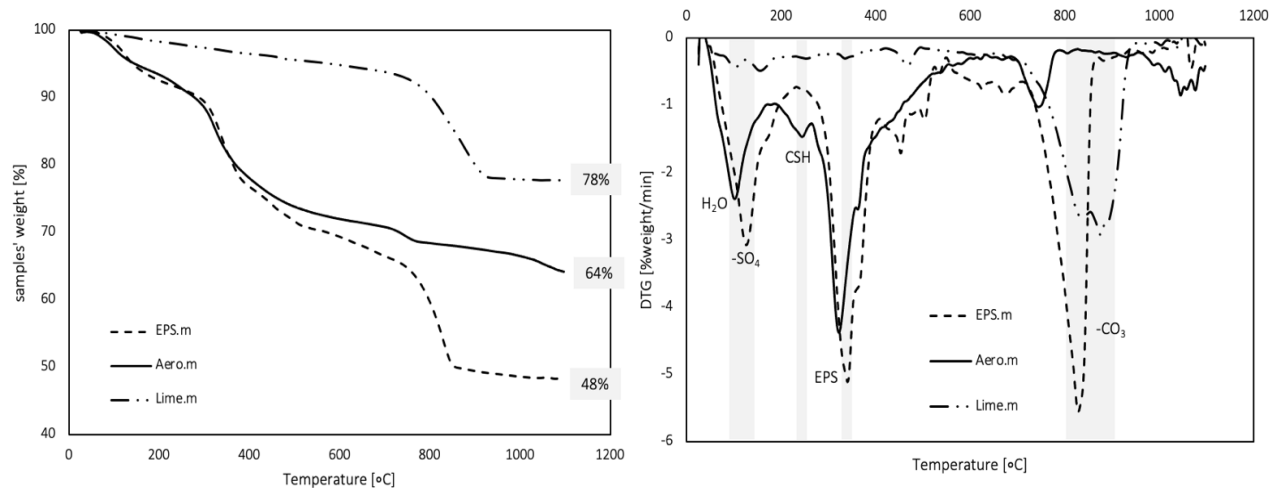
Figure 19. Thermograms, TG (left) and DTG (right), of the prepared mortars (heating rate 25 °C/min, under air flow)

4.4 Microstructural analysis

i)   X-Ray diffraction (XRD)

Firstly, it is important to state again that this technique only allows the detection of mineral and crystalline compounds. In the X-ray diffraction patterns, the peaks enable the identification of minerals and the degree of crystallinity. Higher and narrower peaks reveal higher degrees of crystallinity. Wider, flatter bands/curves are characteristic of amorphous compounds.

The X-ray diffraction pattern of Aero.m at initial conditions (blue) presented in Figure 20, reveals the presence of calcite ($CaCO_3$), gypsum ($CaSO_4$), and gehlenite ($Ca_2Al_2SiO_7$) (technical report is in annex A3) . In the post heating pattern (red) it is noticeable the dehydration process since the representative peaks of gypsum and gehlenite disappear. In both graphs there is a slope between 15° and 35°, which are related to the presence of amorphous/nanocrystalline compounds.
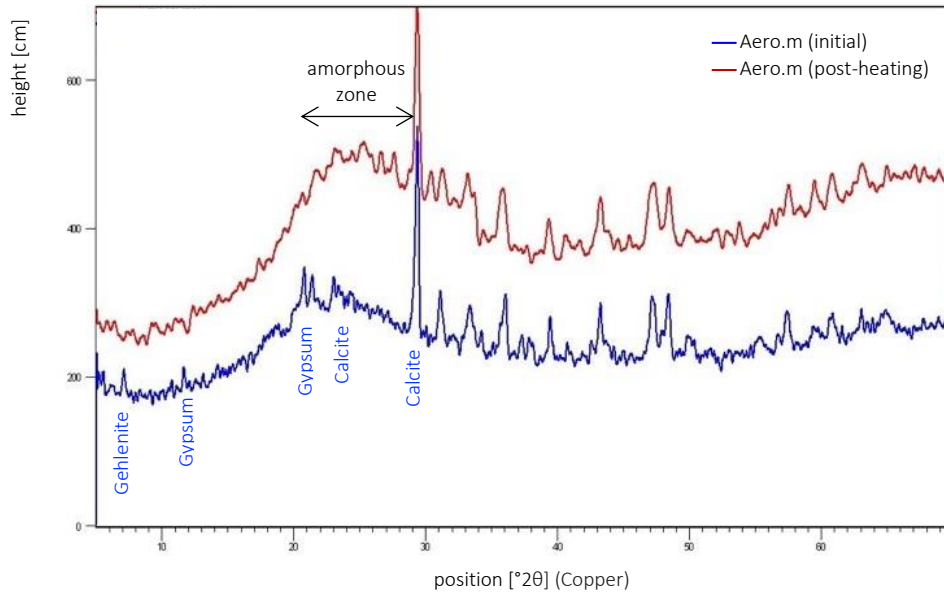
Figure 20. X-ray diffraction pattern of Aero.m at initial conditions and post heating at ≈300 ℃

Regarding the pattern of EPS.m at initial conditions (red curve) in Figure 21, the only detected mineral was calcite (technical report is in annex A4). This proves that the mortar's matrix is lime based. However, as in this test a sample from an old production was used, most of the water had already evaporated, which led the material to be completely carbonated, which can explain the fact that only calcite was detected. The sample used for post heating analyses was recent, therefore it contains portlandite ($Ca(OH)_2$) that, when heated, generates intermediate products (metastable). Indeed, when heated, water is released and the lime (CaO) is reactivated again, promoting the formation of new carbonates, vaterite and aragonite. They are both polymorphous materials from calcite which means they have the same atoms composition ($CaCO_3$), but a different crystalline structure, i.e. the atoms are organized on a different way. The presence of these polymorphs can be attributed to fast carbonation after heating process.

The comparison between Aero.m and EPS.m shows that while the first one has a cementitious matrix, since components of cement were detected, the other presents a lime-based matrix.
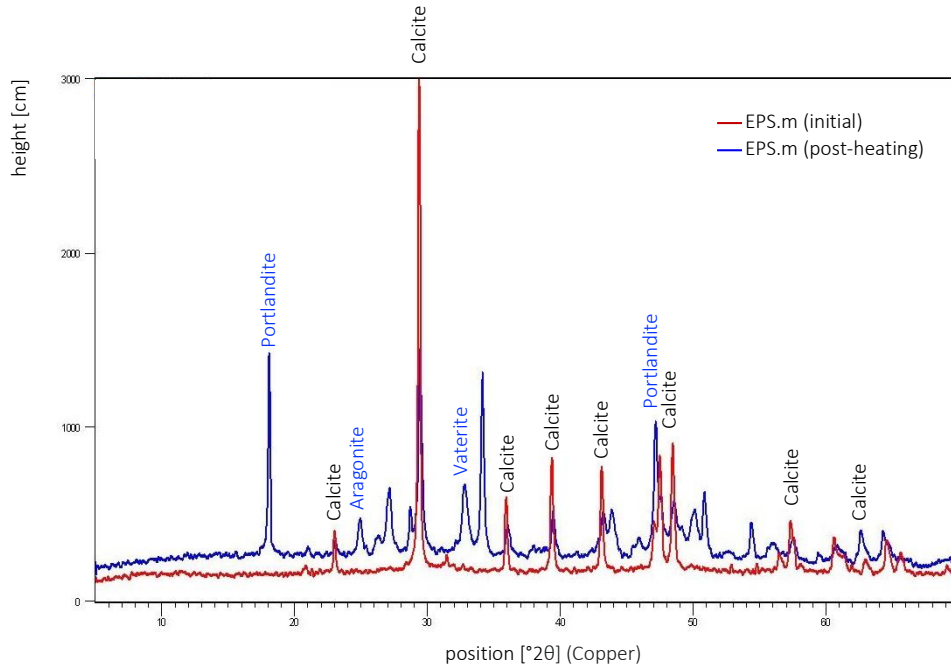
Figure 21. X-ray diffraction pattern of EPS.m at initial conditions and post heating at ≈300 ℃

ii)   Micro CT

This nondestructive technique, described in chapter 0, enables the 3D visualization of objects, based in reconstructed images (slices). The radiation does not detect low dense or lightweight components such as the aggregates, EPS and aerogel, which comprise the thermal mortar analyzed, leading to apparent pores/ voids in the images.

The results presented in Figure 22 do not show significant differences between the initial specimens and the post-heated ones. This technique allows the analyses of the matrix, and it can be concluded that there is no collapse or micro fissures due to the exposure to high temperature, which means the porous network was preserved.
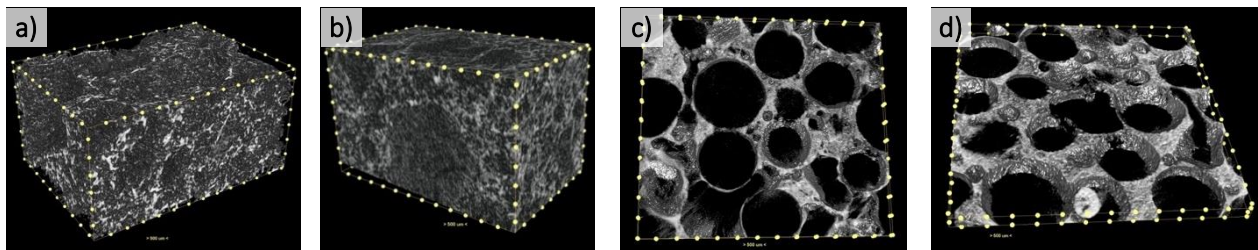
Figure 22. Micro CT images of Aero.m a) initial conditions, b) post heating; and EPS.m c) initial conditions, d) post heating

To add value to these analyses, high-resolution pictures were taken, as shown in Figure 23. The EPS has a honeycomb structure after heating, with a probably more rigid (and presumable brittle) structure resulting from the decomposition of the polymeric components (justifying in part the loss of mechanical strength).

The Aerogel was affected from the chromatic point of view, however, its structure remained rather similar to the unheated specimen.

In both cases, the yellowish-brownish colour can be attributed to the partial combustion of the polymeric parts, as seen in the relative test (smoke release), as well as melting and decomposition (in the case of EPS).

Figure 23. Zoomed photos. From left to right: initial EPS.m, post-heating EPS.m, initial Aero.m, post-heating Aero.m

iii)   Scanning electron microscope (SEM)

According to XRD, Aero.m at initial conditions (pre-heating) contain calcite (hydraulic lime or cement), gehlenite (hydraulic compound of cement), and gypsum. In image a), one can see acicular compounds at the interfaces between siliceous aggregates and the cementitious matrix, which must correspond to the hydraulic compounds mentioned above. The aerogel has a compact microstructure, with some micro-cracks. Spherical particles may correspond to other compounds in the formulation (e.g. perlite, undetected in the XRD, being amorphous). Regarding TG analysis data (on section 4.3), the mass loss was considerably lower than EPS.m, which shows its thermal stability in the considered temperature range.

After heating (300° C, Figure 24(bottom)), the images show an increase in microporosity, possibly dependent on the dehydration of the cementitious products of the matrix, however, the microstructure is rather similar to the initial unheated sample. Dehydration is also confirmed by XRD, by the disappearance of gehlenite and gypsum.
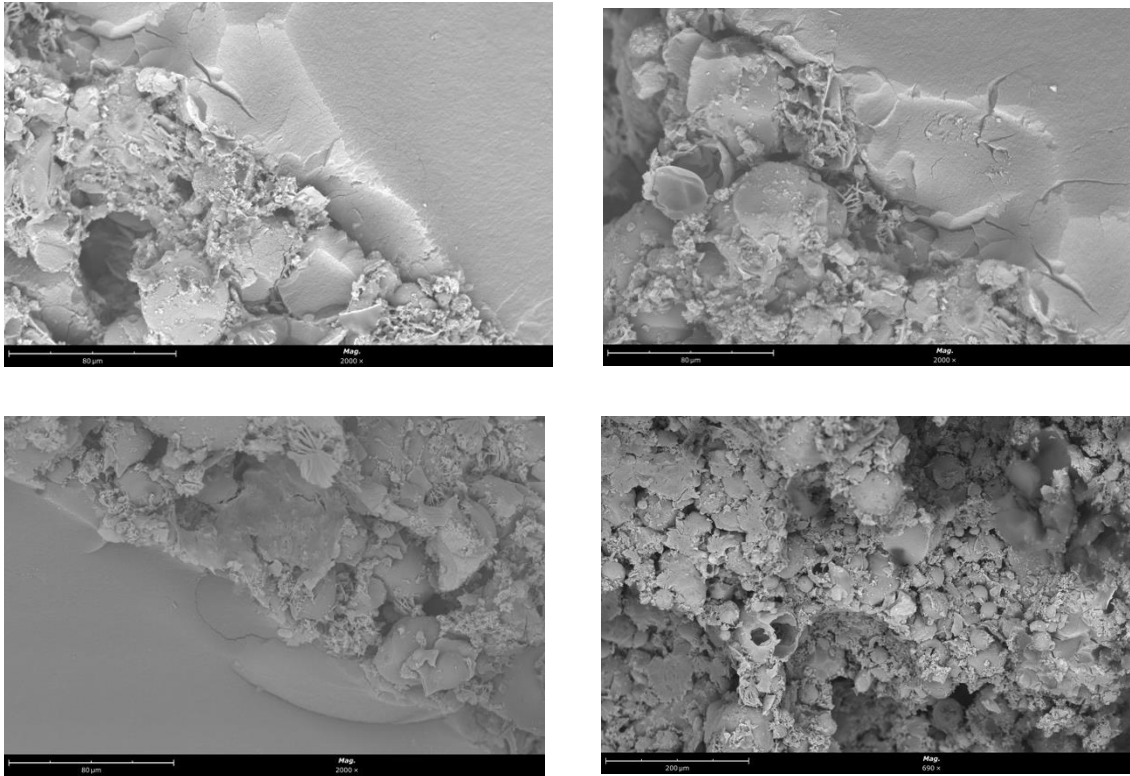
Figure 24. SEM images of Aero.m; initial conditions (top), post heating (bottom)

Regarding EPS.m, initially (pre-heating) - Figure 25 (left), the matrix shows a high porosity, but generally a compact morphology (expanded polystyrene with some cohesion with the calcite-based binder). XRD confirmed a constitution mostly based on calcite (originally natural hydraulic lime). After heating, the formation of metastable phases of $CaCO_3$, e.g. aragonite and vaterite, was confirmed by XRD. As analysed in TGA, the expanded polystyrene undergoes an important thermochemical degradation, accompanied by shrinkage (polystyrene, when expanded, can increase by 50 times its volume; after heating, it exponentially shrinks again, if compared to its expanded state). The SEM images post-heating (Figure 25 (right)) confirmed the macroscopic and tomographic observations, which indicate that there are still residues resulting from the incineration of polystyrene in the matrix (total decomposition around 450°C). On the other hand, the microstructure is maintained, with apparently global preservation of the porous matrix.
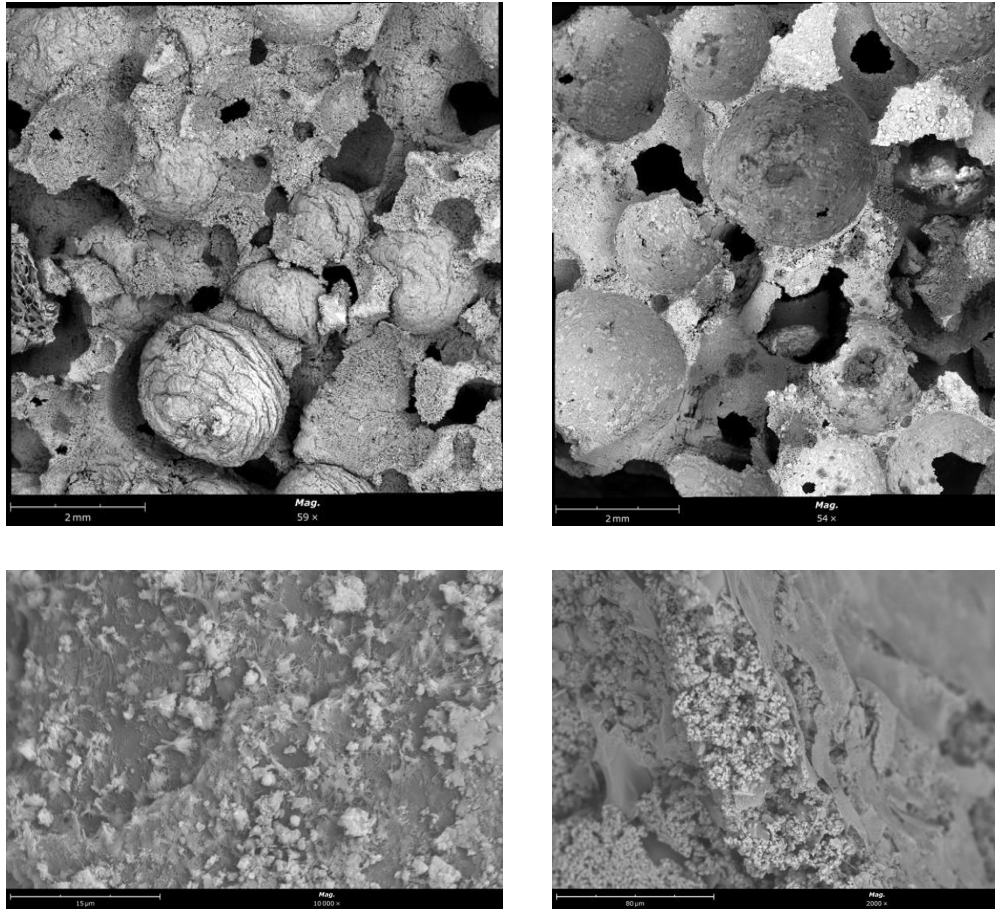
Figure 25. SEM images of EPS.m; initial conditions (left), post heating (right)

4.5 Fire reaction tests

During the ignitability test performed to the thermal mortar with aerogel, neither ignition of the sample nor residues on the filter paper placed on the base of the specimens were observed. There was also no release of flaming droplets or particles. This procedure only allowed to conclude that the material is, at least, classified as E. The technical report provided by the lab where the test took place (ITECONS) is presented in annex A5.

When it comes to the Gross Calorific Potential test conducted on samples of the mortar with aerogel, the PCS (gross calorific potential) value obtained was 6.19 ± 0.25 MJ/Kg (technical report in annex A6), which is significantly above the maximum permitted value to be able to classify a material as A2 (3 MJ/Kg [32]) . However, the bomb calorimeter test, which is not standardized but allows the measurement of the same variable, provided significantly different results. Indeed, the value obtained was 4.3 MJ/Kg.

Although both results provide values above the standard's threshold to classify the product as A2, there are relevant conclusions that can be drawn. Since the sample used for both procedures only have a few milligrams, they may not be representative of a future practical use of the mortar. Furthermore, not being a commercial product yet, it is not optimized, nor there is a manufacturing production method that ensures a proper control of the quantities and proportions of reagents which means that some lack of homogenization may have occurred during specimens' production.

The cone calorimeter results indicate how fast the specimens ignite. The performed heat fluxes were 13.64, 15.82, 17.55 and 22.36 KW/m^2 (Table 11). The EPS.m only ignited for the two higher heat fluxes, which means that the critical heat flux, i.e. the minimum heat flux for material to ignite, should be within the range 17.55-15.82 KW/m^2. Lower heat releases rates should have been studied for Aero.m since it has ignited for the lowest heat flux analyzed. However, due to time constrains regarding the use the equipment in DTU's laboratory, it was not possible to repeat these tests using different heat fluxes.

The graph presented in Figure 26b shows that Aero.m has the fastest delay time which means it ignites earlier than EPS.m. Such result was not expected because: i) in the standardized ignitability test (performed at ITECONS) the specimen, Aero.m, did not ignite when exposed directly to a small flame; ii) during the previous experiments EPS.m has proven to be more susceptible to high temperatures presenting a higher mass loss (TGA), higher disaggregation level on residual compressive strength test; iii) due to the higher polymeric content of EPS.m when comparing to Aero.m.

Another unexpected event was the non-ignition of Aero.m for a heat release of 22.36 KW/m^2. Since it has ignited for lower heat releases, for 17.55 KW/m^2 it only took 8 s for the ignition to start, it was estimated the ignition would start in less than 8 s with 22.36 KW/m^2 (Figure 26a). However, it did not happen. These, apparently, incoherent results may be stem from the fact that Aero.m is a non-commercial mortar with a non-controlled production, therefore some lack of homogenization may have occurred causing the polymeric content, which is what contributes as a combustible material, to get concentrated on top of the specimen, triggering the ignition to happen for heat flux of 17.55 KW/m^2.

Table 11. Experimental results of Cone Calorimeter. Distance cone-specimen: 25 mm

Heat release	Time to ignition [s]	
[KW/m^2]	Aero.m	EPS.m
13.64	22	no ign
15.82	15	no ign
17.55	8	102
22.36	no ign	48
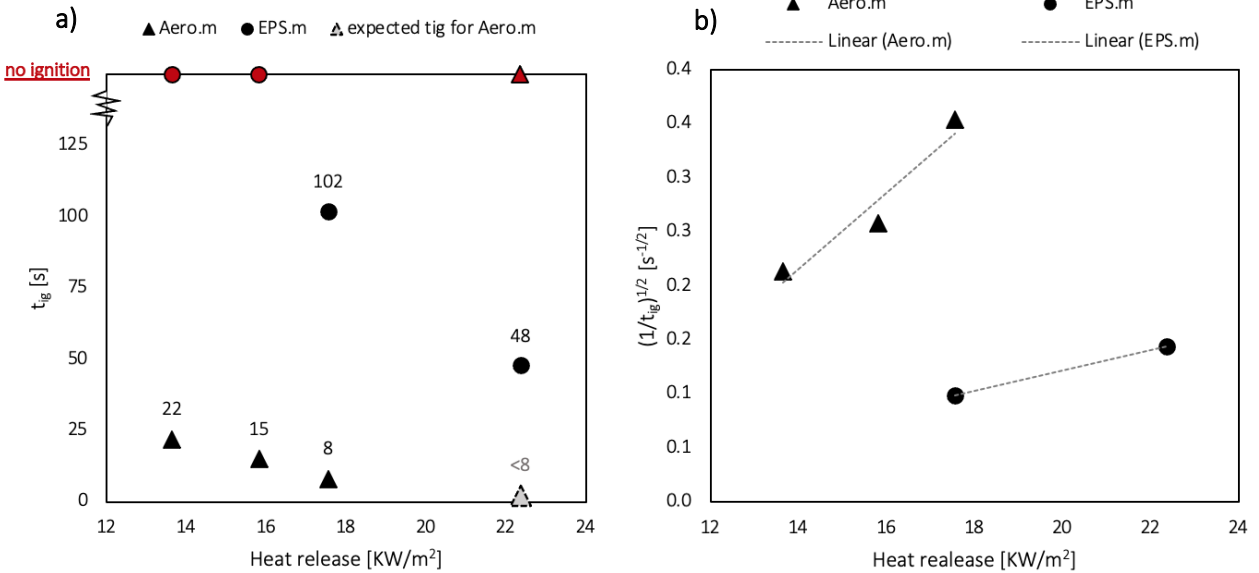
Figure 26. Cone calorimeter results: a) Ignition rate of thermal mortars, b) Linear ignition delay

4.6 Fire exposure tests

Figure 27 shows that the lime-based mortar and the Aero.m presented an overall more gradual temperature increase than the EPS mortar. Regarding the thermal mortars (EPS.m and Aero.m), two distinct behaviors are observed: (i) a first one up to about 100° C, in which the temperature increases at a lower rate (when compared to the one afterwards); at this temperature a plateau is observed that corresponds to the evaporation of water, a plateau that is longer (in time) the more it advances in the mortar thickness (in relation to the exposed surface); for example, at 2 cm from the heat source this plateau lasts about 17 min (1000 s) and at 4 cm about 30 min (1800 s); (ii) and a second characterized by a higher temperature increase rate. In the case of the EPS mortar, an abrupt temperature increase from 100°C to about 400°C is observed at mid-thickness (i.e. at 2 cm), lasting 8 min. This finding may be related to the decomposition of the polymeric compounds, namely the EPS particles that, during this process release energy and contribute to this abrupt increase. In fact, the results within this temperature range agree with the peaks observed in the TGA results (cf. section 4.3), which may reinforce the veracity of this cause-effect relationship.

A similar behaviour is observed in Aero.m, which, however, in a more detailed and amplified evaluation shows some differences to EPS.m. Analysing the curves at mid-thickness of the specimens (Figure 27b), it is clear that Aero.m presents a better insulating capacity than EPS.m; this conclusion is evident, for example, by the longer time required to reach 200°C (1100s for EPS.m vs. 1300s for Aero.m). Furthermore, this figure shows that from 120°C the lime mortar presents the lowest temperature increase rate; this result should

be related to its (mostly) inorganic composition, and therefore less susceptible to changes caused by exposure to high temperatures.

In the initial test conditions, at room temperature, the Lime.m thermal conductivity values are the highest, suggesting that higher temperatures were reached in the specimen of this mortar. However, according to the graph in Figure 27b) it can be observed that both at mid-thickness of the specimen (elevation 2), and on the surface in contact with air (elevation 4), the lime mortar reaches the lowest temperatures. This result indicates that the thermophysical properties (thermal conductivity, density and specific heat) at elevated temperatures of the lime mortar result in a more stable material. This reversal of hierarchy at the level of thermophysical properties is noticeable from 120°C (Figure 27b)) and is justified by the fact that the EPS particles and polymeric components of the aerogel mortar decompose with temperature, compromising the insulating capacity of these mortars.

In Figure 28 are photographs of the thermal mortar specimens after the test. It can be seen that both specimens are significantly degraded after exposure to fire. In mortar EPS.m, the EPS particles were completely burned out and replaced by empty pores, which gave a great fragility also to the mineral matrix, crumbling to the touch. In the aerogel mortar, the lightweight aggregate (i.e. the aerogel particles) is still visible and apparently stable, but on a macro level the specimen presented an curvature causes by the differential temperature exposure (and damage) through-the-thickness.

Finally, it is worth noting that the thermal distribution described in this section were also used as input data in a numerical procedure (described in chapter 5) to calibrate the thermal properties of the mortars at elevated temperatures using an inverse analysis.
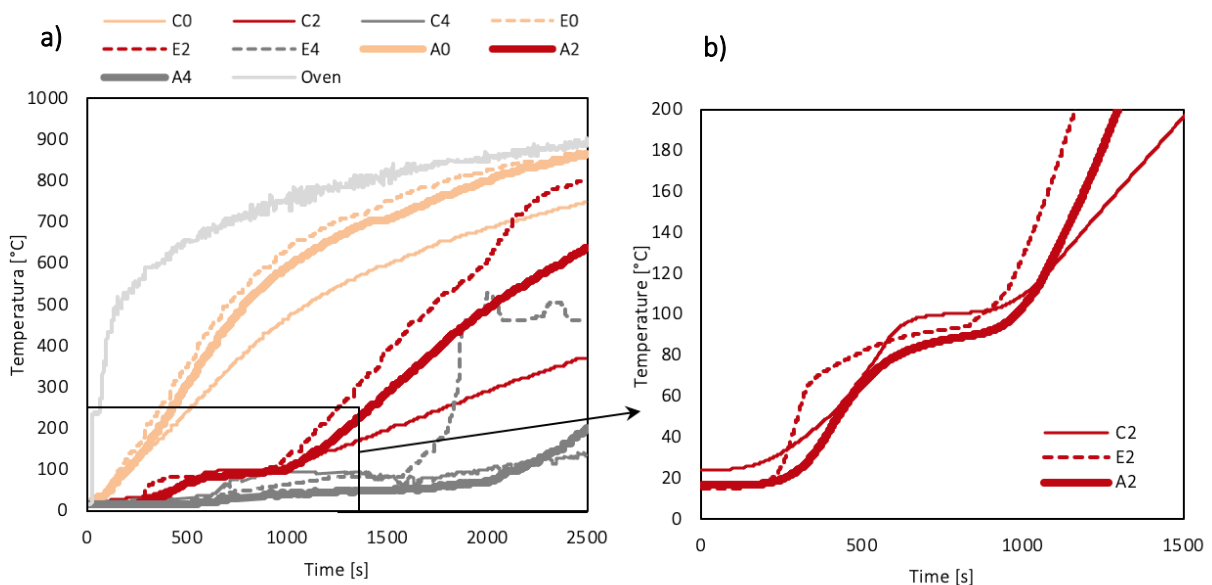
Figure 27. Fire exposure curves a) of the analysed mortars, b) focusing on the initial part of the test and the specimens' half thickness (dimension 2 cm). The colours refer to the thermocouple height (e.g. C0 = thermocouple in contact with the steel plate; C1, C2, C3, C4 = thermocouples installed at 1 ,2, 3, 4 cm from the plate); C – Lime.m, E – EPS.m, A – Aero.m

Figure 28. Thermal mortars post testing: EPS.m (left), Aero.m (right)

4.7 Concluding remarks

With the results presented in this chapter it was possible to analyse thermal mortars at different scales and evaluate the impact of high temperature exposure on thermophysical and mechanical properties, as well as the effects on their microstructure. Finally, the performance under fire was evaluated in terms of (i) fire reaction, in which standard tests were carried out, and (ii) fire exposure tests to a standard fire curve (ISO 834) that allowed to measure the evolution of temperature through the mortars' thickness.

The results of the characterization tests show that both the conventional thermal mortar (with EPS) and the innovative one (with aerogel) are thermally unstable, due to the susceptibility of their constituents when subjected to high temperatures, and in part because of the polymeric additives/components. The microstructural analyses allowed to conclude that the mortars' matrix remains stable after samples had been heated up, emphasizing the idea that the degradation noticed on mechanical and thermophysical properties is caused by the polymeric compounds.

The mechanical tests confirmed what was already expected, the accentuated decrease in mechanical strength, in fact, both thermal mortars present negligible compressive strength after exposed to environmental temperature of slightly above 400 ℃. However, it is worth remembering that in real applications these mortars with be reinforced with fiberglass meshes, therefore, the results of the residual mechanical properties obtained in the present campaign are a lower bound of those would be expected in real scenario.

Since these mortars are pretended to be used in systems whose main purpose is to guarantee thermal insulation, one of the most relevant characteristics is thermal conductivity. It is a well-known property of any commercial thermal mortar. The residual thermal conductivity was measured to see if it could be an indicator of the degree of damage introduced by exposure to high temperatures. The results presented show small changes (<10%) which means it will not be useful to satisfy this purpose.

The microstructural helped to confirm and justify the results already obtained in a visual inspection, allowing a more detailed perception on compounds' degradation.

Regarding fire reaction tests, both thermal mortars present a low performance according to the standards, EN 13501-1. Aero.m is below A2, which is the Euroclass of some thermal commercial mortars with Aerogel. The cone calorimeter results were not conclusive; therefore, further studies/repetitions are needed.

The next chapter comprises a numerical analysis based on the results obtained in fire exposure tests described in section 3.4.5. The input data were the temperatures measured along the samples' thickness during the exposure to fire standard curve (ISO-834), from which it was possible to calibrate thermal conductivity and specific heat as function of temperature. The variation of properties obtained are then analysed to understand its variations along temperature increase.

5 Numerical analysis

5.1 Introductory remarks

Following the fire exposure tests described in section 3.4.5, the present chapter describes the numerical study that was developed in order to determine the thermophysical properties (thermal conductivity and specific heat) as a function of temperature of the mortars under study, through an inverse analysis.

For that end, it was necessary to use (i) a 1D thermal finite element model and (ii) an optimisation routine. The former was used to obtain numerical simulation of the thermal response within the mortars whereas the second was used to perform comparisons between the numerical and experimental results and iteratively approximate both responses by modifying the (unknown) thermophysical properties of the mortars at different elevated temperatures (these were initially assumed to be constant with temperature, and then considered as temperature-dependent).

These properties are intended to provide an additional understanding of what happens to the mortars when exposed to very high temperature, likely to be reached during a fire event. Experimental determination is difficult/impossible due to their sharp degradation, which is why this methodology was implemented. The results can also be used as input to finite element models for future studies that aim at simulating the thermal response during fire exposure of a building element coved with any of these mortars.

5.2 Thermal model and optimization routine

The 1D thermal finite element model allows determining the temperature distribution at different elevations and over time for elements subjected to a certain thermal action, simulating heat transfer phenomena by conduction, convection and radiation. More details on the thermal model can be found in [115].

The optimization program consists in a routine which allows, iteratively, the minimization of the sum of the square of the differences between the numerical and experimental temperatures in each point and for each instant of time, by consecutively changing the thermophysical properties of the material under study.

Whenever the thermophysical properties are changed, the routine invokes and runs again the thermal finite element model to determine new numerical temperatures.

i) Finite elements thermal model

The numerical thermal model used in this dissertation was initially developed in the framework of a PhD thesis [115] through *matlab* software, with the objective of solving one-dimensional (1D) heat transfer problems by conduction, convection, and radiation.

Regarding its usage, the first step was to define the thicknesses of the materials subjected to the standard fire curve: i) a 5 mm steel plate and ii) a mortar layer with 40mm of thickness. The discretization adopted for the materials is a determining factor for obtaining credible results and for the convergence of the model and accuracy of the results. In this sense, 28 elements were adopted for the mortar and 4 elements for the steel plate, each element with 3 nodes. The more refined the mesh, the better the convergence of the model but the longer the duration of the runs.

An illustration of the 1D finite element model is presented in Figure 29.
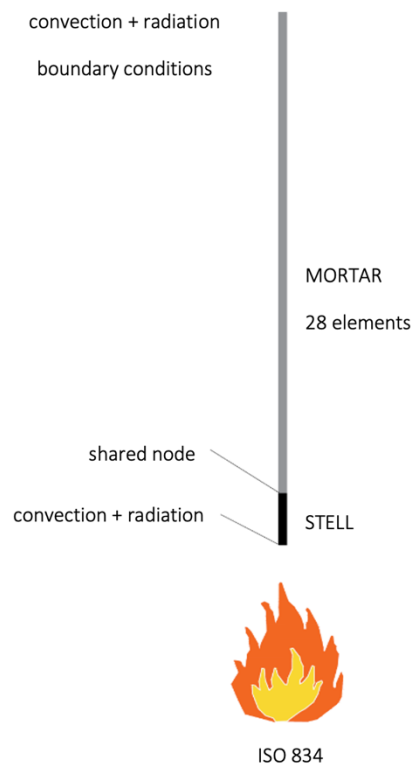
Figure 29. 1D finite element (FE) model

To define the materials in the thermal model, it was necessary to introduce their thermophysical properties as a function of temperature: density, conductivity, and specific heat. For the steel plates, the values given in EN 1993-1-2-2005 [116] were used. For the mortars, these properties were measured at room temperature through the experimental campaign developed in the scope of this dissertation. As stated

above, in the first runs of the models, these values were assumed for all temperatures. Regarding the density of the mortars as a function of temperature, it was assumed to follow that same reduction with temperature of the remaining mass curves obtained in the TGA tests (cf. section 4.3).

The definition of the governing equation in the domain that defines the thermal problem is presented in equation (3) . In this work G = 0 W/m³.

$$\frac{d}{dx}(\lambda\frac{d\theta}{dx}) + G = \rho C_p \dot{\theta} \tag{3}$$

where λ : Thermal conductivity [W/(m.K)]
θ : Temperature [°C]
G : Heat generation per unit volume and time [J/(m³.s)]
ρ : Buk density [Kg/m³]
C_p : Specific heat [J/(Kg.K)]

ii) Optimization routine

The optimization routine was developed according to the principles illustrated in the flowchart presented in Figure 30.
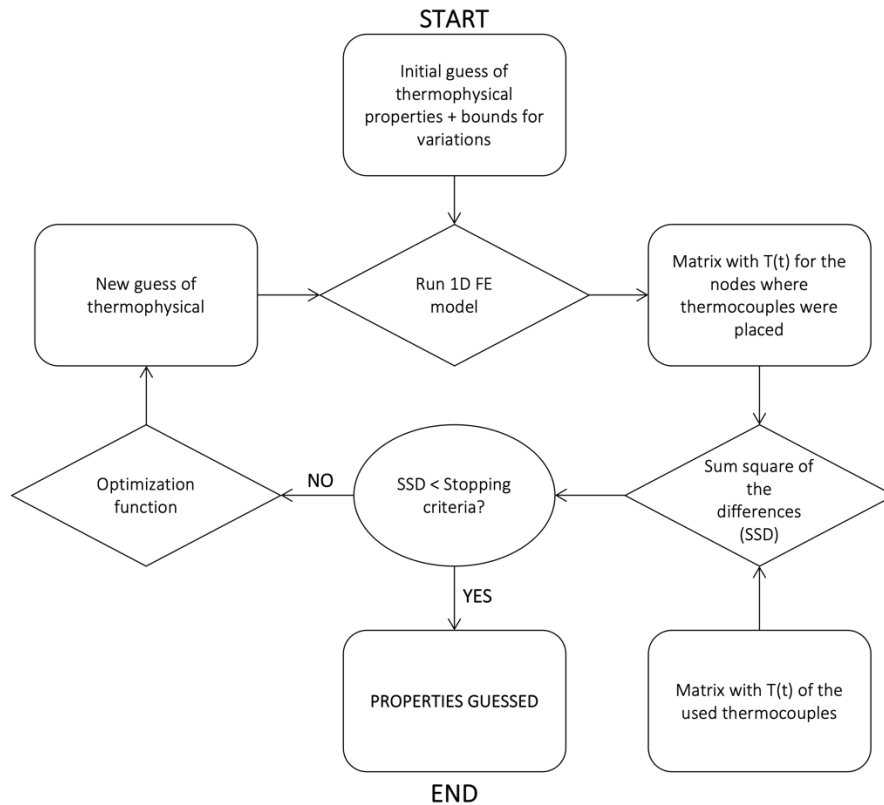
Figure 30. Optimization routine's flowchart

The start of the program is determined by creating a data matrix that is assigned to the thermal conductivity and the specific heat of the material, for different temperatures. Then, the thermal program starts its first run, which ends with obtaining the numerical temperature-time curves for different heights of the specimen.

These temperatures are then compared with those obtained experimentally. The next step is to calculate the sum of squares of the differences (SSD) between numerical and experimental temperatures. This value is compared with the one defined for the stopping criteria (SC=0.1%): i) if SSD < SC the program ends, i.e., the optimised thermophysical properties are reached; ii) otherwise, new thermophysical properties are assigned to the material and the program resumes the described cycle.

5.3 Results and discussion

Figure 31 presented the obtained thermophysical properties (thermal conductivity and specific heat) as a function of temperature of the mortars at the end of the numerical procedure.

For all 3 mortars, the thermal conductivity progression shows similar peaks. It starts with an abrupt increase in conductivity up to 100°C (possibly related to the water evaporation process), followed by a decrease between 200°C and 300°C. Finally, there is a moderate increase until 400°C followed by another decrease where thermal mortars reach the initial values and the Lime.m shows a value slightly higher than the initial one.

Aero.m seems to be the one that undergoes the least changes, i.e., the one that is less affected by the temperature increase. On the other hand, Lime.m is the one that presents the largest peak, at 100°C, in which conductivity almost quadruples in value.

As far as the specific heat is concerned, there is initially a steep increase, where the specific heat peaks between 100 and 200°C; the values at very high temperature are approximately the same to those at ambient temperature conditions. These peaks can be associated to the thermal decompositions; these are generally endothermic (heat consuming) processes as physical theory suggests [116]; this means that when the material is decomposing a lot of energy needs to be provided (*Cp* peaks) in order to decompose the material and to increase its temperature. In this sense it is possible to justify the fact that EPS.m has the highest peak since it has a large percentage of polymeric (organic) components. Although aerogel is an inorganic material, the Aero.m mortar also has polymeric content, thus the peaks observed in the *Cp* (although with lower magnitude than those of the EPS.m).
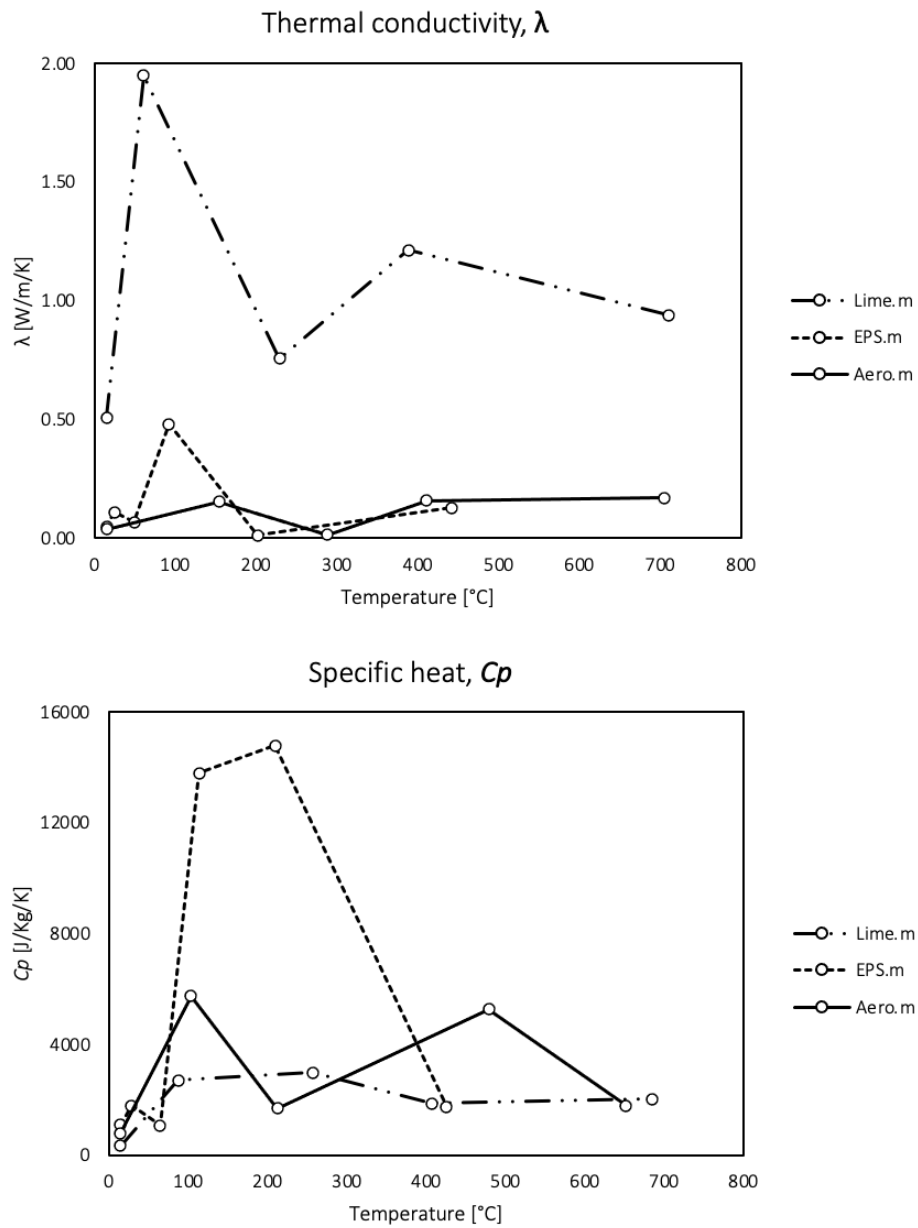
Figure 31. Thermal conductivity and specific heat in function of temperature

The next chapter comprises the general conclusions of the work carried, with a critical analysis of the data obtained in the present research. Considering the difficulties experienced, the proposed objectives, and the results achieved, some proposals on future developments are presented, according to some issues that are considered relevant to deepen.

6 Conclusions and future developments

6.1 General overview

The objective of this dissertation was to compare a conventional thermal mortar with EPS granules with an aerogel-base one, namely in terms of their performance under exposure to elevated temperatures and fire; as well as their post-fire and high temperature (i.e. residual) behaviour. As a reference, due its wide application and for its A1 classification in terms of fire reaction, a conventional hydraulic lime-based mortar was also analysed. The goal was not only to characterize the thermophysical properties of the mortars at different elevated temperatures, but also to understand the degradation of the materials after exposure to high temperatures, namely in terms of residual mechanical resistance and changes in their microstructure.

The literature review was the basis of this study. During this research it was verified that, despite the existence of norms, the high number of facade fire incidents reinforces the need to complement the study of fire behaviour of ETICS, especially those made of inflammable materials, such as EPS or XPS. However, these systems are complex since they comprise multiple layers of different materials, with different thicknesses and purposes. Due to the lack of knowledge, it was decided to analyse only the layer with most impact (according to the analyses made on section 2.5) on fire spread.

Another objective of this study was to propose additional measurements (parameters) that can help comparing solutions beyond the existing standardization. The truth is that most standardized tests to evaluate the fire behaviour of construction elements require a lot of material and have high costs, hence the need arose to develop indirect ways of characterizing on smaller specimens and to extrapolate the results to real situations.

6.2 Final conclusions

Firstly, it is essential to clarify the importance of this study and the choices made. This is a preliminary investigation, with a limited duration in time, on an embryonic subject. In fact, there are not many studies on high temperature and fire behaviour of thermal mortars. Therefore, it was decided to develop an experimental campaign that included a broad testing approach at multiple scales of analysis, conducted in 6 different laboratories: the *Fire Lab* at DTU facilities in Copenhagen, Denmark; ITECONS in Coimbra; and 4 laboratories at IST - LC, LERM and LAMPIST and a chemistry lab form DEQ.

As previously mentioned, four main test categories were conducted: (i) material characterization tests, (ii) microstructural analyses, (iii) fire reaction tests, and (iv) fire exposure tests, for which different objectives were set. In (i) the TGA allowed the definition of peak temperatures associated with the most significant mass losses in which the materials suffer more alterations due to the high temperature exposure. Based on those results, a temperature (400 °C) was set to evaluate the residual mechanical and thermophysical properties in order to compare with the results at initial conditions (pre-heating). With this comparison it was intended to understand if any of these properties could be used as an indirect parameter to assess the damage/alterations in the materials due to the exposure to high temperature. Regarding (ii), the aim was to have complementary information on materials degradation, namely which compounds (matrix and/ or aggregates) were more damaged by the heating. The fire reaction tests, (iii), were the ones that allowed comparisons with standard values presented in EN 13501-1 [32] in order to evaluate the reaction classification of Aero.m, since it's a non-commercial product. Finally, (iv) the fire exposure tests were used to calibrate thermal conductivity and specific heat at high temperatures which are necessary properties to numerically simulate the thermal response of these materials during a fire situation.

The results of the material characterization tests, (i), showed that both the conventional (with EPS) and the innovative thermal mortar (with aerogel) are thermally unstable, due to the susceptibility of their constituents when subjected to high temperatures, especially due to their polymeric adjuvants/components. Regarding Aero.m, despite the referred instability, its residual mass at 800°C was considerably higher than that of EPS.m, showing that its constituents (in particular the aerogel) are less degraded by exposure to high temperatures than the EPS particles. The results obtained for Lime.m showed that, as expected, its constituents are less affected by temperature, however, this mortar does not comply with requirements (considering EN 998-1[54]) to be classified as a thermal mortar.

Through the microstructural analyses, (ii), it was possible to accomplish that, on both thermal mortars, the binder matrix presented few alterations due to the exposure to high temperatures. In fact, whereas the lightweight aggregates (EPS granules) in EPS.m were completely decomposed, the aerogel particles in Aero.m only presented some micro-cracks. It was concluded that the thermal susceptibility of Aero.m was mainly caused by its polymeric additives. It is worth mentioning that Aero.m is a non-commercial product and its formulation (i.e. constituents) is not optimized considering its fire behaviour, nonetheless the results pointed out that there is a considerable potential on aerogel-based thermal mortars as an alternative to EPS-based solutions.

The fire reaction tests (iii) carried out can be divided in two categories: (a) the ones that were developed according to the standardized procedures, and (b) the complementary ones. Regarding (a), it was possible

to concluded that Aero.m will be classified below class A2 and above Euroclass E. Although it has not been possible to perform all standardized tests required to define a specific fire reaction class (as they would involve a significant amount of material and costs), during the ignitability test there was an important observation - the sample did not ignite when exposed to the small flame action, which seems promissory on avoiding fire spread on facades. Regarding the cone calorimeter experiments, (b), the results were not in line with the ignitability ones since samples of Aero.m ignite earlier than EPS.m. Unfortunately, as these tests were carried out during the stay in DTU (Denmark) and due to time constrains, it was not possible to repeat these tests; therefore, further research is needed in the cone calorimeter experiments with new samples.

The results of the fire exposure tests confirmed that EPS.m presents a worse insulating capacity during fire exposure than Aero.m by the shorter time required to reach 200°C in half-thickness of the samples (1100s for EPS.m vs. 1300s for Aero.m); this result may be a consequence of the decomposition of its polymeric compounds and, in particular, of the EPS particles. During the experimental procedures, EPS.m sample released a higher amount of smoke and stronger smell than Aero.m. A more accurate analyses on these parameters was not carried out due to lack of time, material and proper instrumentation for the analysis of the smoke released.

Table 12 shows a matrix which was developed in order to organize the results, to evaluate them and, finally, to be able to compare the performance of EPS and aerogel-based thermal mortars. For that, 13 parameters, both quantitative and qualitative, were identified from A to M and then a value was attributed according to the performance obtained in each the test, followed by a relative classification. This classification was made according to a colour scale: green – great performance; yellow – acceptable performance; read – bad performance. The greens were defined as low alterations (<5%) in performance when comparing the initial performance against the post-heated one (i.e. residual), or a great performance on fire reaction tests (e.g. in ignitability test the specimen did not ignite, so it was identified as green parameter). The yellow ones were considered when the safety of usage of the material post heating/ fire is comprised (i.e. decreasing more than 30% on its initial performance). The red highlight indicates that the material is highly degraded, under no condition of usage (e.g. on the fire exposure the smoke release was so high that the air near the test setup was irrespirable, that is why the qualitative parameter on that test was considered red). When a parameter was inconclusive on assessing the performance of the material it was identified with grey.

This comparison and evaluation (Table 12) can be important when choosing the most appropriate material to apply on a facade in order to know a range of parameters that allow a more informed choice. This need arises to complement the classification suggested at the European level by EN 13501-1 [32].

Table 12. Evaluation and summary of main results

RESULTS SUMMARY MATRIX

Tests		Parameters	ID	Lime.m REFERENCE	Aero.m	EPS.m
Characterization	Mechanical	$\sigma_{c.initial}$ / $\sigma_{c.residual}$	A	6.72 MPa / 6.44 Mpa ↓4%	0.32 Mpa / 0.04 Mpa ↓73%	0.16 Mpa / 0.03Mpa ↓92%
		Qualitative	B	To the eye it looked similar, but more prone to crumbling	The aerogel granules looked intact, however, the matrix seemed more fragile	Very fragile and shatter with a light touch. EPS granules completly burnt - disappear → eye-scale pores
	Thermophysical	$\rho_{initial}$ / $\rho_{residual}$	C	1676 Kg/m³ / 1617 Kg/m³ ≈	160 Kg/m³ / 131 Kg/m³ ↓18%	217 Kg/m³ / 161 Kg/m³ ↓26%
		$\lambda_{initial}$ / $\lambda_{residual}$	D	0.889 W/(m.K) / 0.643 W/(m.K) ↓28%	0.037 W/(m.K) / 0.040 W/(m.K) ↑8%	0.048 W/(m.K) / 0.046 W/(m.K) ↓3%
		$Cp_{initial}$ / $Cp_{residual}$	E	844 J/(Kg.K) / 849 J/(Kg.K) ≈	1078 J/(Kg.K) / 857 J/(Kg.K) ↓15%	1164 J/(Kg.K) / 1003 J/(Kg.K) ↓7%
		TGA - % mass loss	F	↓22%	↓36%	↓52%
Fire reaction		Fire Class (EN 13501-1)	G	A1	(-)	B
		Ignitability — F_s	H	(-)	F_s = 0. No ignition	(-)
		Gross calorific — PCS	I	(-)	6.19 ± 0.25 MJ/Kg ≠ results?: material heterogeneity + small size	(-)
		Bomb calorimeter — Heat release	J	(-)	4.30 MJ/Kg	(-)
		Cone Calorimeter — Time to ignition (Heat flux = 17.55 KW/m²)	K	(-)	8s	102s
Fire exposure		Qualitative	L	Few visible alterations apart from color	Average smoke release + some degradation	High smoke release + high degradation
		Quantitative	M	>40 min to reach 400℃ at 2cm thickness	30 min to reach 400℃ at 2cm thickness	22.6 min to reach 400℃ at 2cm thickness

Legend	(-) not tested	Not conclusive	Low performance	Acceptable performance	Great performance

It is worth mentioning that part the work developed within this dissertation was already published in "IV SImpósio – Argamassas e Soluções Térmicas de Revestimento" which took place in Coimbra during the 10th and 11th march and accepted in "TEST&E 2022 - 3º Congresso de Ensaios e Experimentação em Engenharia Civil".

6.3 Future developments

The study developed within this dissertation showed the potential danger of using EPS-based mortar in facades, especially because of their low fire performance, highlighting the need to develop alternative thermal mortars; in this context, it was showed that aerogel-based renders have the potential to be an alternative to the EPS-based ones, presenting an improved fire performance.

The results obtained in the present dissertation suggest the following path of research:

i) the analyses of commercial formulations of aerogel-based thermal mortars and the comparison with Aero.m would be profitable in order to understand what can be improved to develop a high fire performance aerogel-based thermal mortar;

ii) the optimization of the aerogel mortar formulation analyzed, namely regarding the reduction/replacement of its polymeric admixtures, may be a solution with the potential to originate a material with a better fire performance (similarly to other commercial aerogel mortar formulations available in the foreign market);

iii) to perform tests to evaluate the toxicity of smoke, concentrations of certain gases and measure the amount of smoke released. This topic is particularly relevant since the majority of deaths during fires is caused by gas poisoning;

iv) develop tests to evaluate the fire reaction behaviour of the entire coating system, i.e. mortar + base coat with the fiberglass mesh + finishing coat, in order to understand the expected performance of the whole system in a real situation.

To sum up, the suggestions consist in analyzing the gaps of performance in Aero.m by comparing it with commercial mortars and testing new formulations, followed by the new fire behavior tests on this new formulation and then the evaluation of the entire system.

The development of optimized formulations of aerogel-based thermal mortars, accompanied by specific tests to determine their reaction to fire class, will contribute to improve the safety of buildings with these systems and to expand the field of application of these innovative mortars.

References

[1]   United Nations, Global Alliance for Buildings and Construction 2020 Global Status Report for Buildings and Construction Towards a zero-emissions, efficient and resilient buildings and construction sector, 2020. http://www.un.org/Depts/.

[2]   N. White, M. Delichatsios, M. Ahrens, A. Kimball, Fire hazards of exterior wall assemblies containing combustible components, MATEC Web Conf. 9 (2013). https://doi.org/10.1051/matecconf/20130902005.

[3]   M. Bonner, G. Rein, Flammability and multi-objective performance of building façades: Towards optimum design, Int. J. High-Rise Build. 7 (2018) 363–374. https://doi.org/10.21022/IJHRB.2018.7.4.363.

[4]   M. Bonner, W. Wegrzynski, B.K. Papis, G. Rein, KRESNIK: A top-down, statistical approach to understand the fire performance of building facades using standard test data, Build. Environ. 169 (2020). https://doi.org/10.1016/J.BUILDENV.2019.106540.

[5]   N.N. Brushlinsky, M. Ahrens, S. V. Sokolov, P. Wagner, World Fire Statistics, Center of Fore Statistics (CTIF) Report N°26, 2021.

[6]   N. Hopkins, Huge concentrations' of toxins found in Grenfell soil, Guard. (2018). https://www.theguardian.com/uk-news/2018/oct/12/toxins-found-ingrenfell-   tower-soil-study-finds (accessed 8 September 2021).

[7]   A.A. Stec, K. Dickens, J.L.J. Barnes, C. Bedford, Environmental contamination following the Grenfell Tower fire, Chemosphere. 226 (2019). https://doi.org/10.1016/j.chemosphere.2019.03.153.

[8]   T. Herzog, R. Krippner, W. Lang, Facade construction manual, Gruyter, 2012.

[9]   CEN, EN 1998-1: Design of structures for earthquake resistance, CEN. (1998).

[10]   J. Appleton, Estruturas de Betão, Orion, Lisbon, 2013.

[11]   A. Allouhi, A. Boharb, R. Saidur, T. Kousksou, A. Jamil, 5.1 Energy Auditing, in: Compr. Energy Syst., Elsevier, 2018: pp. 1–44. https://doi.org/10.1016/B978-0-12-809597-3.00503-4.

[12]   M.K. Najjar, K. Figueiredo, A.W.A. Hammad, V.W.Y. Tam, A.C.J. Evangelista, A. Haddad, A framework to estimate heat energy loss in building operation, J. Clean. Prod. 235 (2019) 789–800. https://doi.org/10.1016/J.JCLEPRO.2019.07.026.

[13]   F. Kuznik, K. Johannes, B. Lamrani, Integrating phase change materials in thermal energy storage

systems for buildings, Adv. Therm. Energy Storage Syst. (2021) 381–422. https://doi.org/10.1016/B978-0-12-819885-8.00013-9.

[14] M. do R. Veiga, C. Pina dos Santos, Revestimentos de isolamento térmico de fachada: Eficiência, durabilidade e comprovação de qualidade, Construção Mag. (2009).

[15] V. Kodur, P. Kumar, M.M. Rafi, Fire hazard in buildings: review, assessment and strategies for improving fire safety, PSU Res. Rev. 4 (2019) 1–23. https://doi.org/10.1108/PRR-12-2018-0033.

[16] D. Madrzykowski, Fire Dynamics: The Science of Fire Fighting, Int. Fire Serv. J. Leadersh. Manag. 7 (2013).

[17] T.T. Lie, Fire Temperature-Time Relations, Report, National Research Coucil Canada, Institute for Research in Construction, 1988.

[18] International Fire Service Training Association, Fire and Emergency Services Orientation and Terminology, 6th ed., 2016.

[19] International Organization for Standardization, ISO 834-1: Fire-Resistance Tests - Elements of Building Construction - Part 1: General Requirements, (1999).

[20] B.S. Institution, British Standard 476, Part 20, Method for determination of the fire resistance of elements of construction (General principles), (1987).

[21] American Society for Testing Materials, ASTM E119-11: Standard Test Methods for Fire Tests of Building Construction and Materials, (2010).

[22] National Fire Protection Association (NFPA), NFPA 251, Fire Tests of Building Constructions and Materials, (1995).

[23] S.E. Magnusson et al., Temperature–time curves of complete process of fire development. Bulletin 16, Inst. Technol. (1970).

[24] C.R. Barnett, Replacing international temperature-time curves with BFD curve, Fire Saf. J. 42 (2007) 321–327. https://doi.org/10.1016/J.FIRESAF.2006.11.001.

[25] J. Zehfuss, D. Hosser, A parametric natural fire model for the structural fire design of multi-storey buildings, Fire Saf. J. 42 (2007) 115–126.

[26] I. Oleszkiewicz, Fire exposure to exterior walls and flame spread on combustible cladding, Fire Technol. 26 (1990) 357–375. https://doi.org/10.1007/BF01293079.

[27] D.T. Yung, I. Oleszkiewicz, Fire spread via exterior walls of buildings, in: Proc. 4th Conf. Build. Sci. Technol., 1988.

[28]   CEN, BS EN ISO 11925-2: Reaction to fire tests — Ignitability of products subjected to direct impingement of flame, (2010).

[29]   CEN, EN 13823: Reaction to fire tests for building products. Building products excluding floorings exposed to the thermal attack by a single burning item, (2020).

[30]   CEN, EN ISO 1182: Reaction to fire tests for products — Non-combustibility test, (2020).

[31]   CEN, BS EN ISO 1716: Reaction to fire tests for products - Determination of the gross heat of combustion (calorific value), (2010).

[32]   CEN, EN 13501-1: Fire classification of construction products and building elementes - Part 1: Classification using data from reaction to fire teste, (2009).

[33]   CEN, EN 1992-1-1: Design of Concrete Structures, (1992).

[34]   European Comission, The European Green Deal, Brussels-Belgium, 2019.

[35]   UNFCCC, Adoption of Paris Agreement - Paris Agreement, 2015.

[36]   COM, Energy Efficiency Plan 2011, Brussels-Belgium, 2011.

[37]   European Comission, DIRECTIVE (EU) 2018/844 Of the European Parliament and of the Council of 30 May 2018, (2018).

[38]   The Economist, Investing in energy efficiency in Europe's buildings: A view from the construction and real estate sectors, 2013. www.gbpn.org.

[39]   R. Pasker, The European ETICS market-Do ETICS sufficiently contribute to meet political objectives?, in: 4th Eur. ETICS-Forum, EAE, Warsaw, 2017.

[40]   Pordata, Edifícios segundo os CENSOS, Pordata. (2018). https://www.pordata.pt/Portugal/Edifícios+segundo+os+Censos+total+e+por+época+de+construç ão-93 (accessed 19 September 2021).

[41]   Decreto-Lei 40/90 de 6 de fevereiro, Diário Da República - Série I, N°31. (1990) 490–504.

[42]   Decreto-Lei 118/2013 de 20 Agosto: Regulamento de Desempenho Energético dos Edifícios de Habitação (REH), (2013).

[43]   ARUP, Museums and Galleries | U-Value Guide Museums and Galleries U-Value Guide, (2018).

[44]   APFAC, (n.d.). https://www.apfac.pt/ (accessed 26 March 2022).

[45]   V.P. de Freitas, Manual de Apoio ao Projecto de Reabilitação de Edifícios Antigos, OERN, 2012.

[46]   M. O'Grady, A.A. Lechowska, A.M. Harte, Quantification of heat losses through building envelope

thermal bridges influenced by wind velocity using the outdoor infrared thermography technique, Appl. Energy. 208 (2017) 1038–1052. https://doi.org/10.1016/j.apenergy.2017.09.047.

[47] EURIMA, U-values For Better Energy Performance of Buildings - Report established by ECOFYS for EURIMA, (2007).

[48] J. Yu, C. Yang, L. Tian, D. Liao, A study on optimum insulation thicknesses of external walls in hot summer and cold winter zone of China, Appl. Energy. 86 (2009) 2520–2529. https://doi.org/10.1016/j.apenergy.2009.03.010.

[49] I. Nardi, E. Lucchi, T. de Rubeis, D. Ambrosini, Quantification of heat energy losses through the building envelope: A state-of-the-art analysis with critical and comprehensive review on infrared thermography, Build. Environ. 146 (2018) 190–205. https://doi.org/10.1016/j.buildenv.2018.09.050.

[50] E. Barreira, V.P. de Freitas, External Thermal Insulation Composite Systems (ETICS), Springer, 2016.

[51] E. Cuce, P.M. Cuce, C.J. Wood, S.B. Riffat, Toward aerogel based thermal superinsulation in buildings: A comprehensive review, Renew. Sustain. Energy Rev. 34 (2014). https://doi.org/10.1016/j.rser.2014.03.017.

[52] M.G. Gomes, I. Flores-Colen, H. Melo, A. Soares, Physical performance of industrial and EPS and cork experimental thermal insulation renders, Constr. Build. Mater. 198 (2019) 786–795.

[53] APFAC, Manual ETICS, (2021).

[54] CEN, EN 998-1: Specification for mortar for masonry-Part 1: Rendering and plastering mortar, Specif. Mortar Masonry-Part 1 Render. Plaster. Mortar. (2016).

[55] C. Buratti, E. Moretti, E. Belloni, Aerogel Plasters for Building Energy Efficiency, Nano Biotech Based Mater. Energy Build. Effic. (2016) 17–40. https://doi.org/10.1007/978-3-319-27505-5_2.

[56] U. Berardi, Aerogel-enhanced systems for building energy retrofits: Insights from a case study, Energy Build. 159 (2018) 370–381. https://doi.org/10.1016/J.ENBUILD.2017.10.092.

[57] European Comission, Comission Recommendation of 18 October 2011 on the definition of nanomaterial, Off. J. Eur. Union. (2011). http://ec.europa.eu/health/scientific_committees/emerging/docs/.

[58] J. Alemán, A. V. Chadwick, J. He, M. Hess, K. Horie, R.G. Jones, P. Kratochvíl, I. Meisel, I. Mita, G. Moad, S. Penczek, R.F.T. Stepto, Definitions of terms relating to the structure and processing of sols, gels, networks, and inorganic-organic hybrid materials (IUPAC recommendations 2007), Pure Appl.

Chem. 79 (2007) 1801–1829. https://doi.org/10.1351/pac200779101801.

[59]   S.S. Kistler, Coherent Expanded Aerogels and Jellies, Nature. 127 (1931).

[60]   M. Rubin, C.M. Lampert, Transparent silica aerogels for window insulation, Sol. Energy Mater. 7 (1983) 393–400. https://doi.org/10.1016/0165-1633(83)90012-6.

[61]   S.Q. Zeng, A.J. Hunt, W. Cao, R. Greif, Pore Size Distribution and Apparent Gas Thermal Conductivity of Silica Aerogel, J. Heat Transfer. 116 (1994) 756–759. https://doi.org/10.1115/1.2910933.

[62]   G.M. Pajonk, Transparent silica aerogels, J. Non. Cryst. Solids. 225 (1998) 307–314. https://doi.org/10.1016/S0022-3093(98)00131-8.

[63]   A. Soleimani Dorcheh, M.H. Abbasi, Silica aerogel; synthesis, properties and characterization, J. Mater. Process. Technol. 199 (2008) 10–26. https://doi.org/10.1016/J.JMATPROTEC.2007.10.060.

[64]   J. Frickle, Aerogels — highly tenuous solids with fascinating properties, J. Non-Crystalline Solids . 100 (1988) 169–173.

[65]   J. Fricke, A. Emmerling, Aerogels, J. Am. Ceram. Soc. 75 (1992) 2027–2035.

[66]   S.S. Kistler, A.G. Caldwell, Thermal Conductivity of Silica Aërogel, Ind. Eng. Chem. 26 (1934). https://doi.org/10.1021/ie50294a016.

[67]   F. Orsini, P. Marrone, F. Asdrubali, M. Roncone, G. Grazieschi, Aerogel insulation in building energy retrofit. Performance testing and cost analysis on a case study in Rome, Energy Reports. 6 (2020) 56–61. https://doi.org/10.1016/J.EGYR.2020.10.045.

[68]   K. Richter, P.M. Norris, C.-L. Tien, Aerogels: Applications, Structure, and Heat Transfer Phenomena, Annu. Rev. Heat Transf. 6 (1995). https://doi.org/10.1615/AnnualRevHeatTransfer.v6.40.

[69]   B.K. et al. Ramakrishnan, Modern Aerogels, 2008.

[70]   E. Strobach, B. Bhatia, S. Yang, L. Zhao, E.N. Wang, High temperature stability of transparent silica aerogels for solar thermal applications, APL Mater. 7 (2019) 081104. https://doi.org/10.1063/1.5109433.

[71]   C. Folgar, D. Folz, C. Suchicital, D. Clark, Microstructural evolution in silica aerogel, J. Non. Cryst. Solids. 353 (2007) 1483–1490. https://doi.org/10.1016/j.jnoncrysol.2007.02.047.

[72]   H. Cai, Y. Jiang, J. Feng, S. Zhang, F. Peng, Y. Xiao, L. Li, J. Feng, Preparation of silica aerogels with high temperature resistance and low thermal conductivity by monodispersed silica sol, Mater. Des. 191 (2020) 108640. https://doi.org/10.1016/j.matdes.2020.108640.

[73]   D.-D. Ye, T. Wang, W. Liao, H. Wang, H.-B. Zhao, Y.-T.Y.-Z. Wang, S. Xu, Y.-T.Y.-Z. Wang, Ultrahigh-

Temperature Insulating and Fire-Resistant Aerogels from Cationic Amylopectin and Clay via a Facile Route, ACS Sustain. Chem. Eng. 7 (2019) 11582–11592. https://doi.org/10.1021/acssuschemeng.9b01487.

[74]   J. Ma, F. Ye, C. Yang, J. Ding, S. Lin, B. Zhang, Q. Liu, Heat-resistant, strong alumina-modified silica aerogel fabricated by impregnating silicon oxycarbide aerogel with boehmite sol, Mater. Des. 131 (2017) 226–231. https://doi.org/10.1016/j.matdes.2017.06.036.

[75]   D. Del Curto, V. Cinieri, Aerogel-Based Plasters and Energy Efficiency of Historic Buildings. Literature Review and Guidelines for Manufacturing Specimens Destined for Thermal Tests, Sustainability. 12 (2020). https://doi.org/10.3390/su12229457.

[76]   J.M. Schultz, K.I. Jensen, Evacuated aerogel glazings, Vacuum. 82 (2008). https://doi.org/10.1016/j.vacuum.2007.10.019.

[77]   N.D. Kaushika, K. Sumathy, Solar transparent insulation materials: a review, Renew. Sustain. Energy Rev. 7 (2003). https://doi.org/10.1016/S1364-0321(03)00067-4.

[78]   S. Svendsen, Solar collector with monolithic silica aerogel, J. Non. Cryst. Solids. 145 (1992). https://doi.org/10.1016/S0022-3093(05)80464-8.

[79]   Y. Liang, H. Wu, G. Huang, J. Yang, H. Wang, Thermal performance and service life of vacuum insulation panels with aerogel composite cores, Energy Build. 154 (2017). https://doi.org/10.1016/j.enbuild.2017.08.085.

[80]   P. Zhu, S. Brunner, S. Zhao, M. Griffa, A. Leemann, N. Toropovs, A. Malekos, M.M. Koebel, P. Lura, Study of physical properties and microstructure of aerogel-cement mortars for improving the fire safety of high-performance concrete linings in tunnels, Cem. Concr. Compos. 104 (2019) 103414. https://doi.org/10.1016/j.cemconcomp.2019.103414.

[81]   T. Stahl, S. Brunner, M. Zimmermann, K. Ghazi Wakili, Thermo-hygric properties of a newly developed aerogel based insulation rendering for both exterior and interior applications, Energy Build. 44 (2012) 114–117. https://doi.org/10.1016/j.enbuild.2011.09.041.

[82]   J. Yang, H. Wu, X. Xu, G. Huang, T. Xu, S. Guo, Y. Liang, Numerical and experimental study on the thermal performance of aerogel insulating panels for building energy efficiency, Renew. Energy. 138 (2019). https://doi.org/10.1016/j.renene.2019.01.120.

[83]   EMPA, Technical data sheet: Fixit 222, (2017). www.fixit.ch (accessed 26 March 2022).

[84]   M. Ibrahim, E. Wurtz, P.H. Biwole, P. Achard, H. Sallee, Hygrothermal performance of exterior walls

covered with aerogel-based insulating rendering, Energy Build. 84 (2014) 241–251. https://doi.org/10.1016/J.ENBUILD.2014.07.039.

[85]   K. Ghazi Wakili, T. Stahl, E. Heiduk, M. Schuss, R. Vonbank, U. Pont, C. Sustr, D. Wolosiuk, A. Mahdavi, High performance aerogel containing plaster for historic buildings with structured façades, Energy Procedia. 78 (2015) 949–954. https://doi.org/10.1016/J.EGYPRO.2015.11.027.

[86]   C. Buratti, E. Moretti, E. Belloni, F. Agosti, Development of Innovative Aerogel Based Plasters: Preliminary Thermal and Acoustic Performance Evaluation, Sustainability. 6 (2014) 5839–5852. https://doi.org/10.3390/su6095839.

[87]   Arte e Mestieri Snc., Technical data sheet: Tilica pasta, (n.d.). https://www.naturalcalk.com/tillica/.

[88]   Fucine Architettura Design, Building Bonuses 2020 - Façade bonus, Eco Bonus, Anti-Seismic Bonus - FAD - Fucine Architettura Design, (2020). https://www.fucinead.it/en/building-bonuses-2020-facade-bonus-eco-bonus-anti-seismic-bonus/ (accessed 29 March 2022).

[89]   R. Nosrati, U. Berardi, Long-term performance of aerogel-enhanced materials, Energy Procedia. 132 (2017) 303–308. https://doi.org/10.1016/j.egypro.2017.09.733.

[90]   Austalian Government, Senate Economics References Committee's Inquiry into Non-Conforming Building Products Government Response to the Final Report: Non-conforming building products-the need for a coherent and robust regulatory regime, 2020. www.abcb.gov.au.

[91]   S. Sassi, P. Setti, G. Amaro, L. Mazziotti, G. Paduano, P. Cancelliere, M. Madeddu, Fire safety engineering applied to high-rise building facades, MATEC Web Conf. 46 (2016) 4002. https://doi.org/10.1051/matecconf/20164604002.

[92]   L. Peng, Z. Ni, X. Huang, Review on the Fire Safety of Exterior Wall Claddings in High-rise Buildings in China, Procedia Eng. 62 (2013) 663–670. https://doi.org/10.1016/j.proeng.2013.08.112.

[93]   S. Colwell, T. Baker, Fire performance of external thermal insulation for walls of multistorey buildings, 3rd ed., 2013.

[94]   V. Babrauskas, The Grenfell Tower Fire and Fire Safety Materials Testing, (2018). https://digital.fireengineering.com/fireengineering/201801/MobilePagedArticle.action?articleId=1306692#articleId1306692 (accessed 31 March 2022).

[95]   J. Zehfuß, C. Northe, O. Riese, An investigation of the fire behavior of ETICS facades with polystyrene under fire loads of different size and location, Fire Mater. 42 (2018) 508–516. https://doi.org/10.1002/FAM.2499.

[96] L. Zhou, A. Chen, X. Liu, F. Zhang, The Effectiveness of Horizontal Barriers in Preventing Fire Spread on Vertical Insulation Panels Made of Polystyrene Foams, Fire Technol. 52 (2016) 649–662. https://doi.org/10.1007/S10694-015-0478-X.

[97] M. Pedroso, I. Flores-Colen, J.D. Silvestre, M.G. Gomes, L. Silva, L. Ilharco, Physical, mechanical, and microstructural characterisation of an innovative thermal insulating render incorporating silica aerogel, Energy Build. 211 (2020) 109793. https://doi.org/10.1016/j.enbuild.2020.109793.

[98] Enersens, Product data sheet: Aerogel kwark, (2015). available: http://enersens.fr/en/home/.

[99] M. Pedroso, Eco-efficient and multifunctional thermal renders based on silica aerogel and fibres - Phd Thesis, Instituto Superior Técnico, 2021.

[100] Saint-Gobain Weber, Technical data sheet: Webercal classic (in Portuguese), (2020). www.pt.weber.

[101] Saint-Gobain Weber, Technical data sheet: WeberTherm Aislone (in Portuguese), (2018). www.weber.com.pt.

[102] CEN, EN 1015-2: Methods of test for mortar for masonry Part 2: Bulk sampling of mortars and preparation of test mortars, (1998).

[103] CEN, EN 1015-11: Methods of test for mortar for masonary - Part 11: Determination of ŕexural and compressive strength of hardened mortar, (1999).

[104] Applied Precision Ltd., Isomet 2114 Thermal properties analyser user's guide, Version 1.46, (2011). www.Manualslib.com.

[105] CEN, EN 1015-10: 1999 - Methods of test for mortar for masonry - Part 10: Determination of dry bulk density of hardened mortar, (1999).

[106] S.A. Speakman, Introduction to X-Ray Powder Diffraction Data Analysis, (n.d.). http://prism.mit.edu/xray (accessed 4 April 2022).

[107] X-ray Diffraction Techniques, (n.d.). https://www.doitpoms.ac.uk/tlplib/xray-diffraction/index.php (accessed 4 April 2022).

[108] J.D.B. O'Sullivan, J. Behnsen, T. Starborg, A.S. MacDonald, A.T. Phythian-Adams, K.J. Else, S.M. Cruickshank, P.J. Withers, X-ray micro-computed tomography (µCT): an emerging opportunity in parasite imaging, Parasitology. 145 (2018) 848–854. https://doi.org/10.1017/S0031182017002074.

[109] W. Zhou, R.P. Apkarian, Z. Lin Wang, D. Joy, Fundamentals of Scanning Electron Microscopy, (2006).

[110] LNEC, Caracterização Metrológica e Avaliação de Incertezas no Laboratório de Ensaios de Reação ao fogo (LNEC/LERF) Ensaio de ignitabilidade, Lisbon, 2008.

[111]   Z. Wu, K.H. Khayat, C. Shi, B.F. Tutikian, Q. Chen, Mechanisms underlying the strength enhancement of UHPC modified with nano-SiO2 and nano-CaCO3, Cem. Concr. Compos. 119 (2021) 103992. https://doi.org/10.1016/j.cemconcomp.2021.103992.

[112]   E. Tajuelo Rodriguez, K. Garbev, D. Merz, L. Black, I.G. Richardson, Thermal stability of C-S-H phases and applicability of Richardson and Groves' and Richardson C-(A)-S-H(I) models to synthetic C-S-H, Cem. Concr. Res. 93 (2017) 45–56. https://doi.org/10.1016/j.cemconres.2016.12.005.

[113]   C. Sánchez, Numerical modelling of the thermomechanical behaviour of GFRP pultruded profiles subjected to fire, Universidade de Lisboa - Instituto Superior Técnico, 2017.

[114]   EN 1993-1-2: Eurocode 3: Design of steel structures - Part 1-2: General rules - Structural fire design, (1993).

[115]   D. V. Schroeder, J.K. Pribram, An Introduction to Thermal Physics, Am. J. Phys. 67 (1999) 1284–1285. https://doi.org/10.1119/1.19116.

Annexes

A1 Collection of fire incidents on building façades: 1990 - 2022

| ID	Year	Building	Country	Description	Deads	Injuries	Nº floors affected
1	1990	393 Kennedy St	Canada	8-storey apamnent buildiing with an open-air parking garage located on the Ground Floor. The building's exterior walls were covered with an Exterior Insulation and Finish System. The foam insulation was typically 75 mm	n/a	n/a	4
2	1991	Mercantile Credit Building	UK	The 12 storey high building was of composite steel and concrete construction. The columns and the composite floor beams had applied fire protection but the soffit of the floor slab was unprotected.	n/a	n/a	3
3	1991	Knowsley Heights	UK	An 11-storey block built in 1963 and in 1988 was extensively refurbished as part o f a scheme t o reduce energy consumption which involved the use of a Class 0 GRP rainscreen cladding on aluminium support rails.	0	0	n/a
4	1993	Sun Valley Poultry Factory	UK	It was refurbished in 1990 for meat processing and cold storage. The construction was the typical single storey brick and steel clad with steel roof. Wall and ceiling linings were of composite steel-faced panels containing a range of insulation materials. The panels used for the walls and ceilings were either polyurethane or polystyrene. At the time of the fire there was a deliberate policy to replace ali the panels with polystyrene insulated ones and 25% had been completed.	2	n/a	n/a
5	1996	Düsseldorf Airport fire	Germany	the fire began when a welder working on expansion plates in a roadway above the lower level of the terminal building ignited the polystyrene insulation used in the void above the ceiling on the first level	17	62	n/a
6	1996	Motomachi Apartments	Japan	The fire started in na apartment unit on the 9th floor of a 20 story building and developed to the 20th floor through the balconies in 30 min. The investigations concluded that the principal source of spread were the combustibles on the balconies which had a 8-20mm thick of polymetacrylic (PMMA) fence.	0	2	12
7	1997	Eldorado Hotel-Casino	USA	The facade was reported as being "plastic" in newpaper reports. Indeed, it was believed to be hard coat polyurethane over EPS but there is no detailed information about it. The fire only occured on the façade and did not spread to the building's interior.	0	0	n/a
8	1998	Palace Station Hotel and Casino	USA	The 20 storey hotel fire was confined to the outside of the building. The facade was the only thing that burned. It was specified that polyurethane foam and urethane coated EPS was used.	0	0	n/a
9	1999	Garnock Court fire	Scotland	A 14-storey block of flats. The fire spread via the external cladding, reaching the 12th floor within ten minutes of the start of the fire. In order to eliminate thermal issues and also to improve visual appearance, new window frames of un plastised polyvinylchloride (uPVC) were fixed. The exterior walla round the window was covered with glass reinforced polyester plastic sheet.	1	4	7
10	2002	Tip Top Bakery	Australia	It was na one level factory with a floor area of 10 000m2. The walls and in some areas the roof were constructed of polyestyrene insulated sandwich panels which has caused the rapid fire spread.	0	1	n/a
11	2003	Telstar House	UK	Telstar House is a Thirteen Storey Steel framed concrete Office Building	0	3	4
12	2004	Parque Central Complex	Venezuela	The fire destoyed 16 of the 56 floors government office building. Reinforced concrete building with steel deck floors supported by steel beams.	0	25	17
13	2005	Windsor Tower (Madrid)	Spain	32-story tower framed in steel-reinforced concrete. During this refurbishment work a fire broke out on the 21st floor. The fire spread downwards to the 2nd floor, and upwards to the top of the building. It burnt for some 19 hours and engulfed the entire building.	0	7	32
14	2005	Treskow Strasse Pankow Flats	Germany	The fire started on the second floor of this 7 storey block of flats and spread rapidly (less than 20 min) on the façade to the entire height of the building. The insulating system consisted of 80 millimeters flame retarded expanded polystyrene which was encased with an external mesh and a thin rendering layer.	2	3	5
15	2007	Water Club Tower, Borgata Casino Hotel	USA	A 43-story Borgata hotel tower under construction in Atlantic City. Local fire officials said they never determined what had caused the fire, but concluded the building's combustible exterior panels helped fuel it. The Borgata had used the Alucobond brand of panels made by Alcan Composites, later renamed 3A Composites.	n/a	n/a	39

16	2008	Monte Carlo Hotel	USA	On 25 January 2008, the exterior wall near the roof of the 32-story Monte Carlo Hotel and Casino was ignited by welding activities. Exterior insulation and finish systems (EIFS) were installed at the exterior wall cladding. The polystyrene and polyurethane portions of the EIFS panels and trim installed on the building burned along with the building's parapet.	n/a	n/a	4
17	2008	De Punt	Netherlands	A large commercial building. The Committee of Inquiry has not given an opinion on the exact cause of the fire, but has made a number of provisional conclusions. Many of these relate to the materials used in the construction of the building, whose roof was made of so-called sandwich insulation panels containing polyurethane foam insulation. Built with steel supporting construction the side walls of the building were made largely of profiled steel plate and the lower sections consisted of cavity wall. The roof was built using coated sandwich panels, consisting of two steel plates 0.4 to 0.5 mm thick, with an intermediate layer of polyurethane foam (PUR) 9 cm thick, serving as insulation.	3	0	n/a
18	2009	Beijing Television Cultural Center	China	The fire was initiated on the roof of the 44 story building by fireworks. The sparks from the fireworks on the roof penetrated the metal panels and ignited the insulation materials (extruded polystyrene (XPS) foam) and waterproof sheets (EPDM rubber). There was a cavity between the metal panel and the insulation layers. It was reported that the melting and burning droplets of XPS flew down the facades	1	7	44
19	2009	Lakanal House	UK	A 14 storey tower block. The fire had started in a television in a ninth-floor flat, spread through the 1958-built block of 98 maisonettes with a ferocity that baffled firefighters and terrified residents. An inquest into the deaths found the fire spread unexpectedly fast, both laterally and vertically, trapping people in their homes, with the exterior cladding panels burning through in just four and a half minutes	6	20	n/a
20	2009	Kozepszer Street Flats	Hungary	An eleven storey residential building with a façade made of polystyrene based EIFS was exposed to an external fire. The fire started in a 6th floor apartment kitchen and spread on the combustible façade up to the top of the building	3	n/a	6
21	2010	Al Kuwait Tower	UAE	14-storey residential building. The fire gutted 10 floors	n/a	n/a	10
22	2010	Wooshin Golden Suites	South Korea	The structure was made of steel and in some parts with reinforced concrete. The 38 storie building was made with a curtain wall facade with metal composite panels consisting of aluminium with 3 mm polyethylene core. The fire started on the 4th floor and it took 20 min to reach the top.	0	5	35
23	2010	Immigrant hostel	France	a nine storey immigrant hostel. The fire was reported to spread from a burning waste container over the façade. The EIFS system with expanded polystyrene insulation generated a rapid vertical propagation of fire and significant smoke spread throughout the building. It was concluded that Neither the thin organic render applied on the façade, nor the mineral wool fire barriers were effective in preventing the flames from igniting the insulation and spreading upwards along the façade.	7	11	n/a
24	2010	Jiaozhou Road	China	28-storey residential building in Shanghai. At the time of the fire, the building was undergoing renovations for the installation of exterior wall insulations (polyurethane (PU) foam). It is believed that the fire was caused by welding sparks which ignited the insulation chips or the wood and bamboo scaffolding on the 9th/10th floor. The insulation materials were highly flammable with good access to air supply, and the fire spread externally at a rapid rate. It was reported that the fire spread to the roof in 4 minutes, and within 14 min the entire north-facing facade was utterly burned out.	58	71	28
25	2011	Royal Wanxin Hotel	China	A 219 m high building that housed a 5 star hotel. The Shenyang government said in a statement that the fire was triggered by fireworks that ignited material on the exteriors of the buildings	n/a	n/a	n/a
26	2012	Apartment building	Romania	A 10-storey block of flats façade caught on fire. ccording to the fire brigade investigators the fire started on a mercantile storage space placed on the ground level of the building in the proximity of the façade elements. The EIFS system containing expanded polystyrene was lit on a short time following the ignition and rapidly propagated on the west side of the combustible façade. It was noted that the fire propagation to the upmost level of the flat took nearly 10 minutes.	n/a	n/a	n/a

#	Year	Name	Country	Description			
27	2012	Al Baker Tower	UAE	The fire at the 25-storey Al Baker Tower 4. According to the report, out of a total of 125 apartments, 51 were completely gutted. The fire destroyed 2 of the 40 storey Al Tayer Tower. Flammable cladding materials, comprising plastic or polyurethane fillings – called a thermo-plastic core – sandwiched between aluminium panels, have been blamed for spreading fires at both the Al Baker Tower 4 and the Al Tayer Tower in Sharjah.	n/a	n/a	n/a
29	2012	Mermoz Tower	France	The 18-story residential Mermoz Tower was refurbished in 2003 and metal composite cladding was installed on a part of the exterior wall including walls within the balconies. The cladding above the first story was 3 mm thick polyethylene core sandwiched between two 0.5 mm (0.02 in) thick aluminum sheets. A domestic fire started on a 2nd story balcony on 14 May 2010. The fire spread rapidly to the top of the building.	1	6	17
30	2012	Polat Tower	Turkey	A large blaze broke out in a 42-story tower block in the center of Istanbul. The blaze started on the ground floor caused by a faulty air conditioning unit and tore up one side of the building clad with alluminuem composite materials (ACM). State-run TRT television said the fire, fanned by winds, tore through the building's external wall insulation	0	0	n/a
31	2012	Saif Belhasa Building	UAE	It was a 13 storey residential building clad with metal composite panels consistin of aluminium with a polyethylene core. The fire started in the 4th floor and rapidly spread until the top of the building.	0	2	9
32	2012	Tamweel Tower	UAE	A mixed use building with 34 floors clad with metal composite panels consisting of aluminium wtih a polyethylene core. The fire started at the roof and spread down the exterior of the building.	0	0	n/a
33	2013	Karlstad Hospital	Sweden	The incident took place on a new part of the hospital that was under construction. The EIFS with polystyrene insulation has been chosen to decorate the external part of the building. The combustible façade insulating system allowed the fire to rapidly spread up the outside of the construction. Moreover, the flaming droplets and burning parts of polystyrene caused the development of new small fires over the scaffolding mounted in the proximity of the blazing façade	n/a	n/a	n/a
34	2013	Grozny-City Towers	Russia	A 40 storey tower. It is believed that a short circuit caused the fire and that it spread quickly due to "plastic sheathing and insulation" on the building, but no more details about the exterior cladding were specified.	0	0	40
35	2013	Al Hafeet Tower 2	UAE	A 20-storey tower in Sharjah's Al Taawun. The fire broke at the 7th floor. "Three residents who hail from an African country have been detained on charges of causing the fire. They were trying to make hookah fire. Sparks from the hookah coals touched off fire in the aluminium foils that covered the building façade and soon it spread very fast through the areas covering the piped gas line," said residents who witnessed the fire.	0	n/a	10
36	2014	Krasnoyarsk Apartments	Russia	25 floor apartment block. The fire started at around 1pm local time, but the cause was not immediately known. It began on the lower floors and spread up the building, according to an eyewitness. A spokesperson for the local emergency response team said that the materials cladding the tower were responsible for the fire rapid movement, as well as the thick smoke: vinyl siding and plastic-furnished balconies	1	n/a	25
37	2014	Lacrosse Building	Australia	23-storey apartment building. he fire started via an unextinguished cigarette disposed in a plastic containeron the 6th floor balcony which spread to the timber table top. Aluminium composite panels with apolyethylene core were installed on the side wall of the balcony. Once the fire ignited the external wallcladding, it rapidly spread vertically up the building.	0	0	16
38	2015	The Marina Torch	UAE	The Torch is a 79-storey skyscraper, one of the world's tallest residential towers. n investigation by the management of the Torch after its 2015 fire found that most of the damage was to the cladding (cladding panels with thermoplastic cores), exterior panelling used for decoration or insulation.	0	7	60
39	2015	Baku Residential Flats	Azerbaijan	16-storey building. Authorities blamed the fire-prone exteriors as it was the second case of a residential building bursting into flames. The cladding panels containing polyurethane reportedly produced toxic gas, resulting in the death of those trapped inside the building.	16	63	n/a
40	2015	Al Nasser Tower	UAE	26 floors of the32-storey building were destroyed. A top civil defence department official has blamed the contractor for using banned highly inflammable construction material for the project	0	40	26

C

|							
41	2015	Address Downtown Hotel	UAE	An electrical short circuit on a spotlight was the cause of a fire that engulfed The Address Downtown Dubai hotel. The reason, building and safety experts say, is the material used for the buildings' sidings, called aluminum composite panel cladding.	0	15	n/a
42	2016	Ajman One Complex	UAE	Flames destroyed two 26-storey towers	0	n/a	n/a
43	2016	Sulafa Tower	UAE	75-storey tower. More than 30 floors were affected by the fire. The building was covered with aluminum composite panels (ACP)	1	n/a	30
44	2016	Shepherds Court	UK	A faulty tumble dryer is believed to have sparked a fire that led to people evacuating an 18-storey tower block in west London. The fire spread from the seventh floor via the outside of the building. The fire experts found that panels withstood initial contact with fire but as it developed further, the polystyrene foam under the thin metal sheet began to melt. The metal sheet could then fall away exposing the foam and plywood beneath.	0	1	3
45	2016	Neo Soho Project	Indonisia	Several floors of the Neo Soho apartment building, located by the Central Park superblock in Tanjung Duren, West Jakarta, were engulfed in flame. Fire has spread externally by means of flammable cladding on the outside of a building.	0	0	7
46	2016	Al Bandary Tower B	UAE	23-storey Al Bandary Twin Towers. The fire broke out on the 13th floor of Al Bandary Twin Towers B and quickly spread to some of the upper floors. It was brought under control in 75 minutes. The material is a form of aluminium composite panel cladding	0	4	n/a
47	2016	Oceana Adriatic Building	UAE	Oceana is a beach front resort community and a triangular-shaped luxury residential complex consisting of seven buildings (15 storey). It was believed to have started in a coffee machine in a penthouse apartment, triggered by an electrical fault. The spread of the fire was aided by flammable exterior cladding	0	0	n/a
48	2016	Longsheng Building	China	office building. Black smoke billows down the side of the structure, which measures more than 492 fee. The facade is described as being 'metal' but no more information was found.	0	0	n/a
49	2017	Address Residences Fountain Views	UAE	An under construction tower. the blaze that broke out between the fifth and the seventh floor of Fountain Views. A large plume of black smoke is still visible hours after the blaze broke out. Experts have pinned blame for such fires on flammable building materials, specifically non-fire-rated aluminum panel	0	0	3
50	2017	Grenfell Tower fire	UK	4-storey Grenfell Tower block ofpublic housing flats in North Kensington. The fire is believed to have been started from a refrigerator in a 4th floor apartmentkitchen. The flames spread at an alarming rate up the exterior cladding and thefire quickly became out of control. In addition, the exterior fire re-entered the building, trapping asignificant percentage of residents inside the building	72	70	24
51	2017	The Marina Torch	UAE	Flames shot up the side of the skyscraper, sending debris tumbling from the 337m structure for the 2n time (2015). That fire, and other recent blazes in the city, spread quickly because of external cladding. more than 40 floors of the high-rise tower appeared to be engulfed in flames on one side of the building. Investigators blamed the building's flammable exterior cladding for that blaze's rapid spread.	0	0	64/87
52	2018	Yuansheng International	China	A blaze raged through a 20-storey office block in Zhengzhou. The fire was initially seen on the building's thermal insulation layer. Smoke and flames engulfed the entire eastern side of the building after the blaze broke out among insulation materials on an upper floor. The flames swept through the building facade and burnt window frames were seen falling down.	0	n/a	20
53	2018	Taksim Ilk Yardim Hospital	Turkey	Within seconds, flames had engulfed the side of a 14-floor hospital in the heart of Istanbul. Highly inflammable exterior cladding has been cited by many experts as the reason behind the rapid spread of the hospital fire in central Istanbul on 5 April.	0	0	14
54	2018	Zen Tower	UAE	The Zen Tower caught alight causing over 100 residents to flee their homes. The fire that left the building badly burnt is said to have begun in the kitchen of a downstairs floor business. t as wind speeds of 30 miles per hour whipped-up flames across flammable cladding (aluminium composite panel) that encased the 68-flat high rise in Dubai Marina.	0	0	15
55	2019	Neo 200	Australia	a 41-level apartment complex built in 2004. At issue is the use of flammable aluminium composite cladding, which is made from two skins of aluminium with a fibrous polyethylene material in the middle.	0	0	6

D

56	2019	Kaifeng Apartments	China	25-storey tower block. The blaze was caused by the building's insulation materials, according to the local fire brigade. No casualties have been reported by the authority. The blaze started at the fourth floor on the northern side of the block A in No. 102 of the complex and quickly spread upwards	0	n/a	17
57	2019	Golden Eagle Shopping Mall	China	A fire engulfed the 9th floor of the Golden Eagle International Shopping Center. An initial investigation into the cause of the blaze found construction personnel had ignited combustible material against the rules	0	0	1
58	2019	Residential Flats	Poland	The fire broke out on the ground floor of the 11-story building	n/a	n/a	10
59	2019	The Cube Student Housing	UK	he six-storey building on Bradshawgate, Bolton which was affecting every floor. "To me it looked like the fire was climbing up the cladding. The cladding used on Cube was high-pressure laminate (HPL). The material used in HPL panels can vary and include compressed paper and wood fibre having different combustibility ratings.	0	2	1
60	2020	Abbco Tower	UAE	48-floor UAE skyscraper goes up in flames. The Abbco Tower was fitted with cladding banned (alluminium composite cladding) in 2016 for buildings over 23 meters in Sharjah	0	12	48
61	2020	Business Centre	Turkey	The building appears to be engulfed in flames from top to bottom while burning debris can be seen falling onto nearby roads.	0	n/a	n/a
62	2020	Madrid Tower Block	Spain	The flames on the 20 storey residential building, originating from the roof, fell down the facade without causing injurie. In view of the images of the tower, the insulation used is glass wool (mineral wool) and the outer cladding is very similar to a metallic product of the ACM type (Aluminum Composite Material), with a filling not yet specified, but a priori it has contributed to the spread of flame with falling flaming droplets.	1	n/a	3
63	2020	Apartment Block	South Korea	A 33 storey tower block. The fire broke out between the 8th and 12th floors of the Samhwan Art Nouveau commercial and residential building, which has about 120 households and shopping units. he Ministry said it appears to have spread from one of the lower floors up to the top floor, burning the building's outer wall. The Ulsan Fire Department said fire seeds were hidden throughout the bulding's exterior made with aluminum panels, which also caused delays in extinguishing the fire. Aluminum panels are more susceptible to fire as they are connected with polyester.	0	91	33
64	2021	Apartment Building	China	A huge fire engulfed a 26-storey building in Shijiazhuang, China.According to reports, the fire started on the ground floor before spreading.	0	0	26
65	2021	Torre dei Moro fire	Italy	The fire in the Torre del Moro apartment block, an 18-storey residential building in Milan, started on the 15th floor and first rose to the top of the building. The 60-metre-high building was clad in materials including aluminium and polystyrene. According to Corriere della Ser (an italian newspapper), the inner lining of the cladding panels on the building's facade would have "acted as gasoline".	0	0	20
66	2022	Tunjungan Plaza	Indonesia	A retail complex. The cause was a short circuit in the air conditioning circuit or the AC supplying the cinema. The fire spread quickly because it passed through the aluminum composite (ACP) building TP 5 which then made the facade (outer side of the building) collapse to the tenants below it and the terrace	0	0	n/a

E

A2 Time-temperature curves of samples inside muffle

Lime.m

EPS.m & Aero.m
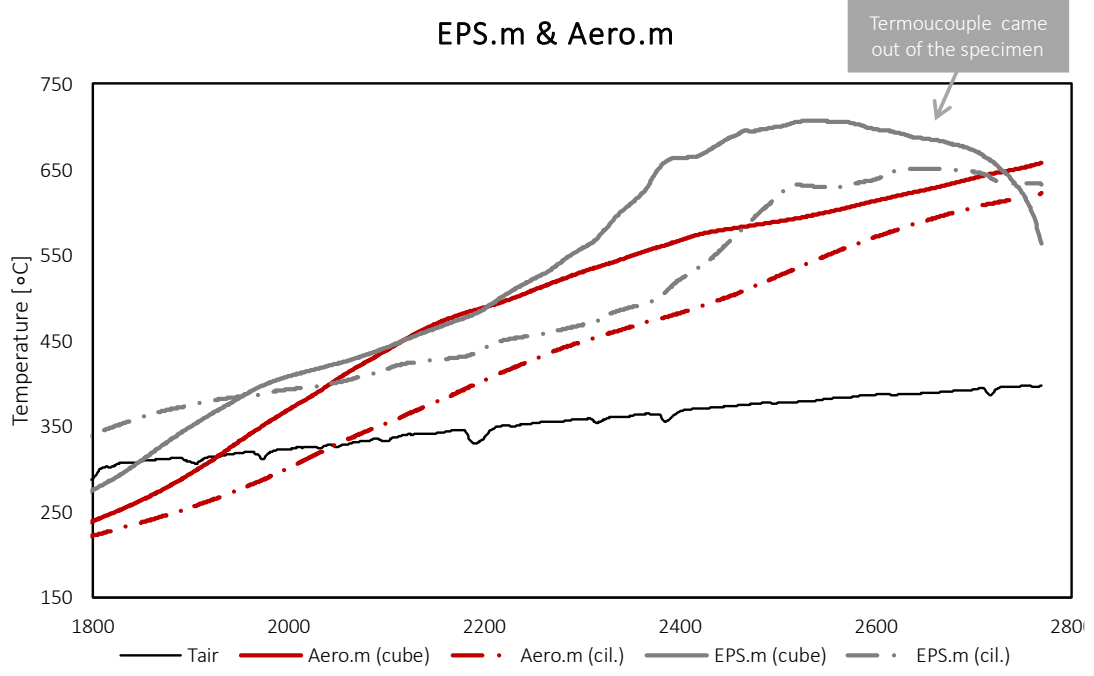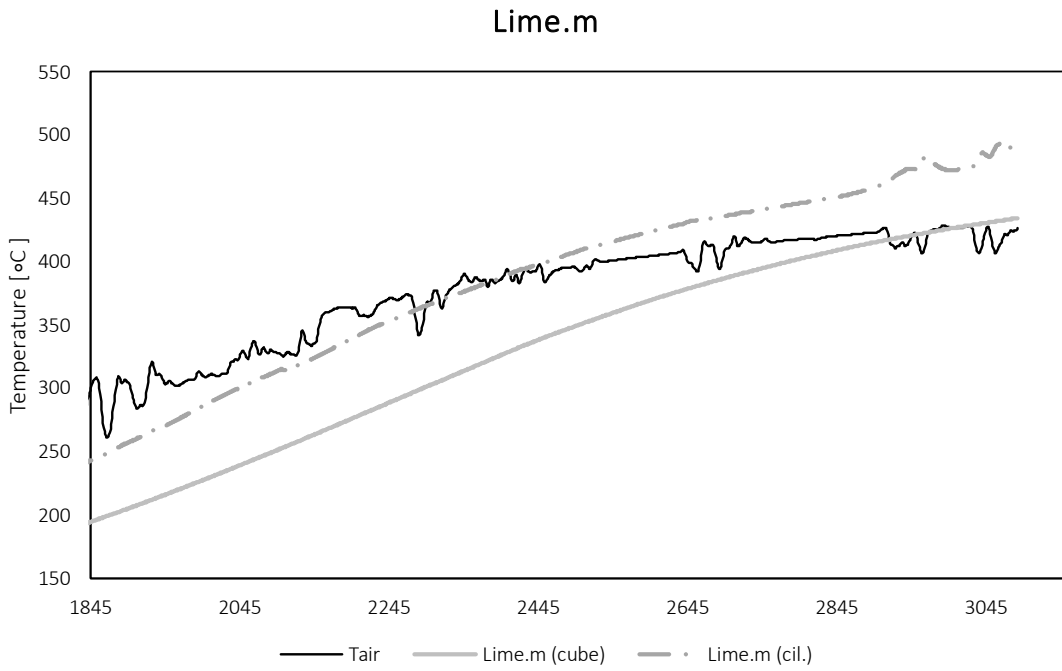
A3 Reports of XRD analyses– Aero.m

A3.1 Diffractometers of sample at initial conditions

Main Graphics, Analyze View: (Bookmark 2)
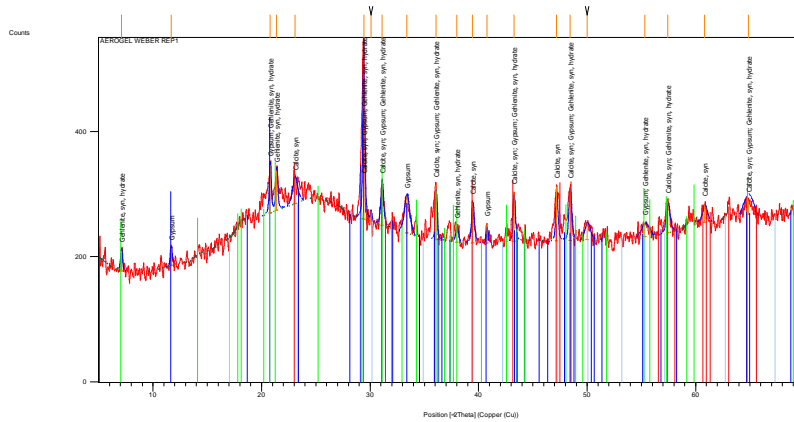
Peak List: (Bookmark 3)

Pos. [°2Th.]	Height [cts]	FWHM [°2Th.]	d-spacing [Å]	Rel. Int. [%]
7.0985	31.78	0.2007	12.45318	11.01
11.6813	27.02	0.2007	7.57587	9.36
20.7845	76.01	0.2007	4.27381	26.34
21.3868	63.26	0.2007	4.15479	21.92
23.0763	39.24	0.5353	3.85429	13.60
29.4070	288.54	0.1840	3.03737	100.00
30.0910	16.91	0.1506	2.96987	5.86
31.0975	69.77	0.2676	2.87601	24.18
33.3866	58.04	0.5353	2.68387	20.12
36.0790	86.96	0.1673	2.48953	30.14
37.9829	23.55	0.2676	2.36900	8.16
39.4513	63.52	0.2676	2.28415	22.02
40.7669	29.74	0.1338	2.21342	10.31
43.2558	78.35	0.2007	2.09166	27.16
47.1753	87.11	0.2007	1.92661	30.19
48.4150	86.15	0.2676	1.88014	29.86
50.0089	26.34	0.5353	1.82389	9.13
55.3190	20.18	0.8029	1.66073	6.99
57.4229	50.13	0.3346	1.60479	17.37
60.8101	26.89	0.4684	1.52326	9.32
64.8400	21.72	0.9792	1.43680	7.53

A3.2 Diffractometers of sample post heating

Main Graphics, Analyze View: (Bookmark 2)
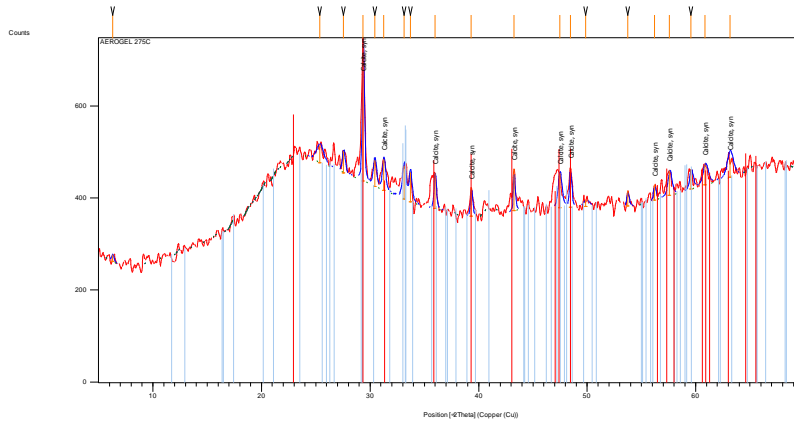
Peak List: (Bookmark 3)

Pos. [°2Th.]	Height [cts]	FWHM [°2Th.]	d-spacing [Å]	Rel. Int. [%]
6.2926	14.52	0.2598	14.04618	4.67
25.3769	37.07	0.7793	3.50985	11.91
27.5596	46.43	0.3247	3.23663	14.92
29.3640	311.16	0.1948	3.04172	100.00
30.4323	57.15	0.3247	2.93734	18.37
31.2682	67.41	0.3247	2.86069	21.67
33.1325	71.68	0.3897	2.70387	23.04
33.7123	63.18	0.2922	2.65868	20.31
35.9819	77.26	0.2273	2.49602	24.83
39.3273	61.30	0.1948	2.29106	19.70
43.2631	90.23	0.1624	2.09132	29.00
47.4695	75.05	0.3897	1.91536	24.12
48.4407	86.29	0.1948	1.87920	27.73
49.8721	13.80	0.6494	1.82857	4.44
53.7224	32.92	0.1948	1.70625	10.58
56.1890	32.71	0.2273	1.63706	10.51
57.5824	53.94	0.3897	1.60072	17.34
59.5632	43.37	0.3247	1.55213	13.94
60.8636	44.14	0.5196	1.52205	14.19
63.1349	40.24	0.6336	1.47144	12.93

Pattern List: (Bookmark 4)

A4 Diffractometers from XRD – EPS.m

A4.1 Diffractometers of sample at initial conditions

Main Graphics, Analyze View: (Bookmark 2)
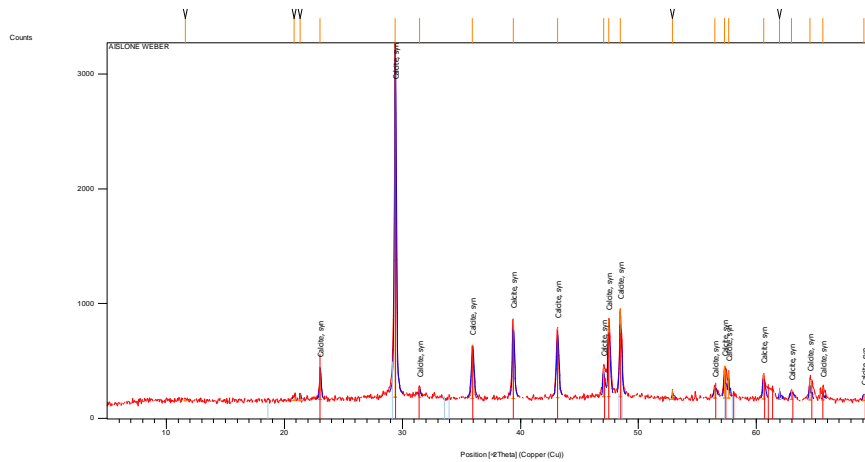
Peak List: (Bookmark 3)

Pos. [°2Th.]	Height [cts]	FWHM [°2Th.]	d-spacing [Å]	Rel. Int. [%]
11.6162	17.20	0.9092	7.61816	0.54
20.8274	32.51	0.3897	4.26510	1.03
21.3309	62.39	0.0974	4.16556	1.97
23.0321	285.86	0.1299	3.86159	9.02
29.3883	3170.27	0.1624	3.03927	100.00
31.4664	87.00	0.0974	2.84312	2.74
35.9192	469.27	0.2273	2.50023	14.80
39.3716	700.04	0.1624	2.28858	22.08
43.1250	614.47	0.1948	2.09770	19.38
47.0425	265.82	0.1299	1.93174	8.38
47.4738	671.17	0.1624	1.91519	21.17
48.4491	768.85	0.1624	1.87890	24.25
52.8922	79.20	0.0974	1.73106	2.50
56.4859	97.13	0.2598	1.62916	3.06
57.2941	281.23	0.1299	1.60809	8.87
57.6347	238.70	0.0974	1.59939	7.53
60.5966	227.87	0.1624	1.52811	7.19
61.9486	99.52	0.0974	1.49797	3.14
62.9435	79.46	0.2598	1.47667	2.51
64.5054	167.59	0.1299	1.44464	5.29
65.6224	114.18	0.0974	1.42273	3.60
69.1088	51.71	0.2376	1.35810	1.63

A4.2 Diffractometers of sample post heating

Main Graphics, Analyze View: (Bookmark 2)

***Peak List:*** (Bookmark 3)

Pos. [°2Th.]	Height [cts]	FWHM [°2Th.]	d-spacing [Å]	Rel. Int. [%]
15.6695	27.23	0.1948	5.65550	1.91
18.1095	1427.55	0.1299	4.89863	100.00
19.4567	17.07	0.3247	4.56237	1.20
21.0343	54.23	0.1948	4.22362	3.80
23.0640	79.18	0.1299	3.85631	5.55
24.9892	214.72	0.0974	3.56341	15.04
26.2762	93.33	0.3897	3.39173	6.54
27.1546	372.83	0.2273	3.28398	26.12
28.7304	345.98	0.0974	3.10735	24.24
29.4570	1238.93	0.1948	3.03233	86.79
32.7443	373.36	0.1624	2.73503	26.15
34.1385	1109.00	0.1948	2.62646	77.69
36.0226	192.82	0.1299	2.49329	13.51
38.0353	67.90	0.1624	2.36586	4.76
39.4113	227.72	0.1624	2.28637	15.95
41.2783	26.25	0.2598	2.18717	1.84
43.2280	269.19	0.1624	2.09294	18.86
43.8970	290.26	0.2598	2.06258	20.33
45.9545	120.77	0.1948	1.97491	8.46
47.1574	831.51	0.2273	1.92730	58.25
47.5716	373.32	0.1299	1.91148	26.15
48.6371	321.69	0.2273	1.87207	22.53
50.1192	288.80	0.4546	1.82013	20.23
50.8242	417.81	0.1299	1.79653	29.27
52.6842	50.91	0.6494	1.73740	3.57

J

A5   Ignitability test report

Relatório de Ensaio

Relat**ó**rio n.**º**   ETE 157/21   Data de emiss**ão**:   26/11/2021

Ensaio de ignitabilidade de produtos de cons**trução**
(M**ét**odo de ensaio: ISO 11925-2:2020)

Dados relativos ao cliente:

Nome: IST-ID - Associação do Instituto Superior Técnico para a Investigação e Desenvolvimento

Endere**ço:** Instituto Superior Técnico, Av. Rovisco Pais, 1. 1049-003 Lisboa

Contacto: Inês Flores-Colen

Fax: ---   Tel.:   218 418 354   e-mail: ines.flores.colen@tecnico.ulisboa.pt

Dados relativos **à** amostra ensaiada:

Ref**erê**ncia Itecons: ETE166A/21   Ref**erê**ncia do Cliente *:   Argamassa com aerogel

Fabricante/ fornecedor *:   IST-ID   Identifica**ção do** produto *:   a)

Descri**çã**o do produto *: Produto ensaiado apresentava massa volúmica de 160 kg/m³, massa por unidade de área de 6400 g/m² e espessura nominal de 40 mm.

Substratos utilizados: ---

Data de rece**ção:**   21/10/2021

Responsabilidade da amostragem: Cliente. A amostragem efetuada não se encontra incluída no âmbito da acreditação.

Local de rea**lização d**o ensaio: Itecons

Resultados obtidos:

Detalhes do condicionamento: Os provetes foram condicionados à temperatura de (23±2) ºC e a humidade relativa de (50±5) %, por um período de 96 horas, até alcançarem massa constante. Durante os ensaios, o laboratório encontrava-se a (23±5) ºC de temperatura e a (50±20) % de humidade.

Data in**íci**o do condicionamento: 08/11/2021   Data fim do condicionamento: 12/11/2021

Data do ensaio: 12/11/2021   Tempo de aplica**çã**o da chama: 15 s   A duração total do ensaio foi de 20 s, desde o instante de aplicação da chama.

APLICA**ÇÃ**O DA CHAMA NA FACE PRINCIPAL					
Ref**erê**ncia dos provetes	Oco**rrê**ncia de ign**ição**	Prop**agaçã**o da chama a 150 mm acima do ponto de aplica**çã**o, Fs > 150 mm	Instante em que a chama atinge os 150 mm acima do ponto de aplica**çã**o, t_{150} (S)	Got**íc**ulas ou part**íc**ulas incandescentes	Ign**ição d**o papel de filtro
ETE166A/21.1	Não	Não	---	Não	Não
ETE166A/21.2	Não	Não	---	Não	Não
ETE166A/21.3	Não	Não	---	Não	Não
ETE166A/21.4	Não	Não	---	Não	Não
ETE166A/21.5	Não	Não	---	Não	Não
ETE166A/21.6	Não	Não	---	Não	Não

K

Ensaio de ignitabilidade de produtos de construção
(Método de ensaio: ISO 11925-2:2020)

		APLICAÇÃO DA CHAMA NO BORDO INFERIOR			
Referência dos provetes	Ocorrência de ignição	Propagação da chama a 150 mm acima do ponto de aplicação, Fs > 150 mm	Instante em que a chama atinge os 150 mm acima do ponto de aplicação, t_{150} (S)	Gotículas ou partículas incandescentes	Ignição do papel de filtro
---	---	---	---	---	---
---	---	---	---	---	---
---	---	---	---	---	---
---	---	---	---	---	---
---	---	---	---	---	---
---	---	---	---	---	---

Observações:

a) Argamassa com a seguinte composição, indicada pelo cliente, em percentagem de massa do produto: 37% (silica aerogel), 35,01% (ligante), 1,47% (aditivos) e 25,53% (filler leve).

Ensaios realizados por: _____ Katya Coelho _____

Autoria técnica   Responsabilidade técnica   A Direção

ETE157/21

António Nascimento
António Nascimento
Técnico Superior

Isabel Torres
Isabel Torres
Supervisora Técnica e Científica

Documento validado

Notas:

Os resultados apresentados referem-se ao desempenho dos provetes do produto quando submetidos às condições particulares do ensaio realizado. Estes resultados não pretendem ser o único critério de avaliação do risco potencial de incêndio associado às condições de utilização do produto em causa.

Os resultados apresentados referem-se, exclusivamente, aos itens ensaiados e aplicam-se à amostra conforme rececionada.

Os dados assinalados com * foram fornecidos pelo cliente e são da sua inteira responsabilidade.

O presente relatório não pode ser reproduzido, exceto na íntegra, sem o acordo escrito do Itecons.

L

A6 Gross calorific potential tests report

Rel**atóri**o de Ensaio

Rel**atóri**o n.**º**   ETE 156/21

Data de em**issão**:   26/11/2021

Determina**çã**o do calor de combus**tão** de produtos de cons**truçã**o
(M**éto**do de ensaio: ISO 1716:2018)

Dados relativos ao cliente:

Nome: IST-ID - Associação do Instituto Superior Técnico para a Investigação e Desenvolvimento

Endere**ç**o: Instituto Superior Técnico, Av. Rovisco Pais, 1. 1049-003 Lisboa

Contacto: Inês Flores-Colen

Fax: --- Tel.: 218 418 354 e-mail: ines.flores.colen@tecnico.ulisboa.pt

Dados relativos **à** amostra ensaiada:

Refer**ê**ncia Itecons: ETE165A/21

Refer**ê**ncia do cliente*: Argamassa com aerogel

Fabricante/fornecedor*: IST-DT

Identifica**çã**o do produto*: a)

Descri**çã**o do produto*: Produto ensaiado apresentava massa volúmica de 160 kg/m³, massa por unidade de área de 6400 g/m² e espessura nominal de 40 mm.

Data de rece**çã**o: 21/10/2021

Responsabilidade da amostragem*: Cliente. A amostragem efetuada não se encontra incluída no âmbito da acreditação.

Local de reali**zaçã**o do ensaio: Itecons

Resultados do ensaio:

Equivalente de **á**gua, E: 0,00393976 MJ/K

Data de determina**çã**o do equivalente de **á**gua, E: 27/09/2021

Detalhes do condicionamento: A amostra foi condicionada à temperatura de (23±2) °C e a humidade relativa de (50±5) %, por um período de 96 horas, até alcançar massa constante.

Data do início de condicionamento: 01/11/2021   Data do fim de condicionamento: 05/11/2021   Data de ensaio: 05/11/2021

Refer**ê**ncia do provete	ETE165A21.1	ETE165A21.2	ETE165A21.3	Valor **mé**dio**
Calor de Combus**tão** bruto, Q_{PCS} (MJ/kg)	6,24	6,27	6,06	6,19 ± 0,25

Observa**çõ**es:

Os resultados obtidos são válidos conforme os requisitos expressos na Tabela 1 da norma ISO 1716:2018. **A incerteza de medição expandida apresentada, calculada de acordo com o documento ILAC-G17, está expressa pela incerteza-padrão combinada multiplicada pelo fator de expansão k = 3,3, o qual, para uma distribuição normal, corresponde a um nível de confiança de aproximadamente 95 %. A incerteza de medição expandida não inclui a etapa relativa à amostragem. a) Argamassa com a seguinte composição, indicada pelo cliente, em percentagem de massa do produto: 37% (silica aerogel), 35,01% (ligante), 1,47% (aditivos) e 25,53% (filler leve).

Ensaios realizados por: Nuno Tinoco

Autoria técnica	Responsabilidade técnica	A Direção
António Nascimento	*Isabel Torres*	*Documento validado*
António Nascimento	Isabel Torres	
Técnico Superior	Supervisora Técnica e Científica	

Notas: Os resultados apresentados referem-se ao desempenho dos provetes do produto quando submetidos às condições particulares do ensaio realizado. Estes resultados não pretendem ser o único critério de avaliação do risco potencial de incêndio associado às condições de utilização do produto em causa.

Os resultados apresentados referem-se, exclusivamente, aos itens ensaiados e aplicam-se à amostra conforme rececionada.

Os dados assinalados com * foram fornecidos pelo cliente e são da sua inteira responsabilidade.

O presente relatório não pode ser reproduzido, exceto na íntegra, sem o acordo escrito do Itecons.

INSTITUTO DE INVESTIGAÇÃO E DESENVOLVIMENTO TECNOLÓGICO PARA A **CONSTRUÇÃO, ENERGIA, AMBIENTE E SUSTENTABILIDADE**

Rua Pedro Hispano, s/n
3030-289 Coimbra
Tel: (+351) 239 79 89 49

www.itecons.uc.pt
itecons@itecons.uc.pt

M